



**THE EFFECT OF THE PITCH ANGLES OF CHARGED
PARTICLES ON THEIR SEPARATION FROM
MAGNETIC FIELD LINES**

CHART WIKEE

**MASTER OF SCIENCE
IN
COMPUTATIONAL SCIENCE**

**SCHOOL OF SCIENCE
MAE FAH LUANG UNIVERSITY**

2013

©COPYRIGHT BY MAE FAH LUANG UNIVERSITY

**THE EFFECT OF THE PITCH ANGLES OF CHARGED
PARTICLES ON THEIR SEPARATION FROM
MAGNETIC FIELD LINES**

CHART WIKEE

**THIS THESIS IS A PARTIAL FULFILLMENT OF
THE REQUIREMENTS FOR THE DEGREE OF
MASTER OF SCIENCE
IN
COMPUTATIONAL SCIENCE**

**SCHOOL OF SCIENCE
MAE FAH LUANG UNIVERSITY**

2013


©COPYRIGHT BY MAE FAH LUANG UNIVERSITY


**THE EFFECT OF THE PITCH ANGLES OF CHARGED
PARTICLES ON THEIR SEPARATION FROM
MAGNETIC FIELD LINES**

CHART WIKEE


THIS THESIS HAS BEEN APPROVED
TO BE A PARTIAL FULFILLMENT OF THE REQUIREMENTS
FOR THE DEGREE OF MASTER OF SCIENCE
IN
COMPUTATIONAL SCIENCE
2013

THESIS COMMITTEE


.....CHAIRPERSON
(Dr. Anant Eungwanichayapant)


.....ADVISOR
(Dr. Piyanate Chuychai)


.....CO-ADVISOR
(Prof. Dr. David Ruffolo)


.....EXTERNAL EXAMINER
(Dr. Watcharawuth Krittinatham)

ACKNOWLEDGEMENTS

First of all, I wish to sincerely express my gratitude to my co-advisor, Prof. Dr. David Ruffolo, for always giving me new creative ideas, suggestions for my study and finding a scholarship for me. I am also grateful to Dr. Piyanate Chuychai, my advisor, for her help and many suggestions. I have learned a lot of astrophysics and computer techniques from her. Without her guidance, I could not finish this work.

I would like to thank Dr. Paisan Tooprakai for his paper and allowing me to use it for presentation in the first seminar. I would like to give my gratitude to my thesis committee members, Dr. Anant Eungwanichayapant and Dr. Watcharawuth Krittinatham, for their comments and suggestions.

I would like to thank Thailand Center of Excellence in Physics very much for giving me financial support for the master's degree program. For computation, I also would like to thank the Thailand Research Fund and Thailand Center of Excellence in Physics for supporting a computing cluster in our research group.

Finally, I would like to thank my family, who have given me inspiration, and also all of my teachers who taught me how to think well, and my colleges who always helped me when I was mistaken.

Chart Wikee

Thesis Title	The Effect of The Pitch Angles of Charged Particles on their Separation From Magnetic Field Lines
Author	Chart Wikee
Degree	Master of Science (Computational Science)
Advisor	Dr. Piyanate Chuychai
Co-Advisor	Prof. Dr. David Ruffolo

ABSTRACT

When the charged particles are moving in a magnetic field, the charged particles follow the right hand rule due to Newton-Lorentz force. The pitch angle is defined as the angle between the particle velocity and the magnetic field. In a uniform magnetic field, the charged particles released at a 90 degree pitch angle move around the magnetic field line in a circular orbit, while the charged particles released with a pitch angle less or more than 90 degrees have helical orbits around the magnetic field. Magnetic fields are found not only on the earth, but also in interplanetary space. The interplanetary magnetic field is turbulent and always comes out from the Sun. In this work, we are interested to study the transport of charged particles in a turbulent magnetic field as in the interplanetary space by using computer simulations. We use a 2D+slab model for the magnetic field. We compare two cases which are a simple 2D field+slab turbulence case and a case where both 2D and slab components are turbulent. Then we release the charged particles by varying the pitch angle for study of the separation of charged particles and magnetic field lines. We solve the Newton-Lorentz and field line equations to find trajectories of charged particles and magnetic field lines by using the Runge-Kutta method with adaptive

time stepping regulated by a fifth-order error estimate. We analyze the positions of guiding centers of the charged particle trajectories and compare them with the magnetic field lines that are released from the initial guiding centers of the charged particles at various times. We present the effect of initial pitch angle on the separation between guiding centers and magnetic field lines when we set the initial pitch angle to 0, 30, 60 and 90 degrees. From overall results, we found that the initial pitch angle has an effect on the separation of the charged particles and their corresponding magnetic field lines. For the simple case, the separations of the charged particles are related to distance from the center of the Gaussian flux tube and intensity of 2D Gaussian field. For the 2D+slab turbulent field, we can find that the separation of the charged particles is different at each initial pitch angle and the critical initial pitch angle that gives the most separation at any time is also computed. Moreover, we found that in an intermediate range the particles released at a 90 degree pitch angle have more separation than the others. In the long time limit, all initial pitch angles give similar results for the separation. This work is useful to help us understand the mechanisms of the transport of the solar energetic particles in heliosphere and developing the theory of diffusion of charged particles in turbulent magnetic fields.

Keywords: Charge particles/Magnetic field/Pitch angle/Turbulence/
Newton-Lorentz force/Guiding center

TABLE OF CONTENTS

	Page
ACKNOWLEDGEMENTS	(3)
ABSTRACT	(4)
TABLE OF CONTENTS	(6)
LIST OF FIGURES	(9)
 CHAPTER	
1 INTRODUCTION	1
1.1 Overview	1
1.2 Objectives	2
1.3 Expected outcome	2
1.4 Scope of study	2
1.5 Literature review	3
1.6 Thesis outline	4
1.7 Usefulness of this work	5
 2 THEORETICAL BACKGROUND	6
2.1 Background	6
2.2 Two-component magnetic field model	9
2.3 Characteristics of turbulence and its power spectrum	14
2.4 Correlation functions and power spectrum	16
2.5 Charged particles in uniform magnetic field	18
2.6 Guiding center	22
2.7 Pitch angles	23
2.8 Charged particles in non-uniform magnetic field	24

TABLE OF CONTENTS (continued)

	Page
CHAPTER	
3 METHODOLOGY	30
3.1 Generation of magnetic field	30
3.2 Particle simulations	33
3.3 Field line simulation	35
3.4 Pitch angle setup	36
3.5 Parameter setup	40
3.6 Procedure of simulations	41
3.7 Data analysis	43
3.8 Research tools	45
4 RESULTS FOR THE CHARGED PARTICLES IN SIMPLE 2D FIELD+SLAB TURBULENCE	46
4.1 The effect of initial released position to the separation	46
4.2 The effect of fixed initial pitch angles to the separation	54
5 RESULTS FOR THE CHARGED PARTICLES IN 2D+SLAB TURBULENCE	60
5.1 The effect of various initial pitch angle ranges on the separation	60
5.2 The effect of fixed initial pitch angles on the separation	64
6 CONCLUSIONS	75
REFERENCES	78

TABLE OF CONTENTS (continued)

	Page
APPENDICES	84
APPENDIX A THE LINEAR INTERPOLATION AND BI-LINEAR INTERPOLATION FOR 2D+SLAB TURBULENT FIELD	85
APPENDIX B THE CORRECTION OF UNIT VECTOR OF CROSS PRODUCT BETWEEN VELOCITY AND UNIT VECTOR FOR GENERATING A NEW VELOCITY VECTOR	88
CURRICULUM VITAE	90

LIST OF FIGURES

Figure	Page
2.1 Illustration of the structure of interplanetary magnetic field and solar wind.	7
2.2 Illustration of the slab fluctuation and the arrows demonstrate the slab fluctuation \vec{b}^{slab} .	10
2.3 Illustration of the 2D fluctuation. The solid arrows show the 2D field (\vec{b}^{2D}) and dashed arrows show examples of the directions of $\vec{\nabla}a(x, y)$. For a positive potential function, the 2D field is in a counter-clockwise direction, while a 2D field having a negative potential function is in the clockwise direction.	11
2.4 Illustration of the contours of Gaussian potential function and the arrows demonstrate the 2D field.	12
2.5 The spectrum of turbulence from Kolmogorov's theory.	15
2.6 Relationship between the autocorrelation $A(k_x, k_y)$ and the potential function $a(x, y)$. The scales of the $A(k_x, k_y)$ plot indicate the number of modes in (k_x, k_y) space and the contour plots of $a(x, y)$ in the right panel are only small pieces cut from the large simulation area.	18
2.7 The right-hand rule for determining the direction of magnetic force. (a) If q is positive and (b) if q is negative.	19
2.8 Showing component parallel ($\vec{v}_{ }$) and perpendicular (\vec{v}_{\perp}) of the velocity of charged particle in the magnetic field.	20

LIST OF FIGURES (continued)

Figure	Page
2.9 The motion of positive charged particle in a uniform magnetic field (when $\vec{v}_{//} = 0$).	21
2.10 Showing the example of a trajectory of positive charged particle to the direction of magnetic field (when $\vec{v}_{//}$ and $\vec{v}_{\perp} \neq 0$).	21
2.11 Illustration of a particle orbit, magnetic field line and guiding center.	22
2.12 The example of trajectory of charged particle at each pitch angle.	24
2.13 Charged particle drift due to magnetic field gradient.	27
2.14 Illustration of direction of the particle guiding center drift velocity \vec{v}_C and \vec{v}_G due to the curvature and gradient of the magnetic field line.	29
3.1 Generation of slab magnetic field.	31
3.2 The positions of the magnetic field obtained at each grid point.	33
3.3 The sketch of the positions of releasing the charged particles.	34
3.4 Showing the example of trajectory of the magnetic field line.	36
3.5 Illustration the change of magnetic field vector from Cartesian coordinate to Spherical coordinate at each position.	37
3.6 Illustration of setting a velocity vector.	38
3.7 Illustration of rotating of a new velocity vector (\vec{v}') by method random β angle around the magnetic field.	39
3.8 The cross section from rotation of velocity vector around the magnetic field.	40
3.9 Showing radius of curvature, particle position and guiding center position.	42
3.10 The diagram of separation between the guiding center and magnetic field line.	44

LIST OF FIGURES (continued)

Figure	Page
4.1 Example of the trajectory of a charged particle in our model; red line demonstrates trajectory of magnetic field line, black line and blue line demonstrate trajectories of charged particle and its guiding centers, respectively.	47
4.2 The results of the separation of charged particles and their corresponding field lines in the log-log scale.	48
4.3 The profile of the 2D Gaussian magnetic field along the distance from the center of the flux tube.	50
4.4 Showing shape of drift speed of guiding center due to the gradient of the magnetic field, radius of curvature of the magnetic field line and the summation of the gradient drift and curvature drift in arbitrary units.	51
4.5 Showing the separation of the charged particles at a) inside the 2D island and b) outside the 2D island.	52
4.6 The mean squared perpendicular displacement and time in the final range.	53
4.7 Example of the trajectories of a charged particles are released at radius as 0.1λ when the initial pitch angle as a) 0 degree and b) 90 degrees; the red line demonstrates trajectory of magnetic field line, the black line and the blue line demonstrate trajectories of charged particle and its guiding centers, respectively.	55
4.8 Showing the separation of the charged particles at the radii as 0.1, 0.3, 0.5, 0.7, 0.9λ in the figure 4.8a)-e) respectively.	56

LIST OF FIGURES (continued)

Figure	Page
4.9 Showing the separation of the charged particles at the radius as 0.1λ , 0.3λ and 0.9λ by using fix initial pitch angles as a) 0 degree and b) 90 degrees in the simple pure 2D field.	58
4.10 Showing the separation of the charged particles in log-log scale at the radius as 0.1λ , 0.3λ and 0.9λ by using fix initial pitch angles as a) 0 degree and b) 90 degrees in simple pure 2D field.	58
5.1 Illustration of the examples of charged particles and their corresponding magnetic field line trajectories. a) The charged particle is released at initial pitch angle near 0 degree. b) The charged particle is released at initial pitch angle near 90 degrees. They are released at the same position where the green arrow indicates. The red line shows trajectory of magnetic field line, the blue line shows trajectory of guiding center, and dark line show trajectory of charged particle.	61
5.2 Displacement mean squared perpendicular to the mean field between guiding centers of charged particles (x_{GC}, y_{GC}) and their corresponding magnetic field lines (x_{FL}, y_{FL}) at initial in linear-linear scale.	62
5.3 Showing relation between mean squared displacement perpendicular to the mean field between guiding centers of charged particles (x_{GC}, y_{GC}) and their corresponding magnetic field lines (x_{FL}, y_{FL}) and time in log-log scale.	63

LIST OF FIGURES (continued)

Figure	Page
5.4 Showing the separation of the charged particles between guiding centers of charged particles (x_{GC}, y_{GC}) and their corresponding magnetic field lines (x_{FL}, y_{FL}) at any each time in a) linear-linear scale and b) log-log scale(5.4b).	65
5.5 The results of the separation of charged particles and their corresponding field lines in the log-log scale.	67
5.6 Showing the results between the initial pitch angles and the separation of the charged particles in log scale on the same picture at the time as $tc/\lambda = 0.1, 1.0, 10.0, 100.0$ and 1000.0 .	68
5.7 Showing the results between the cosine initial pitch angles and the separation of the charged particles in log scale on the same picture at the time as $tc/\lambda = 0.1, 1.0, 10.0, 100.0$ and 1000.0 .	69
5.8 These figures show the separation of a charged particles in turbulence magnetic field model when initial pitch angle and time are different.	71
5.9 These figures show the critical points of initial pitch angles at the time as $tc/\lambda = 0.1, 1.0, 10.0, 100.0$, and 1000.0 by using linear least square fitting.	72
5.10 These figures show the changing of pitch angles and time in a) a selected particle at initial pitch angle as 0 degree and b) the average pitch angle of 1000 particles at initial pitch angles as 0, 30, 60 and 90 degrees.	73

CHAPTER 1

INTRODUCTION

1.1 Overview

The solar wind is a turbulent ionized gas that is flow out from the outer layer of the Sun into the entire heliosphere. The solar wind also drags the Sun's magnetic field into interplanetary space. Therefore, the magnetic field is also turbulent. When the temperature on the surface of the Sun is very high, the Sun's gravity cannot hold on to the high energy particles, called solar energetic particles or SEPs. Since most SEPs are charged particles, thus they move along the magnetic field. There are many researches to study transport of charged particles and magnetic field in interplanetary space, but it is not yet enough to completely understand about the mechanism, due to their complexity.

In this work, we are interested in the transport of charged particles in interplanetary space, by studying the separation of guiding center of charged particles and their corresponding magnetic field lines. In particular, we are interested in the relationship between the initial pitch angles of charged particles and their separation corresponding magnetic field lines. It is easy to understand behavior of charged particles in space if the magnetic field is uniform and we know that the charged particles will spiral around the magnetic field lines. When the magnetic field in space is non-uniform and more complicated we have to use new numerical techniques to set up in the simulations. To succeed this work, we use the 2D+slab turbulence field to model the simulations of turbulent magnetic field in interplanetary space and numerical method to solve the Newton-Lorentz equation and field line equation to

obtain the trajectories of particles and field lines. This work may help us to produce new idea and develop the theories and numerical simulation techniques for particle diffusion in space.

1.2 Objectives

1. To study the separation and the effect of initial pitch angles of the charged particles and their initial magnetic field lines by performing the simulations in simple model (2D Gaussian field + slab turbulence).
2. To study the effect of initial pitch angle of the charged particles on their separation behavior of magnetic field lines and the charged particles in turbulent magnetic field model called two-component model or 2D+slab turbulence.

1.3 Expected outcome

We can understand the effect of the pitch angles on the separation of the charged particles and the magnetic field lines in two-component model (2D+slab) of the magnetic field turbulence. Moreover, we develop the theory and numerical techniques in order to study separation between the charged particles and the magnetic field lines. This study can help us to explain the transport of the charged particles in interplanetary space in our system.

1.4 Scope of study

To study the effect of initial pitch angles of the charged particles the separation of the charged particles and their initial magnetic field lines in 2D+slab model of the magnetic field turbulence which is an appropriate model for interplanetary magnetic field (Matthaeus, Goldstein & Roberts, 1990; Bieber, Wanner & Matthaeus, 1996).

1.5 Literature review

Since we are interested in moving charged particles in interplanetary magnetic field, the trajectories of charged particles are described by the motion due to the Lorentz force in an irregular magnetic field which is the superposition of a uniform field and a smaller fluctuating. Usually, the charged particles are followed the magnetic field. Therefore, there are many papers assumed that the diffusion of charged particles along the magnetic field related to the diffusion of field lines and they study the behavior of field line random walk instead. The classic field line random walk theory is presented and measured by the observed power spectrum of field fluctuations (Jokipii, 1966; Jokipii & Parker, 1968). There is also evidence that the behavior of the particle distribution can be better understood if we know the separation rate of the random field line and it is found that the rate of separation is very sensitive to the precise form of the power spectrum (Jokipii, 1973). For better understanding the interplanetary magnetic field, they describe the theory of quasi-two-dimensional turbulence in terms of a perturbation expansion (Matthaeus et al., 1990). After that the two-component model is used to study solar wind and interplanetary magnetic field (Bieber et al., 1996). The field line random walk in two-component model is first introduced by Matthaeus, Gray, Pontius and Bieber (1995). Later the theory is modified and applied for various cases including the numerical confirmation in order to explain the behavior of diffusion of charged particles in space (Ruffolo, Matthaeus & Chuychai, 2004; Chuychai, Ruffolo, Matthaeus & Meechai, 2007; Shalchi, 2010). However, considering only the field line random walk is not enough to have complete explanation about the behavior of the charged particles.

Although the magnetic field will be interested by a lot of scientists, but it is not enough to describe all transport behavior of charged particles in space. The study about trajectories of charged particles in interplanetary is also developed by various group such as the transport of charged particles are examined by direct computational of a large number of charged test particles trajectories, these will be subdiffusive transport of charged particles perpendicular to the large scale magnetic field (Qin, Matthaeus & Bieber, 2002). For high accuracy, the trajectory of charged particles are

traced by using Runge-Kutta method to solve Newton-Lorentz equation, transform particles position coordinates to guiding center coordinate and transform the kinematic momentum from Cartesian coordinate to spherical coordinate (Achara Seripienlert, 2006). Moreover, the motion of charged particles in interplanetary was described for more understanding is drift motion of energetic particles in an interplanetary magnetic cloud (Watcharawuth Krittinatham, 2010). The transport of the charged particles is investigated in non-axisymmetric 2D+slab turbulence by numerical simulations (Ruffolo, Chuychai, Wongpan, Minnie, Bieber & Matthaeus, 2008) and compare with the nonlinear guiding center (NLGC) theory (Mathaeus, Qin, Bieber & Zank, 2003). The theory is not yet fully explained the results from the simulations. The improvement of theory is still needed in order to understand the mechanism of the motion of the charged particles. However, there are many ways are waiting to prove and learn about relationship between the magnetic field and charged particles.

In this study, we consider both charged particles and magnetic field lines and find their separation. We focus on the effect of the initial pitch angle of charged particles on the separation from the magnetic field lines. Perhaps, this work could help us to understand behavior of the charged particles in interplanetary space.

1.6 Thesis outline

The dissertation is divided into six chapters. In chapter 1, we explain the scope of study, objectives, and usefulness of this work. After that we present the theoretical background such as the model of turbulent magnetic field and charged particle motion and related diffusion theories in chapter 2. In the next chapter, the methodology that we use to generate magnetic field and to analyze the data is shown and we describe the numerical methods to setup initial parameters of charged particles and magnetic field. Furthermore, we show all results from this work in the following two chapters. Chapter 4 is presented the effect of initial pitch angles to the separation in Gaussian 2D field+slab turbulence and the results for 2D+slab turbulence are shown in chapter 5. Finally, we discuss and conclude in the last chapter.

1.7 Usefulness of this work

This work provides a better understanding the effect of initial pitch angles of the charged particles on their separation behavior of magnetic field lines. Moreover, this research can be applied to produce new idea and numerical technique in order to describe the problems of particles diffusion in turbulent magnetic field or phenomena that occur in nature, and it is useful for scientific knowledge that motivate young blood scientist to study astrophysics.

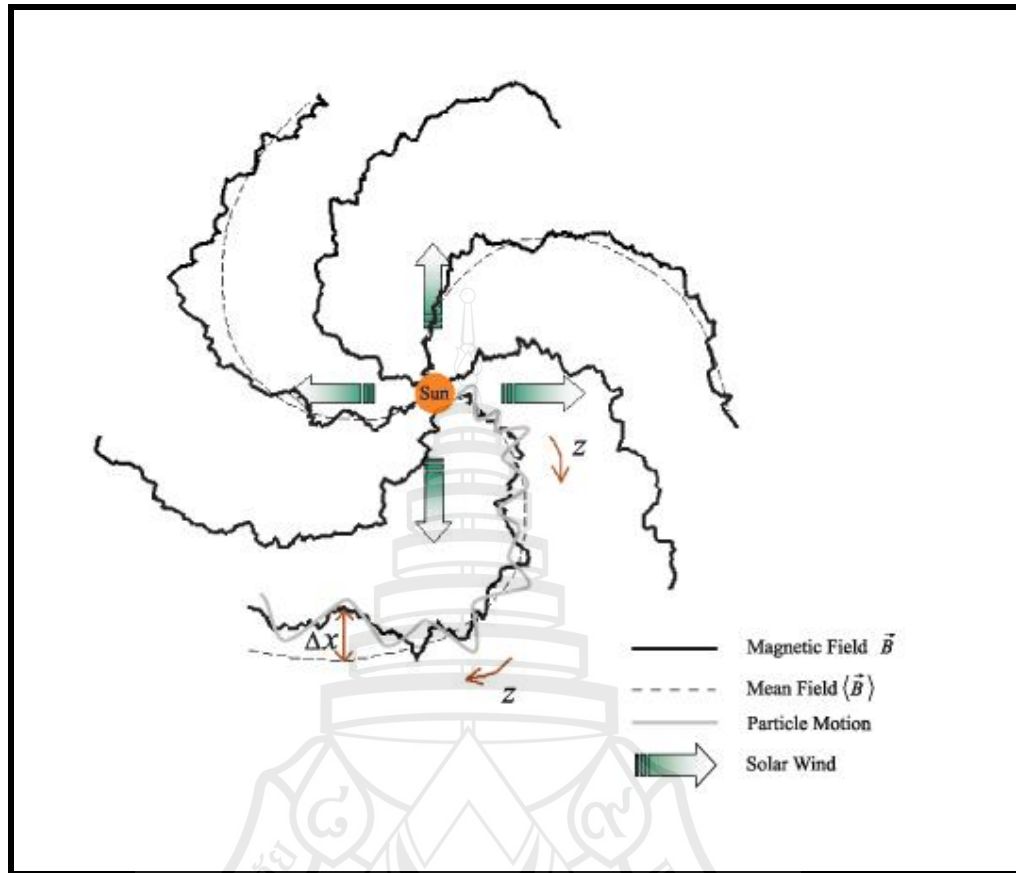


CHAPTER 2

THEORETICAL BACKGROUND

2.1 Background

The Sun consists of plasma i.e., ionized gas such as helium, hydrogen, protons and electrons. These charged particles covered by magnetic field of the Sun collide and exchange energy all the time. If the magnetic field of the Sun has less energy, these charged particles flow out from the Sun to the interplanetary space with the velocity about 400 km/s and drag the magnetic field of the Sun into the space as well. We call these charged particles as “solar wind” as shown in Figure 1. Because the Sun is turned around itself and solar wind comes out from the Sun in radial direction, the magnetic field that comes out from the Sun has spiral shape as illustrated in Figure 2.1. Since the solar wind is turbulent, the interplanetary magnetic field (IMF) is also turbulent.



Source Piyanate Chuychai (2004).

Figure 2.1 Illustration of the structure of interplanetary magnetic field and solar wind.

When the eruption of magnetic energy occurs at the surface of the Sun, it will suddenly released highly energetic particles to interplanetary space. We call “solar flare”. Moreover, coronal mass ejections (or CMEs) (Schindler, 2007) are huge bubbles of ionized gas threaded with magnetic field lines that are ejected from the Sun over the course of several hours, and the energetic charged particles also come out from the shock in front of the CME. These high energy charged particles are called solar energetic particles (SEPs). They are diffusive because they orbit around the turbulent magnetic field in space.

Usually, when the charged particles are moving in the magnetic field lines, it orbit around the magnetic field as helical orbit due to the Lorentz force. The angle between the velocity of the charged particle and the magnetic field called pitch angle determine the direction and the shape of helix. For a constant magnetic field, the center of trajectories of charged particles called guiding center exactly follow their initial magnetic field lines. In interplanetary space, the magnetic field is turbulent. The charged particles initially move along their initial magnetic field lines, scatter back and forth, and later they deviate from the initial field lines because of the effect of the drift (Ruffolo et al., 2008; Chuychai, Ruffolo, Wikee & Matthaeus, 2011). In this work, we are interested in the angles that release charged particles called pitch angles and regard to the effect of those to separation between the magnetic field lines and the guiding center of charged particles.

From previous work, the charged particle transport is described by the quasi-linear approximation and assumed irregularities that it depended only on one coordinate such as slab turbulence. The charged particles are scattered back and forth and move along the magnetic field lines. After that the other studies of particle scattering in a fully three-dimensional turbulent magnetic field system show that the cross-field diffusion should be occurred (Giacalone & Jokipii, 1994) which the reduced dimensionality to the slab field model cannot give this characteristic. Whenever the charged particles are in electromagnetic field with at least one ignorable coordinate, they are tied forever to the magnetic field (Jones, Jokipii & Matthaeus, 1998). Moreover, the charged particles cannot be under any circumstances to stray more than about a gyro-radius normal to the field line on which it started and it is possible that due to drift or some other mechanism. The particle is accelerated to a high energy, so that its gyro-radius becomes large (Jokipii, Kota & Giacalone, 1993). If the charged particles released at the turbulent magnetic field with a weak transverse structure, subdiffusion is a long-lived state and mostly likely permanent state. For magnetic turbulence with strong transverse structure, a regime of second diffusion is recovered for a long time (Qin et al., 2002). Furthermore, a strong two-dimensional field can inhibit the random walk of field lines due to a slab field component. The field lines are trapped near the center of the Gaussian and rapidly diffuse with the slab rate only at a radial distance $r \geq \sigma$. We explain the suppression

of the field line diffusion inside the two-dimensional island by a quasi-linear theory (Chuychai, Ruffolo, Matthaeus & Rowlands, 2005).

The numerical experiments of the charged particles in simple turbulence magnetic field, the charged test particles can be temporarily trapped in flux tubes and escape due to random turbulent perturbations in the magnetic field. The results are calculated in order to relationship of the charged particles in turbulent magnetic field by using the average of the squared perpendicular displacement and a running diffusion coefficient of the particles at time. When they are plotted in log-log scale, the behaviors of the charged particles at each range are divided into 4 regimes. Firstly, the range has slope >0 but <1.0 , this range is called as subdiffusion regime. Secondly, the range has slope ≈ 1.0 , this range is called as diffusion regime. Thirdly, the range has slope >1.0 but <2.0 , this range is called as superdiffusion regime. Finally, the range has slope ≈ 2.0 , this range is called as free streaming regime (Tooprakai, Chuychai, Minnie, Ruffolo, Bieber & Matthaeus, 2007).

2.2 Two-component magnetic field model

Two component model or 2D+slab model was developing by the observations that solar wind fluctuations are concentrated at nearly parallel and nearly perpendicular wave numbers (Matthaeus et al., 1990). For two-dimensional (2D) turbulence, the fluctuation is perpendicular to the mean field and this component is motivated by laboratory experiments. The slab component is motivated by Alfvénic wave (Bittencourt, 2004) in solar wind. The two-component model provides a good explanation of the parallel transport of SEPs (Bieber et al., 1996).

The magnetic field turbulence in 2D+slab model which is composed of the mean field and fluctuations can be written as

$$\vec{B} = \vec{B}_0 + \vec{b}(x, y, z), \quad (2.1)$$

where \vec{B}_0 is a constant mean field in z direction and \vec{b} is the transverse fluctuation perpendicular to the mean field. The transverse fluctuation can be divided into two parts which are slab and 2D components. The slab component (\vec{b}^{slab}) depends only on z

coordinate as shown in Figure 2.2 and the 2D component (\vec{b}^{2D}) depends only on the x and y coordinates as shown in Figure 2.3. Therefore, we can write the fluctuation as

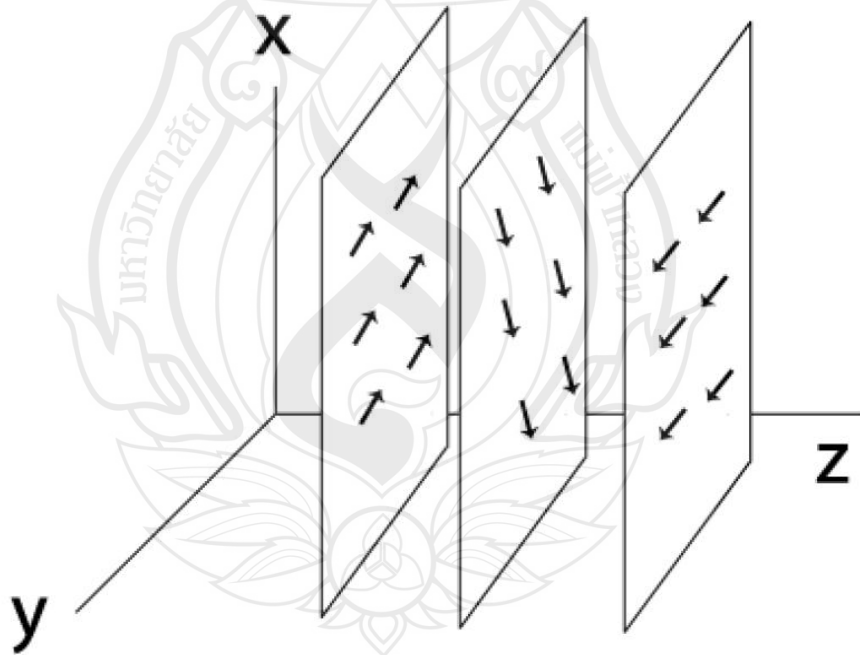
$$\vec{b}(x,y,z) = \vec{b}^{2D}(x,y) + \vec{b}^{slab}(z). \quad (2.2)$$

For the 2D component, we can generally write

$$\vec{b}^{2D}(x,y) = \vec{\nabla} \times [a(x,y)\hat{z}], \quad (2.3)$$

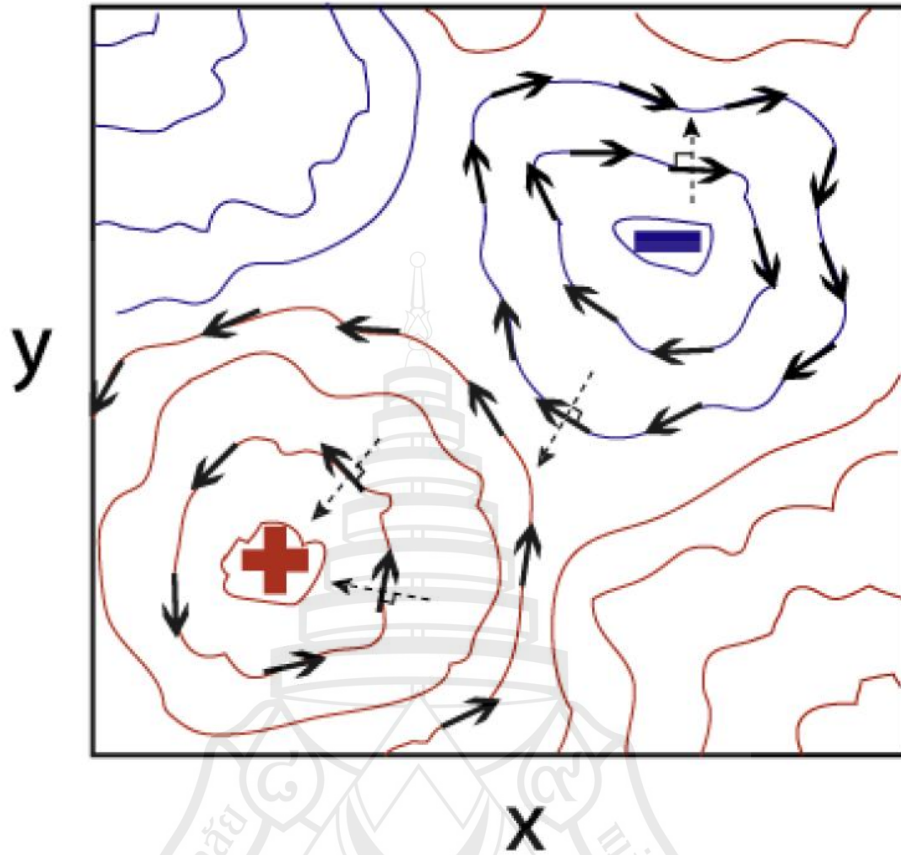
where $a\hat{z}$ is a vector potential for the 2D component and $a(x,y)$ can be called the potential function (Ruffolo, Matthaeus & Chuychai, 2003). The total magnetic field for the two-component model includes the mean field, slab and 2D field, so we write again the total magnetic field,

$$\vec{B}(x,y,z) = B_0\hat{z} + [b_x^{2D}(x,y) + b_x^{slab}(z)]\hat{x} + [b_y^{2D}(x,y) + b_y^{slab}(z)]\hat{y}. \quad (2.4)$$



Source Piyanate Chuychai (2004).

Figure 2.2 Illustration of the slab fluctuation and the arrows demonstrate the slab fluctuation \vec{b}^{slab} .



Source Piyanate Chuychai (2004).

Figure 2.3 Illustration of the 2D fluctuation. The solid arrows show the 2D field (\vec{b}^{2D}) and dashed arrows show examples of the directions of $\vec{\nabla}a(x, y)$. For a positive potential function, the 2D field is in a counter-clockwise direction, while a 2D field having a negative potential function is in the clockwise direction.

In this work, we explore the charged particles moving in two cases of magnetic field. One is the 2D+slab turbulence which both of 2D and slab fields are turbulent. In this case, we will specify the power spectrum for both 2D and slab magnetic field as Kolmogorov spectrum (see more explanation in subsection 2.3 and

2.4). Another one is a simple case which is 2D Gaussian field + slab turbulence. For the simple case, we model 2D field as a Gaussian function while the slab field is turbulent (Chuychai et al., 2005; Tooprakai et al., 2007). That would provide us more understanding about the mechanism of the motion of the charged particles when we vary the initial pitch angles. The potential function for simple 2D case can be written as

$$a(r) = A_0 \exp\left(-\frac{r^2}{2\sigma^2}\right), \quad (2.5)$$

where A_0 is the maximum value at the center of the island, σ represents the half-width of the Gaussian, and r is measured from the center of island. The contours of $a(x, y)$ in this model are circles as shown in Figure 2.4.

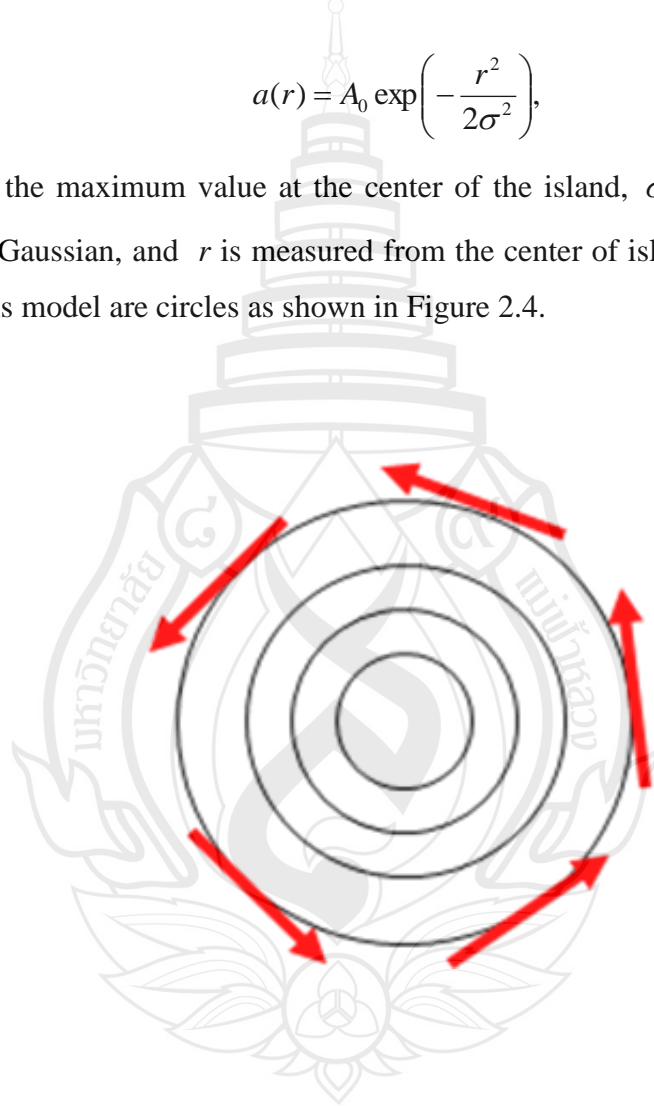


Figure 2.4 Illustration of the contours of Gaussian potential function and the arrows demonstrate the 2D field.

From $\vec{B} = \vec{\nabla} \times \vec{A}$, we can write

$$\vec{b}^{2D}(r) = \frac{ra(r)}{\sigma^2} \hat{\theta}, \quad (2.6)$$

where $\hat{\theta}$ is the unit vector associated with the angular coordinate in a cylindrical coordinate system defined by the flux tube axis and $b^{2D}(r)$ has a maximum value at $r = \sigma$. To find the location that has an extreme value of $b^{2D}(r)$, we compute the derivative of the component in equation (2.6) and set it equal to zero. Then it becomes

$$\frac{db^{2D}(r)}{dr} = \frac{d}{dr} \left[\frac{ra(r)}{\sigma^2} \right] = 0.$$

We substitute $a(r) = A_0 \exp\left(-\frac{r^2}{2\sigma^2}\right)$ into the above equation to obtain

$$\begin{aligned} \frac{d}{dr} \left[\frac{rA_0 e^{-\frac{r^2}{2\sigma^2}}}{\sigma^2} \right] &= 0 \\ -\frac{r^2}{\sigma^2} \frac{A_0 e^{-\frac{r^2}{2\sigma^2}}}{\sigma^2} + \frac{A_0 e^{-\frac{r^2}{2\sigma^2}}}{\sigma^2} &= 0 \\ \frac{A_0 e^{-\frac{r^2}{2\sigma^2}}}{\sigma^2} \left[1 - \frac{r^2}{\sigma^2} \right] &= 0. \end{aligned} \quad (2.7)$$

After that

$$\begin{aligned} \left[1 - \frac{r^2}{\sigma^2} \right] &= 0 \\ r^2 &= \sigma^2 \text{ so } r = \sigma. \end{aligned}$$

We found that the $b^{2D}(r)$ have a maximum or minimum value at $r = \sigma$, thus we find the derivative of equation (2.7) again:

$$\begin{aligned} \left[-r^2 \left(\frac{-2r}{2\sigma^2} \right) \right] \frac{A_0 e^{-\frac{r^2}{2\sigma^2}}}{\sigma^4} - \frac{2rA_0 e^{-\frac{r^2}{2\sigma^2}}}{\sigma^4} - \frac{2r}{2\sigma^2} \frac{A_0 e^{-\frac{r^2}{2\sigma^2}}}{\sigma^2} &= 0 \\ \frac{r^3 A_0 e^{-\frac{r^2}{2\sigma^2}}}{\sigma^6} - \frac{3rA_0 e^{-\frac{r^2}{2\sigma^2}}}{\sigma^4} &= 0, \end{aligned} \quad (2.8)$$

and we substitute $r = \sigma$ into equation (2.8),

$$\begin{aligned}
\frac{\sigma^3 A_0 e^{\frac{\sigma^2}{2\sigma^2}}}{\sigma^6} - \frac{3\sigma A_0 e^{\frac{\sigma^2}{2\sigma^2}}}{\sigma^4} &= 0 \\
\frac{A_0 e^{\frac{1}{2}}}{\sigma^3} - \frac{3A_0 e^{\frac{1}{2}}}{\sigma^3} &= 0 \\
-\frac{2A_0 e^{\frac{1}{2}}}{\sigma^3} &< 0.
\end{aligned} \tag{2.9}$$

From equation (2.9), we know that the $b^{2D}(r)$ have a maximum value at $r = \sigma$.

2.3 Characteristics of turbulence and its power spectrum

Turbulence is phenomena that it can occur in nature and we can see that such as the cloud in the sky, smoke from the car, as well as the plasma in the space. The turbulence is one type of fluid flow. The important for characteristic of turbulence is random walk and diffusivity, so we cannot predict the direction of turbulent flow.

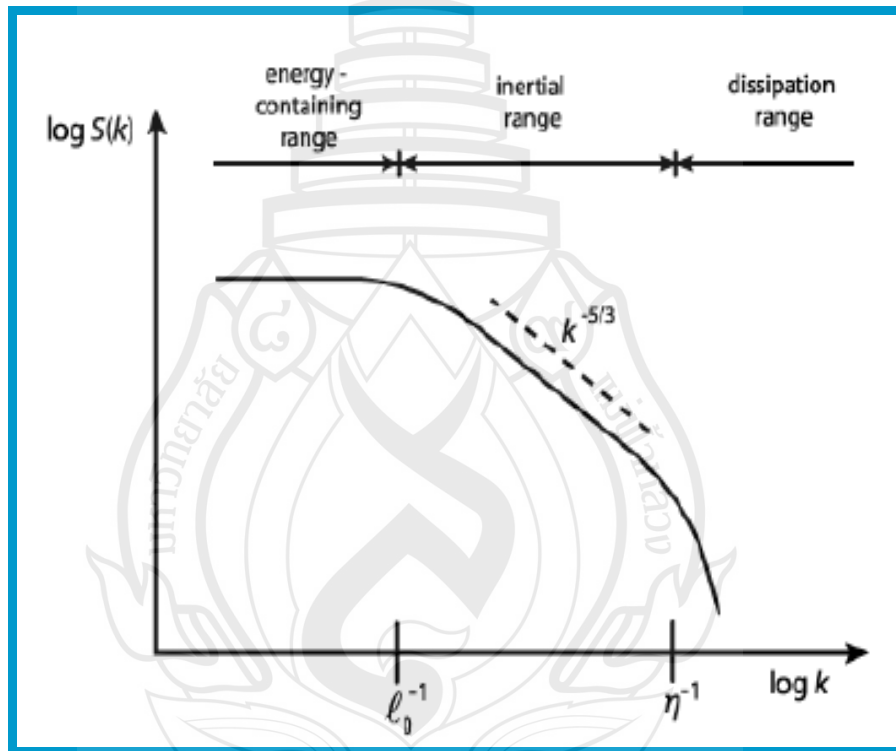
One important characteristic of turbulence is the shape of power spectrum in inertial range could obey Kolmogorov spectrum. The theory about this comes from the largest scales to smallest scales in the turbulent flow. The first introduced by Richardson (1922). This idea of Richardson has been again considered and greatly developed by Kolmogorov (1941). In the important hypothesis for turbulence given by Kolmogorov is that in every turbulent flow the statistics of the motion of scale ℓ in the range called "inertial range", $\ell_0 \gg \ell \gg \eta$ where ℓ_0 is a typical length scale of the large eddies and η is Kolmogorov microscale, have a universal form, which can be determined by the rate of energy transfer per unit mass (ε). We consider the spectrum in the inertial range. We can write the average of energy per unit mass by

$$\bar{u}^2 = \int_0^\infty S(k) dk, \tag{2.10}$$

where $S(k)$ is the wave number spectrum and k is the wave number. Therefore, the power spectrum of turbulence flow is mention as "Kolmogorov spectrum" (Kolmogorov, 1941). From dimensional analysis, it is found that in the inertial range

$$S(k) \propto \varepsilon^{2/3} k^{-5/3}. \quad (2.11)$$

Then the shape of the spectrum of turbulence looks like Figure 2.5. This is usually called Kolmogorov's $k^{-5/3}$ law which this theory is confirmed by many observations in the nature such as in ocean and solar wind observations (Grant, Stewart & Moilliet, 1962; Tu & Marsch, 1995). In our research, since the interplanetary magnetic field is frozen in the solar wind, the magnetic field also has the characteristic of turbulence (Goldstein, Roberts & Matthaeus, 1995).



Source Piyanate Chuychai (2004).

Figure 2.5 The spectrum of turbulence from Kolmogorov's theory.

2.4 Correlation functions and power spectrum

To describe the random field of the magnetic field turbulence, in our model we set that $\langle \vec{b} \rangle = 0$, where $\langle \rangle$ denotes the ensemble average, but it is not enough information to describe the random field. Thus we use statistical quantity tell spatial structure that is the “two-point correlation” or “correlation function” (Piyanate Chuychai, 2004). It is defined by

$$R_{ij}(\vec{x}, \vec{r}) = \langle b_i(\vec{x}) b_j(\vec{x} + \vec{r}) \rangle, \quad (2.12)$$

where i and j are x , y and z components.

The correlation function tells us how the magnetic field at two different points is correlated. That is if we obtain a high value from the correlation function, it shows that these two points are still in the same direction while a low value or nearly zero of the correlation shows a little or no relation.

Another quantities tell us about the relationship between the correlation function and power spectrum are the length scales in slab and 2D turbulence. We first evaluate the slab correlation length ℓ_c , defined by

$$\ell_c = \frac{\int_0^\infty R_{xx}^{slab}(z) dz}{R_{xx}^{slab}(z=0)}. \quad (2.13)$$

Thus model for the magnetic field turbulence be written as

$$\vec{b}(x, y, z) = \vec{b}^{2D}(x, y) + \vec{b}^{slab}(z). \quad (2.14)$$

Normally, the power spectrum is the Fourier transform of the correlation function. For example, the power spectrum for slab field can be written as

$$P_{xx}^{slab}(k_z) = \frac{1}{\sqrt{2\pi}} \int_{-\infty}^{\infty} R_{xx}^{slab}(z) \exp(ik_z z) dz. \quad (2.15)$$

Since we consider the magnetic field that is turbulent which the shape power spectrum in inertial range should be Kolmogorov spectrum. Therefore, in numerical simulation, we model the shape of power spectrum as

$$P_{xx}^{slab}(k_z) = \frac{C_1}{[1 + (k_z \ell_c)^2]^{5/6}}, \quad (2.16)$$

where C_1 is constant that can be calculated if we know the turbulence energy, k_z is magnitude of the wave vector and ℓ_z is the coherence length which is associated with $k_{0z} = 1/\ell_z$. This function gives us the shape of -5/3 power law in inertial range. For 2D turbulence, we instead specify power spectrum $A(k_x, k_y)$, which is the Fourier transform of auto correlation $\langle a(0,0)a(x,y) \rangle$, we can see that the shape of the spectrum affects the contour plot of the 2D potential function from Figure 2.6, and it can be written as

$$A(k_\perp) = \frac{C_2}{[1 + (k_\perp \ell_\perp)^2]^{7/3}}, \quad (2.17)$$

$$\vec{b}^{2D} = \vec{\nabla} \times [a(x,y)\hat{z}], \quad (2.18)$$

where $k_\perp = \sqrt{k_x^2 + k_y^2}$, C_2 is normalization constant, ℓ_\perp is characteristic scale length (Piyanate Chuychai, 2004). From equation (2.18), we can derive that the magnetic power spectrum for 2D component (P_{ii}^{2D}) is related to $A(k_x, k_y)$, as

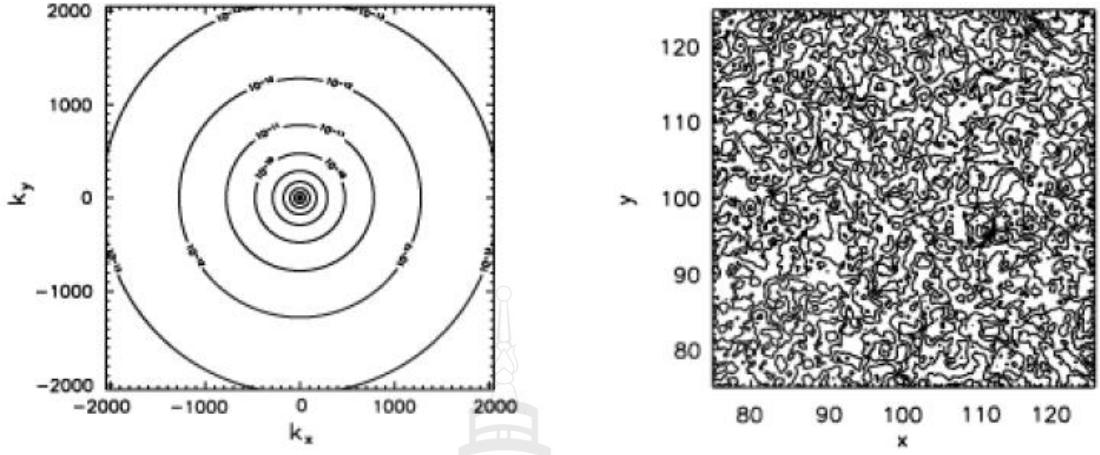
$$P_{xx}^{2D}(k_x, k_y) = k_y^2 A(k_x, k_y) \quad (2.19)$$

$$P_{yy}^{2D}(k_x, k_y) = k_x^2 A(k_x, k_y). \quad (2.20)$$

Therefore, we have

$$P_{xx}^{2D}(k_x, k_y) = \frac{k_y^2 C_2}{[1 + (k_\perp \ell_\perp)^2]^{7/3}} \quad (2.21)$$

$$P_{yy}^{2D}(k_x, k_y) = \frac{k_x^2 C_2}{[1 + (k_\perp \ell_\perp)^2]^{7/3}} \quad (2.22)$$



Source Piyanate Chuychai (2004).

Figure 2.6 Relationship between the autocorrelation $A(k_x, k_y)$ and the potential function $a(x, y)$. The scales of the $A(k_x, k_y)$ plot indicate the number of modes in (k_x, k_y) space and the contour plots of $a(x, y)$ in the right panel are only small pieces cut from the large simulation area.

2.5 Charged particles in uniform magnetic field

For the charged particle q and mass m , moving with velocity (\vec{v}) a magnetic field (\vec{B}), without electric field (\vec{E}), we can write motion equation by Newton's Lorentz force (F_B):

$$\vec{F}_B = m \frac{d\vec{v}}{dt} = q(\vec{v} \times \vec{B}). \quad (2.23)$$

For our work, we a bit adapt equation (2.23) for simulation (Tooprakai et al., 2007),

$$\frac{d\vec{v}'}{dt'} = \alpha(\vec{v}' \times \vec{B}'), \quad (2.24)$$

where $\alpha = (qB_0\tau_0)/(\gamma m_0)$ and the quantities \vec{v}' , \vec{B}' , and t' are normalized quantities which have units as scale to the speed of light (c), the mean magnetic field

(B_0), the time scale $\tau_0 = \lambda/c$, respectively. Note that $\lambda = \ell_z$ which is the slab turbulence coherence length.

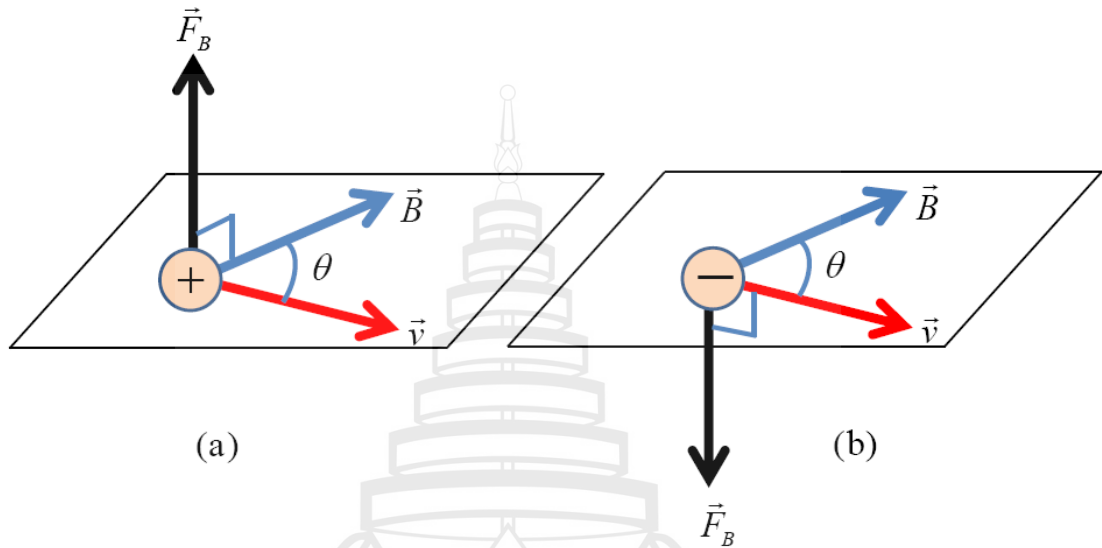


Figure 2.7 The right-hand rule for determining the direction of magnetic force (F_B).
(a) If q is positive and (b) if q is negative.

The direction of force is determined by the right-hand rule (see Figure 2.7). Usually, the velocity can be separated into two components as shown in Figure 2.8, with components parallel (\vec{v}_{\parallel}) and perpendicular (\vec{v}_{\perp}) to the magnetic field,

$$\vec{v} = \vec{v}_{\parallel} + \vec{v}_{\perp}. \quad (2.25)$$

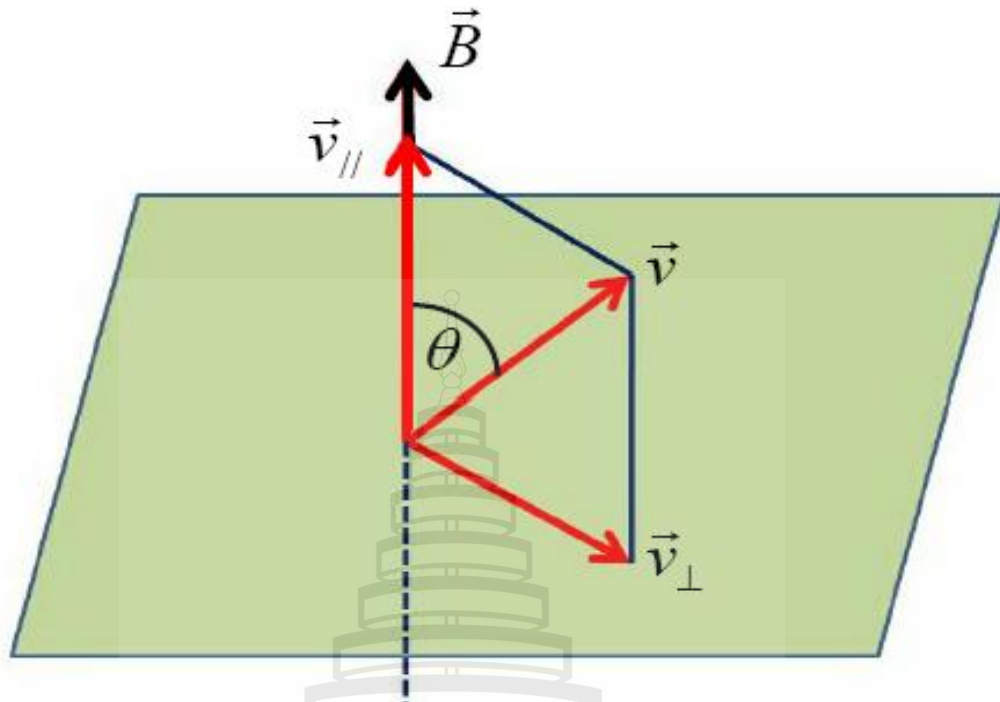


Figure 2.8 Showing component parallel ($\vec{v}_{||}$) and perpendicular (\vec{v}_{\perp}) of the velocity of charged particle in the magnetic field.

If the charged particle has velocity in component parallel ($\vec{v}_{||}$) and is equal to zero ($\vec{v}_{||} = 0$) the trajectory of the charged particle is a circular around the guiding center (GC) in the magnetic field \vec{B} with the constant speed (v_{\perp}) as illustrated in Figure 2.9. If the charged particle has velocity in component parallel is not zero ($\vec{v}_{||} \neq 0$) and also component perpendicular, the trajectory of charged particle will be a helix or spiral around guiding center in the magnetic field, such as Figure 2.10.

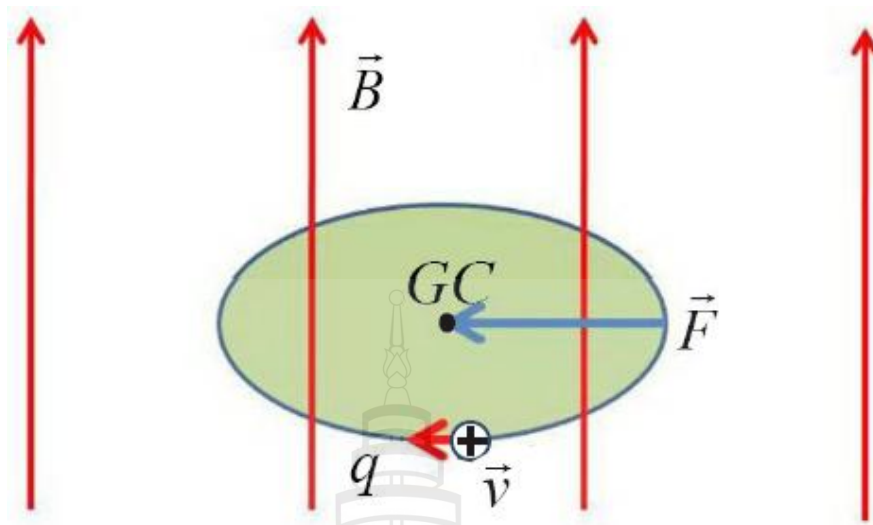


Figure 2.9 The motion of positive charged particle in a uniform magnetic field (when $\vec{v}_{\parallel} = 0$).

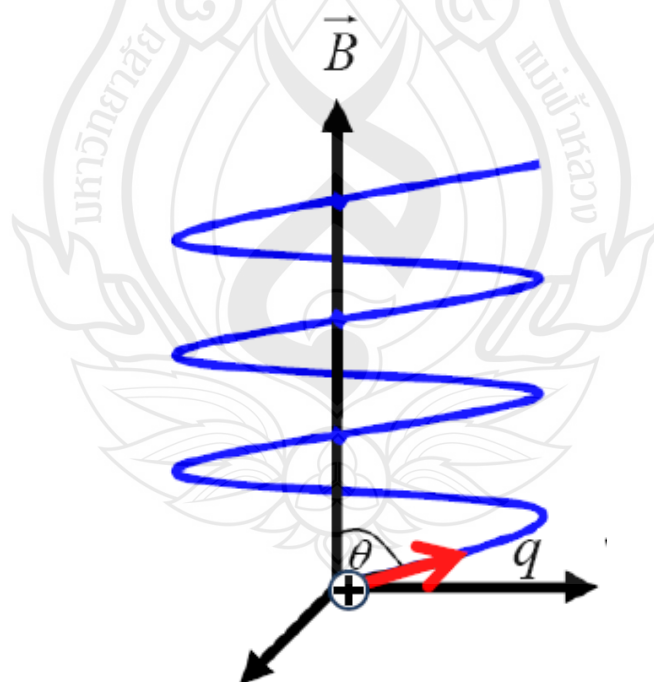


Figure 2.10 Showing the example of a trajectory of positive charged particle to the direction of magnetic field (when \vec{v}_{\parallel} and $\vec{v}_{\perp} \neq 0$).

2.6 Guiding center

When the charged particle moves in a magnetic field, it will spiral around a magnetic field line due to the magnetic force acts as a centrifugal force with gyrofrequency ω . Thus the center of particles orbit is called the “guiding center”. From Figure 2.11, determine \vec{r} , \vec{r}_{GC} and $\vec{\rho}$ as the particles vector position, guiding center’s vector position and gyration vector. The equation for these three vectors is defined as

$$\vec{r}_{GC} = \vec{r} - \vec{\rho}. \quad (2.26)$$

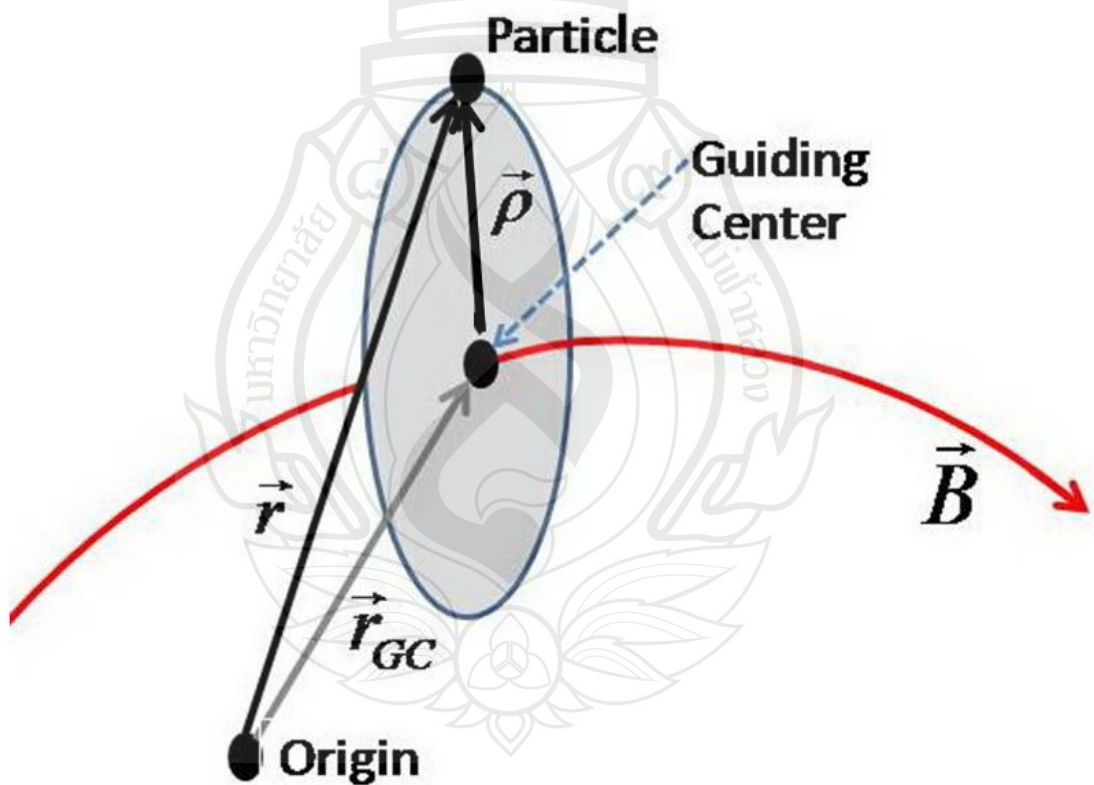


Figure 2.11 Illustration of a particle orbit, magnetic field line and guiding center.

If we consider centrifugal force of magnetic field to charged particle and Newton’s Lorentz force, the equation of the relation between these two forces is

$$\begin{aligned}\vec{F}_c &= \vec{F}_m \\ \frac{-\gamma m v^2}{\rho} \hat{\rho} &= q \vec{v} \times \vec{B},\end{aligned}\tag{2.27}$$

where $v = \omega \rho$ and rest mass of proton m , it be written as

$$\gamma m \omega^2 \rho \hat{\rho} = -q \vec{v} \times \vec{B},\tag{2.28}$$

where $\omega = |q|B/(\gamma m)$ is gyrofrequency and $\vec{P} = \gamma m \vec{v}$ is the momentum of the particle.

Thus we have

$$\rho \hat{\rho} = -\frac{\vec{P} \times \vec{B}}{q B^2} \quad \text{or}\tag{2.29}$$

$$\rho \hat{\rho} = \frac{\vec{B} \times \vec{P}}{q B^2}.\tag{2.30}$$

The radius of gyration is $\rho = m v_{\perp} / (|q|B)$, when v_{\perp} is the velocity of charged particle perpendicular to the magnetic field.

2.7 Pitch angles

The angle between the magnetic field \vec{B} and the direction of the charged particle velocity \vec{v} is called the pitch angle θ (Bittencourt, 2004) as shown in Figure 2.8. Since the velocity in parallel component to magnetic field is $v_{\parallel} = v \cos \theta$ and the velocity in perpendicular component to magnetic field is $v_{\perp} = v \sin \theta$, the pitch angle is given by

$$\theta = \tan^{-1} \left(\frac{v_{\perp}}{v_{\parallel}} \right).\tag{2.31}$$

Figure 2.12 presents the examples of trajectories of the particles in different pitch angles.

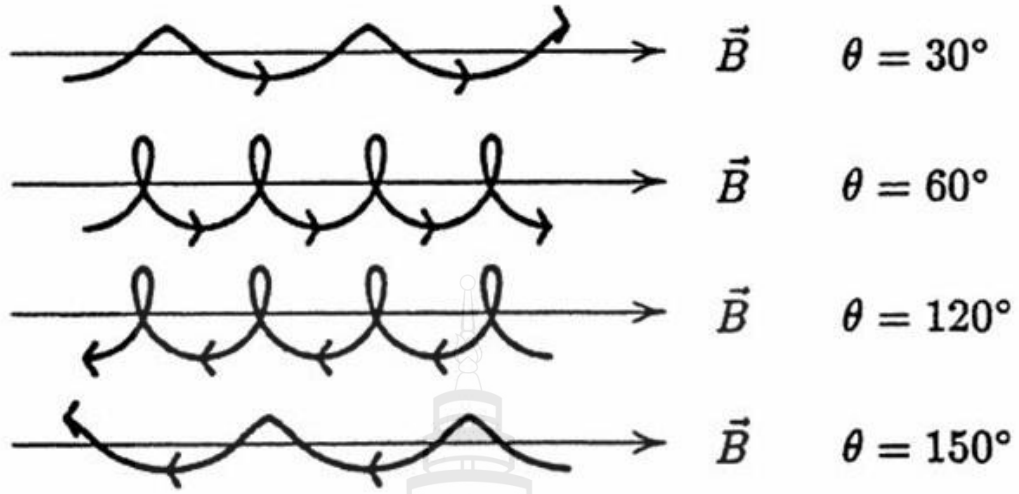


Figure 2.12 The example of trajectory of charged particle at each pitch angle.

Moreover, if the pitch angle is angle between charged particle and magnetic field, it written as

$$\vec{B} \cdot \vec{v} = |\vec{B}| |\vec{v}| \cos \theta. \quad (2.32)$$

Then we define $\mu \equiv \cos \theta$, the equation becomes

$$\vec{B} \cdot \vec{v} = |\vec{B}| |\vec{v}| \mu. \quad (2.33)$$

The cosine of the pitch angle or μ is important for this work and see the next chapter for more detail.

2.8 Charged particles in non-uniform magnetic field

When the charged particle moves in constant magnetic field, we can analytically calculate trajectory of it and also find the radius of trajectory of charged particle by using Larmor radius method. In our work, the magnetic field in interplanetary space is turbulent and it is difficult to solve and obtain the analytic solution of charged particle motion. Thus, to analyze the charged particle motion in non-uniform magnetic field, we can approximate the trajectories of charged particles

in magnetic field by numerically solving Newton Lorentz equation and then find guiding center of them. The guiding center is a great utility for studying the separation of charged particles and their corresponding magnetic field line. So it is easy to study the separation between trajectory of charged particles and guiding center, if we focus on the guiding center motion. We found that it drifts across magnetic field line due to the gradient drift and curvature drifts.

If the motion of the guiding center is perpendicular to a magnetic field line, it is called drift motion. From Figure 2.11, define \vec{r} , \vec{r}_{GC} , and $\vec{\rho}$ as the particle's vector position, guiding center's vector position, and gyration vector respectively. Then the velocity of the guiding center (\vec{v}_{GC}) can be calculated by differentiating equation (2.26),

$$\vec{v}_{GC} = \frac{d\vec{r}_{GC}}{dt} = \frac{d\vec{r}}{dt} - \frac{d\vec{\rho}}{dt}. \quad (2.34)$$

If there is an additional, non magnetic force \vec{F}_{add} acting on them, then the equation of motion should be

$$\frac{d\vec{P}}{dt} = q\vec{v} \times \vec{B} + \vec{F}_{add}. \quad (2.35)$$

If $\frac{d\vec{r}}{dt}$ is the particle velocity (\vec{v}), the formula for the guiding center velocity is

$$\begin{aligned} \vec{v}_{GC} &= \frac{d\vec{r}}{dt} + \frac{d}{dt} \left(\frac{\vec{P} \times \vec{B}}{qB^2} \right) \\ \vec{v}_{GC} &= \vec{v} + \frac{1}{qB^2} \frac{d\vec{P}}{dt} \times \vec{B}. \end{aligned} \quad (2.36)$$

Replace $\frac{d\vec{P}}{dt}$ from equation (2.35) into equation (2.36), we obtain

$$\vec{v}_{GC} = \vec{v} + \frac{1}{qB^2} (q\vec{v} \times \vec{B} + \vec{F}_{add}) \times \vec{B}, \quad (2.37)$$

and substitute $(\vec{v} \times \vec{B}) \times \vec{B} = -\vec{v}_{\perp} B^2$ and $\vec{v} - \vec{v}_{\perp} = v_{\parallel} \vec{B} / B$ in equation (2.37), the equation of the guiding center velocity is

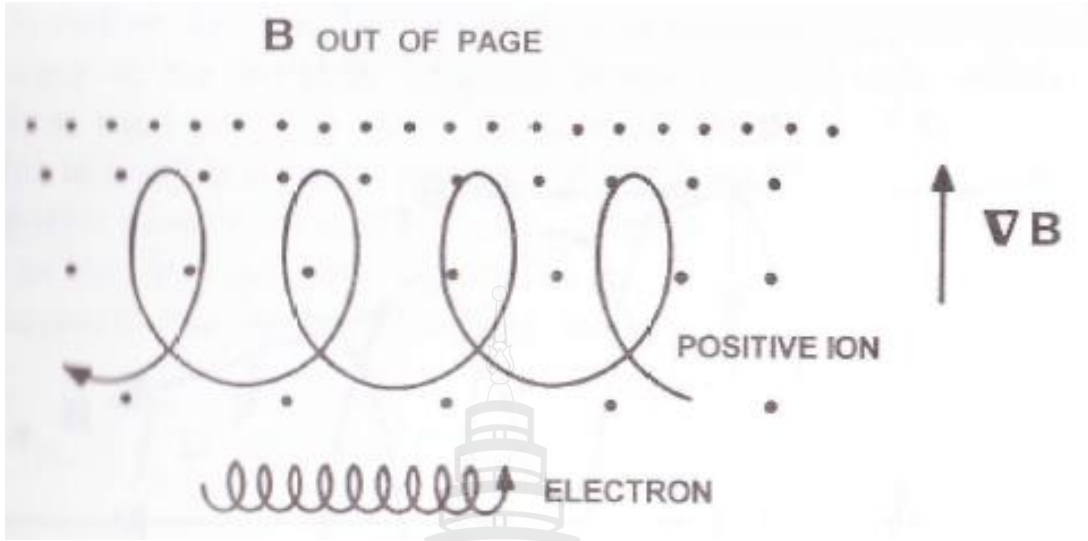
$$\vec{v}_{GC} = v_{\parallel} \frac{\vec{B}}{B} + \frac{\vec{F}_{add} \times \vec{B}}{qB^2}. \quad (2.38)$$

The upper equation shows that the additional force results in a drift velocity perpendicular to the magnetic field. Thus if the charged particle travels in a uniform magnetic field, it does not have an additional force, the guiding center will move parallel to the magnetic field along with the parallel component of the particle velocity.

However, the magnetic field in interplanetary space is not uniform. Since the characteristic of magnetic field lines are curvature and gradient, these give more effect to the drift motion of the guiding center and it will be explained in next subsection.

2.8.1 Gradient drift

When the charged particle gyrates around a magnetic field line and the position of the guiding center of charged particle is at its magnetic field line for uniform magnetic field. The positive charges spiral in the clockwise direction when magnetic field line pointing toward the observer while the electrons spiral in the counterclockwise direction, as shown in Figure 2.13. When the particle is in non-uniform magnetic field, it experiences the difference of intensity magnetic field. For the stronger magnetic field, the radius of particle's trajectory is small, while the weaker field gives a larger radius. Due to the change of magnetic field intensity, the guiding center of the charged particle drifts from their magnetic field line which we call "gradient drift" (\vec{v}_G). Moreover, it is perpendicular to \vec{B} and to the magnetic field gradient (∇B) and its direction depends on the charged sign.



Source Bittencourt (2004).

Figure 2.13 Charged particle drift due to magnetic field gradient.

Consider the magnetic field intensity at the particle's position can be expanded by using a Taylor expansion, to find the equation of the gradient drift,

$$\vec{B}(r) = \vec{B}_0 + (\vec{\rho} \cdot \nabla) \vec{B} + \dots, \quad (2.39)$$

where \vec{B}_0 is the magnetic field at the guiding center and $\vec{\rho}$ is gyration vector or the Larmor vector from the guiding center to the position of the particle. From Newton's Lorentz force will be $q\vec{v} \times (\vec{B}_0 + (\vec{\rho} \cdot \nabla) \vec{B} + \dots)$, we will consider the first order term $(\vec{\rho} \cdot \nabla) \vec{B}$, there is additional force that corresponds to the term $q\vec{v} \times (\vec{\rho} \cdot \nabla) \vec{B}$. Because Larmor vector is rotating, so the force is not constant, the additional force is considered by using average over a gyration orbit,

$$\vec{F}_{add} = \langle q\vec{v} \times (\vec{\rho} \cdot \nabla) \vec{B} \rangle. \quad (2.40)$$

In general term, it be written as

$$\vec{F}_{add} = -\frac{qv_{\perp}^2}{2\omega_c} \nabla B, \quad (2.41)$$

the relativistic gyrofrequency is $\omega_c = qB/(\gamma m)$ (Watcharawuth Krittinatham, 2010). Thus the drift velocity of guiding center due to the gradient of the magnetic field is

$$\vec{v}_G = \frac{v_\perp^2}{2\omega_c} \frac{\vec{B} \times \nabla \vec{B}}{B^2}. \quad (2.42)$$

2.8.2 Curvature drift

In the interplanetary space, the magnetic field lines have both gradient and curvature. When a charged particles spiral around the magnetic field line, they will move along the field line with a constant angular velocity ($\omega_c = v/\rho$), the guiding center have a centrifugal acceleration due to the field curvature as $v_\parallel^2 \vec{R}_c / R_c^2$, where R_c is the field line's radius of curvature, as shown in Figure 2.14. Due to the curvature of magnetic field, the moving charged particle has acceleration relate to the field line curvature, so equation of motion is

$$\vec{F}_{curv} = mv_\parallel^2 \vec{R}_c / R_c^2. \quad (2.43)$$

This can be applied from an effective electric field, and it can be rewritten as

$$\vec{E}_{eff} = \frac{mv_\parallel^2}{q} \frac{\vec{R}_c}{R_c^2}. \quad (2.44)$$

In uniform electric and magnetic fields, the charged particle will experience an electric force $q\vec{E}_{eff}$, so the drift velocity is

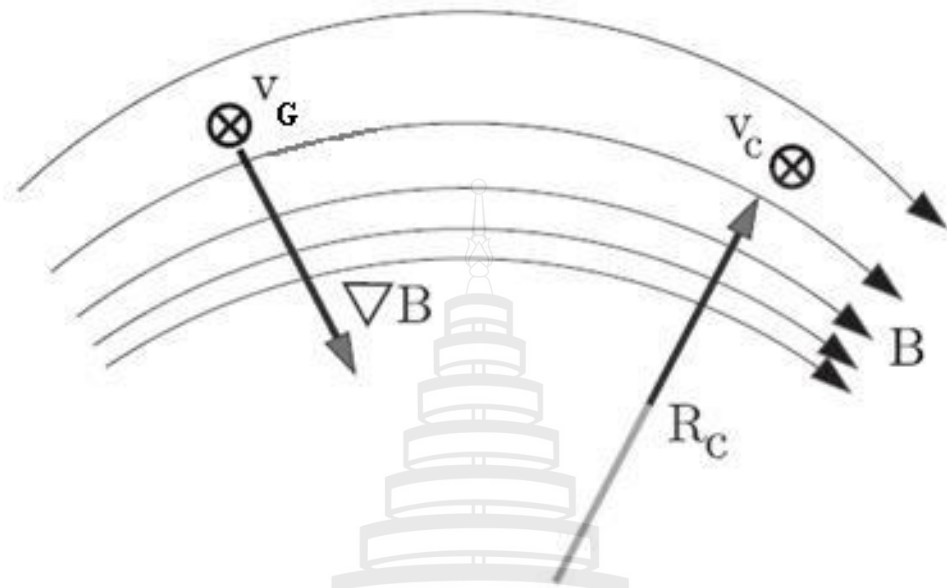
$$\vec{v}_E = \frac{\vec{E}_{eff} \times \vec{B}}{B^2}. \quad (2.45)$$

If we combine the effect of the effective electric field and the magnetic field and substitute equation (2.44) into equation (2.45), finally, we obtained the curvature drift \vec{v}_c as

$$\vec{v}_c = \frac{mv_\parallel^2}{qB^2} \frac{\vec{R}_c \times \vec{B}}{R_c^2}. \quad (2.46)$$

For relativistic particles,

$$\vec{v}_c = \frac{\gamma mv_\parallel^2}{qB^2} \frac{\vec{R}_c \times \vec{B}}{R_c^2}. \quad (2.47)$$



Source Watcharawuth Krittinatham (2010).

Figure 2.14 Illustration of direction of the particle guiding center drift velocity \bar{v}_c and \bar{v}_G due to the curvature and gradient of the magnetic field line.

CHAPTER 3

METHODOLOGY

We generate magnetic field, which is static and homogeneous by using 2D+slab model of magnetic field turbulence. To study the separation between magnetic field line and charged particle trajectories, we simulate magnetic field lines corresponding to the initial guiding centers of the charged particles by numerically solving field line equation while the trajectories of particles is traced by solving equation of motion. The initial data and parameters are setup and various cases of pitch angles are defined in order to see the effect of angles to the separation. After that the data are collected and analyzed by using new statistical approach.

3.1 Generation of magnetic field

The magnetic field in interplanetary is turbulence, thus we will simulate magnetic field that is turbulent by setting up magnetic field parameters and specify power spectrum.

In our simulations, we generate the magnetic field in the simulation box. We need to consider the effects of the simulation box, representations of turbulent field, and suitable length scale for simulated field lines. The magnetic field is generated in wave number space (k -space) before conversion to real space. We instead define the power spectrum as a function in k -space, which is the Fourier transform of the magnetic correlation function.

$$R_{ij}(\vec{r}) = \langle b_i(0)b_j(\vec{r}) \rangle. \quad (3.1)$$

The spectrum that we usually use for the magnetic turbulence is a Komolgorov spectrum over a wide range of wave numbers. The magnetic fluctuation in $b_x(x, y, z)$ and $b_y(x, y, z)$ are composed of slab and 2D turbulence as in equation (2.4). Because the slab turbulence depends only on z and the 2D turbulence depends on x and y positions, we separately generate them in k_z and (k_x, k_y) spaces, respectively. After that, the magnetic field in Fourier space is converted to position space by using an inverse fast Fourier transform as illustrated in Figure 3.1.

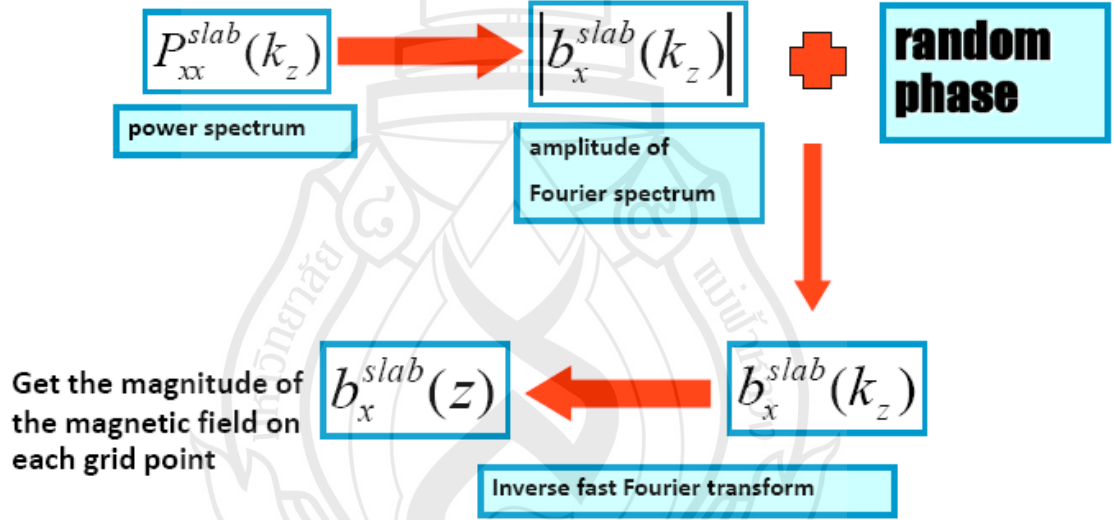


Figure 3.1 Generation of slab magnetic field.

For slab turbulence field, we set the power spectrum for simulation as

$$P_{xx}^{slab}(k_z) = P_{yy}^{slab}(k_z) = \frac{C^{slab}}{[1 + (k_z \ell_z)^2]^{5/6}}, \quad (3.2)$$

where C^{slab} is a normalization constant that depends on the slab energy and ℓ_z is the parallel coherence length. The function of the slab spectrum, it can written in k_z space are

$$b_x^{slab}(k_z) = \sqrt{P_{xx}^{slab}(k_z)} \exp[i\varphi_x(k_z)] \quad (3.3)$$

$$b_y^{slab}(k_z) = \sqrt{P_{yy}^{slab}(k_z)} \exp[i\varphi_y(k_z)], \quad (3.4)$$

where k_z is a discrete number which is $k_z = j2\pi/L_z$, for $j=1,2,3,\dots, N_z/2-1$, φ_i is a random phase number. Equations (3.3) and (3.4) are used only for $k_z > 0$. For slab turbulence, we use only one representation but we random by start initial positions along z in a large simulation box and trace the field lines or particles only less than 10% of the box size.

For 2D turbulence field, we determine the power spectrum for simulation as

$$P_{xx}^{2D}(k_x, k_y) = k_y^2 A(k_x, k_y) \quad (3.5)$$

$$P_{yy}^{2D}(k_x, k_y) = k_x^2 A(k_x, k_y), \quad (3.6)$$

where $A(k_x, k_y) = |a(k_x, k_y)|^2 / (2\pi V)$, V is the total volume and we specify the power spectrum instead of the correlation function. Thus the power spectra of the 2D turbulence can written in terms of $A(k_x, k_y)$ space as

$$b_x^{2D}(k_x, k_y) = -ik_y \sqrt{A(k_\perp)} \exp[i\varphi(k_x, k_y)] \quad (3.7)$$

$$b_y^{2D}(k_x, k_y) = ik_x \sqrt{A(k_\perp)} \exp[i\varphi(k_x, k_y)], \quad (3.8)$$

when the Fourier transform of the autocorrelation function of the vector potential as

$$A(k_\perp) = \frac{C^{2D}}{[1 + (k_\perp \ell_\perp)^2]^{7/3}}, \quad C^{2D} \text{ is a normalization constant, } \ell_\perp \text{ is perpendicular}$$

coherence lengths, $k_\perp = \sqrt{k_x^2 + k_y^2}$, $\varphi(k_x, k_y)$ is a random phase and k_x, k_y are discrete numbers. For 2D turbulence, we change representation of the magnetic field every 10 particles.

We obtain the magnitude of the magnetic field at any grid point from the simulations as in Figure 3.2. To obtain the magnetic field at any location, we use the linear interpolation for slab turbulence and bi-linear interpolation for 2D turbulence from the nearby grid points (see Appendix A for more detail).

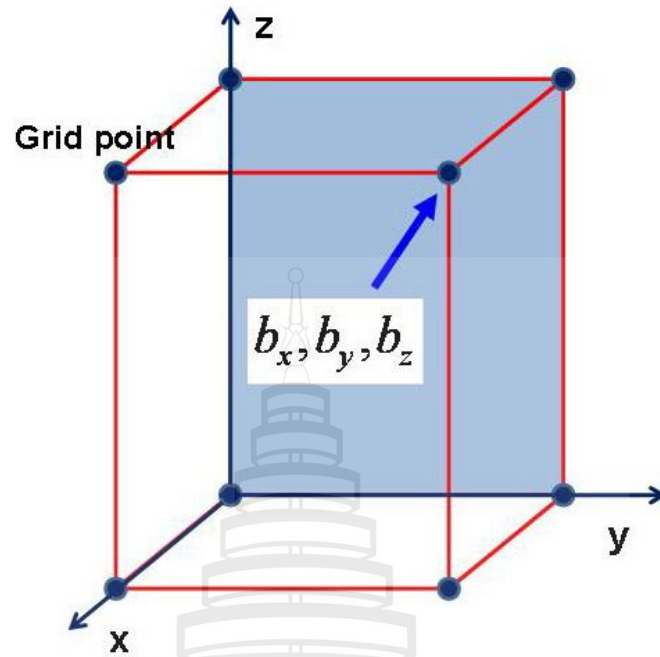


Figure 3.2 The positions of the magnetic field obtained at each grid point.

3.2 Particle simulations

We choose protons as the charged particles in this work. They are released from initial random positions and different pitch angles (see Figure 3.3). The particle positions are initially random (x,y,z) positions for the ensemble average statistics of perpendicular displacement.

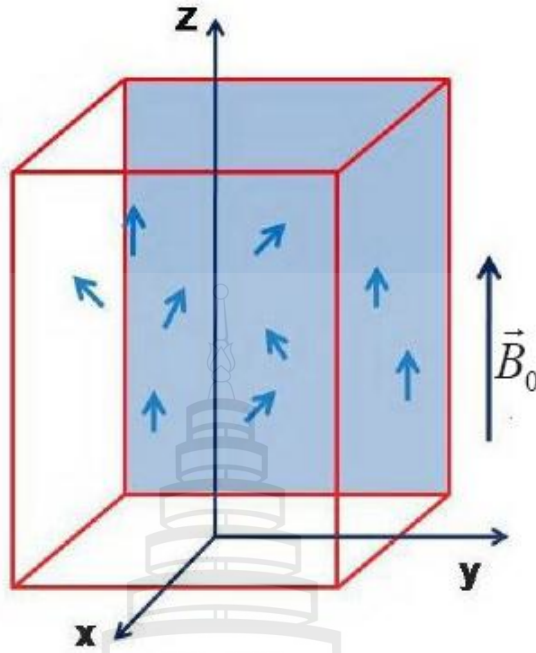


Figure 3.3 The sketch of the positions of releasing the charged particles.

We can find trajectories of the charged particles, when we know the equation of motion of the charged particles. In this work, we use Newton's Lorentz force equation to find positions of the charged particles by using fourth-order Runge-Kutta method with adaptive time stepping regulated by a fifth-order error estimate step (Press, Teukolsky, Vetterling & Flannery, 1992; Dalena, Chuychai, Mace, Greco, Qin & Matthaeus, 2012). From equation (2.24) of motion we can imply it to be

$$\frac{dv'_x}{dt'} = \alpha(v'_y b_z - v'_z b_y) \quad (3.9)$$

$$\frac{dx}{dt'} = v'_x \quad (3.10)$$

$$\frac{dv'_y}{dt'} = \alpha(v'_z b_x - v'_x b_z) \quad (3.11)$$

$$\frac{dy}{dt'} = v'_y \quad (3.12)$$

$$\frac{dv'_z}{dt'} = \alpha(v'_x b_y - v'_y b_x) \quad (3.13)$$

$$\frac{dz}{dt'} = v'_z, \quad (3.14)$$

where $\alpha = (qB_0\tau_0)/(\gamma m)$, $\vec{v}' = \vec{v}/c$, $\vec{B}' = \vec{B}/B_0$, $t' = t/\tau_0$ and $\gamma \equiv 1/\sqrt{1 - \frac{v^2}{c^2}}$ (Tooprakai et al., 2007).

3.3 Field line simulation

When we know the value of the magnetic field at each grid point, we can trace the magnetic field line that is tangent everywhere to the magnetic field (\vec{B}). The differential equation of the magnetic field line is

$$\vec{dl} \times \vec{B} = 0. \quad (3.15)$$

In Cartesian coordinates, \vec{dl} is (dx, dy, dz) and (\vec{B}) is (B_x, B_y, B_z) . From equation (3.15), it can be written as

$$\frac{dx}{B_x} = \frac{dy}{B_y} = \frac{dz}{B_z}. \quad (3.16)$$

In our model, we use $\vec{B} = B_0\hat{z} + b_x\hat{x} + b_y\hat{y}$ so we obtain

$$\frac{dx}{b_x} = \frac{dy}{b_y} = \frac{dz}{B_0}. \quad (3.17)$$

Finally, we can write the differential equation for the magnetic field line as

$$\frac{dx}{dz} = \frac{b_x(x, y, z)}{B_0} = \frac{b_x^{slab}(z) + b_x^{2D}(x, y)}{B_0} \quad (3.18)$$

$$\frac{dy}{dz} = \frac{b_y(x, y, z)}{B_0} = \frac{b_y^{slab}(z) + b_y^{2D}(x, y)}{B_0} \quad (3.19)$$

After that the differential equation of the magnetic field line is solved by using fourth-order Runge Kutta method with adaptive step size as same as we use in particle simulation to find positions of the magnetic field lines x_{FL}, y_{FL}, z_{FL} as shown in Figure 3.4.

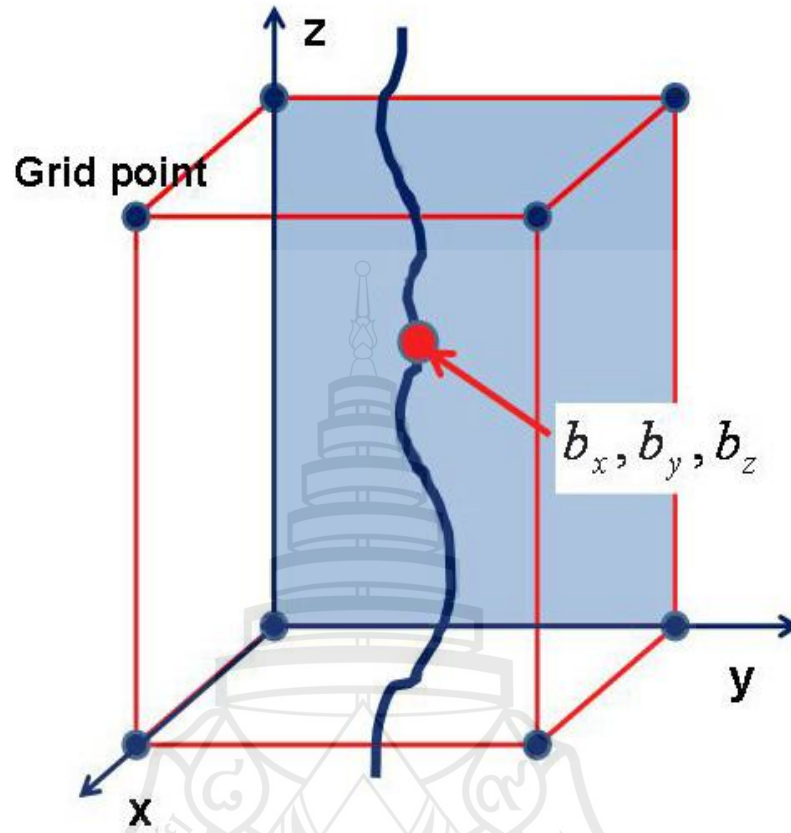


Figure 3.4 Showing the example of trajectory of the magnetic field line.

3.4 Pitch angle setup

The pitch angle is angle between magnetic vector and velocity vector. For setting initial pitch angles we use two methods to generate the initial pitch angle.

3.4.1 Setting ranges for initial pitch angle

For some case, we set ranges for initial pitch angle as 0-30 degrees, 30-60 degrees and 60-90 degrees. When the positions and velocity of the charged particles are set in simulation box by using random method, we can compute the magnetic field at any position. Then the initial pitch angles are computed by using equation (2.32),

we choose the positions and velocity of the charged particles to have initial pitch angle follow our ranges condition.

3.4.2 Fix initial pitch angle

We want to set a velocity vector with the desired pitch angle. After the positions of the charged particles are set in simulation box by using random position, we compute the magnetic field at any position of the charged particles, we convert the magnetic field vector from Cartesian coordinate to Spherical coordinate as shown in Figure 3.5.

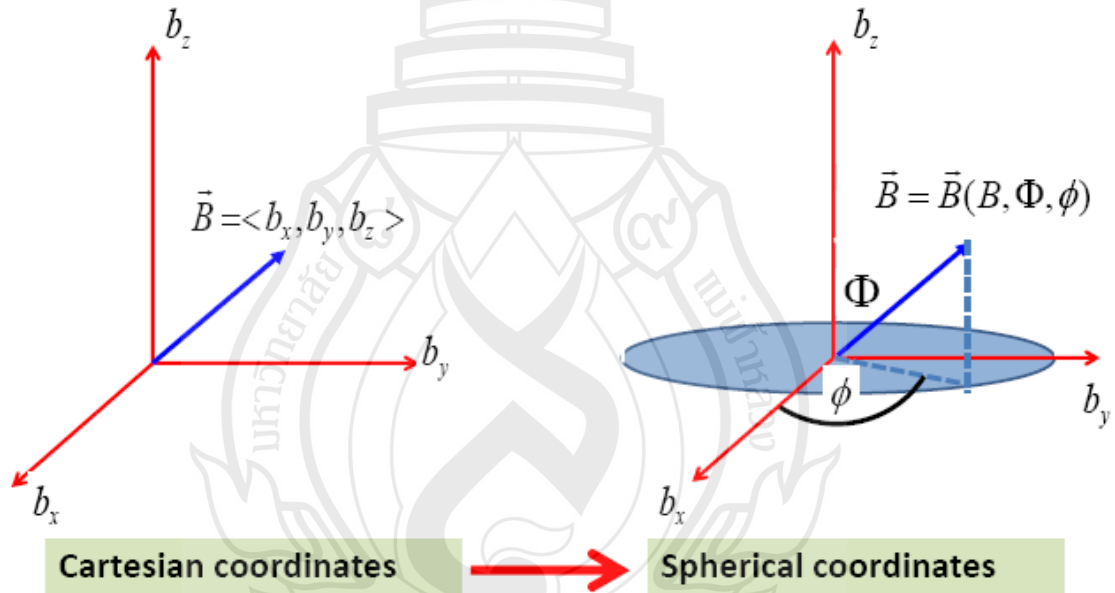


Figure 3.5 Illustration the change of magnetic field vector from Cartesian coordinate to Spherical coordinate at each position.

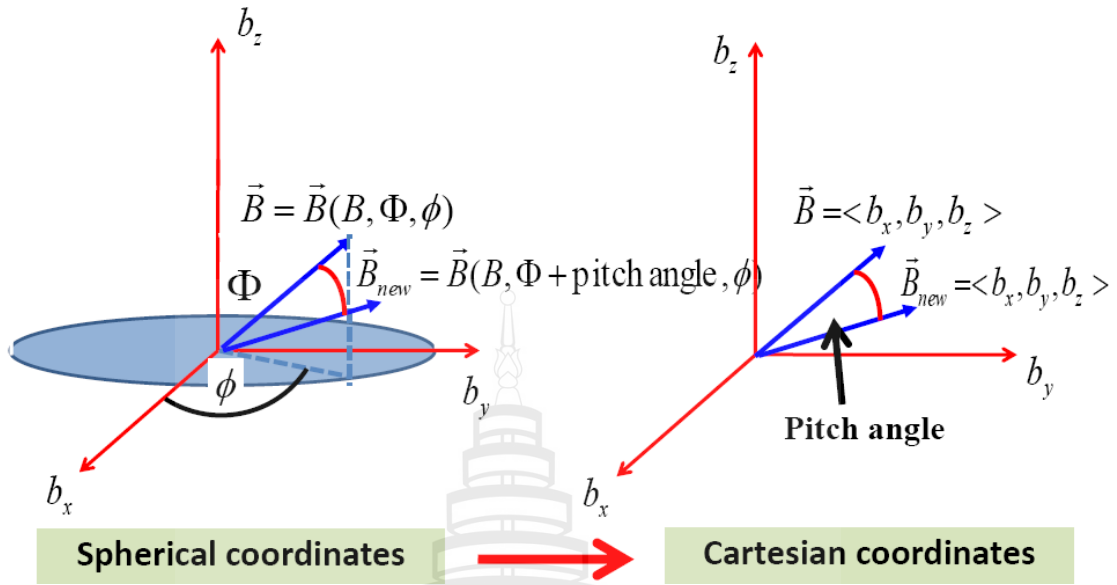


Figure 3.6 Illustration of setting a velocity vector.

Next, we add initial pitch angle such as 0, 30, 60 and 90 degrees at Φ component and after that we convert magnetic field vector from Spherical coordinate to Cartesian coordinate again as shown in Figure 3.6. When we obtained new magnetic field vector (\vec{B}_{new}), it is changed to be velocity vector by using the equation

$$\vec{B}_{new} \frac{|\vec{v}|}{|\vec{B}_{new}|} = \vec{v}, \quad (3.20)$$

where vector \vec{v} now make pitch angles with \vec{B} as we want and $|\vec{v}|$ corresponds to the particle energy.

To make the general method, we rotate velocity vector by method random β angle from 0-360 degrees around the magnetic field (\vec{B}). From the Figure 3.7 and Figure 3.8, let \vec{v}' to be a rotating vector and $\vec{v}' = \overrightarrow{OQ}$. It can be written as

$$\overrightarrow{OQ} = \overrightarrow{ON} + \overrightarrow{NR} + \overrightarrow{RQ}, \quad (3.21)$$

when $\overrightarrow{ON} = \hat{n}(\hat{n} \cdot \vec{v})$, $\overrightarrow{NR} = [\vec{v} - \hat{n}(\hat{n} \cdot \vec{v})]\cos \beta$ and $\overrightarrow{RQ} = (\vec{v} \times \hat{n})\sin \beta$. Thus the equation (3.21) it become to be

$$\vec{v}' = \hat{n}(\hat{n} \cdot \vec{v}) + [\vec{v} - \hat{n}(\hat{n} \cdot \vec{v})] \cos \beta + (\vec{v} \times \hat{n}) \sin \beta, \quad (3.22)$$

if we instead unit vector (\hat{n}) in term magnetic field (\vec{B}), the formula as

$$\begin{aligned} \vec{v}' = \frac{\vec{B}}{|\vec{B}|} (|\vec{v}| \cos \theta) + \left[\vec{v} - \frac{\vec{B}}{|\vec{B}|} (|\vec{v}| \cos \theta) \right] \cos \beta + \left[\left(\frac{v_y b_z - v_z b_y}{|\vec{B}|} \right) \sin \beta \hat{x} + \left(\frac{v_z b_x - v_x b_z}{|\vec{B}|} \right) \sin \beta \hat{y} \right. \\ \left. + \left(\frac{v_x b_y - v_y b_x}{|\vec{B}|} \right) \sin \beta \hat{z} \right]. \end{aligned} \quad (3.23)$$

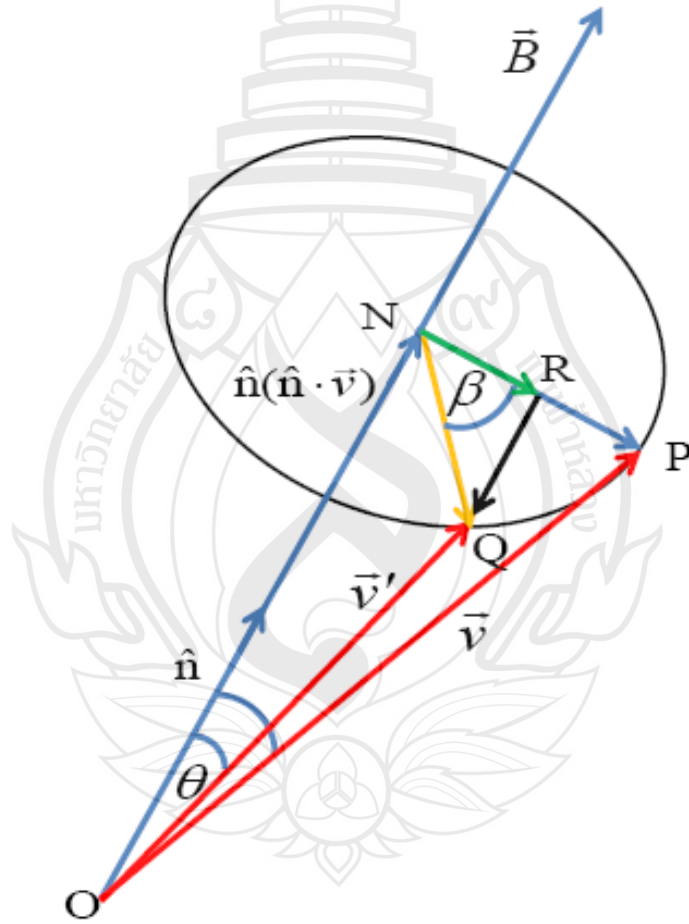


Figure 3.7 Illustration of rotating of a new velocity vector (\vec{v}') by method random β angle around the magnetic field.

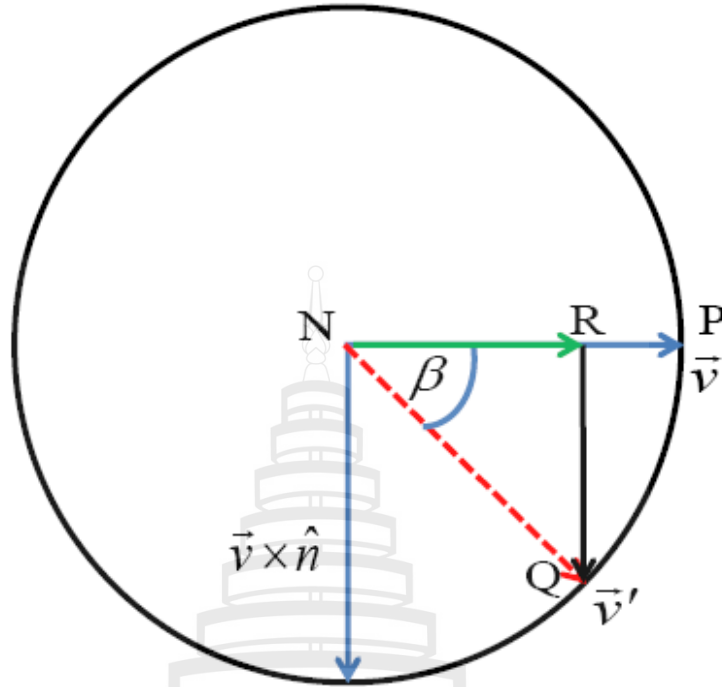


Figure 3.8 The cross section from rotation of velocity vector around the magnetic field.

The equation (3.23) is corrected if $|\vec{v} \times \hat{n}| = |\overline{NP}|$, when $|\vec{v} \times \hat{n}| = |\vec{v}||\hat{n}|\sin\theta$, $|\hat{n}| = 1$ (see Appendix B). Finally, we obtained velocity vector (\vec{v}') and magnetic field vector (\vec{B}) in the same direction and there are initial pitch angles which are follow the setting conditions.

3.5 Parameter setup

This subsection shows the parameters and initial condition for the magnetic field and the charged particles that we use in the simulations.

3.5.1 Magnetic field setup

We set these following parameters for the magnetic field.

1. $B_0 = 5 \text{ nT}$
2. $\ell_z = \lambda = 0.02 \text{ AU} = 3 \times 10^9 \text{ m}$
3. $\ell_\perp = 0.1\lambda$
4. $\tau_0 = \lambda/c \approx 10 \text{ seconds}$
5. The ratio of Gaussian 2D and slab magnetic energy in simple case as $(b_{2D}^{\max} / \delta b_{slab})^2 = 20$.
6. The ratio of 2D and slab magnetic energy in (2D+Slab) turbulence case as $(\delta b_{2D} / \delta b_{slab})^2 = 4$.

3.5.2 Initial setup for charged particles

3.5.2.1 Particle energy

We perform of particle energies as 100 MeV by specifying the magnitude of particle velocities.

3.5.2.2 Positions of protons.

1. The positions are set randomly in simulation box for 2D+slab turbulence cases.
2. For a simple case, Gaussian 2D field + slab turbulence, x and y will be randomly on a given contour of potential function ($r_0 = 0.1\lambda, 0.3\lambda, 0.5\lambda, 0.7\lambda$, and 0.9λ) while z is random in simulation box.

3.5.3 Simulation box setup

The box length and the number of grid points are

1. $L_x = L_y = 100\lambda$ and $L_z = 100,000\lambda$.
2. $N_x = N_y = 4096$ and $N_z = 2^{22} = 4,194,304$.

3.6 Procedure of simulations

3.6.1 The charged particles are released at initial positions and velocities in the magnetic field that we model with the parameter setup as we describe in above

sections. After that the program will compute trajectories of charged particles and their velocities by solving Newton Lorentz-force in equation (2.23) and then compute of the radius of curvature ($\vec{\rho}$) of charged particles for all trajectories from

$$\vec{\rho} = \frac{\vec{B} \times \vec{p}}{qB^2}, \quad (3.24)$$

where $\vec{p} = \gamma m_0 \vec{v}$ is the particle momentum. Next we find guiding centers from the radius of curvature of the particle orbits from $\vec{r}_{GC} = \vec{r} - \vec{\rho}$ (Chuychai et al., 2011, see also in Figure 3.9).

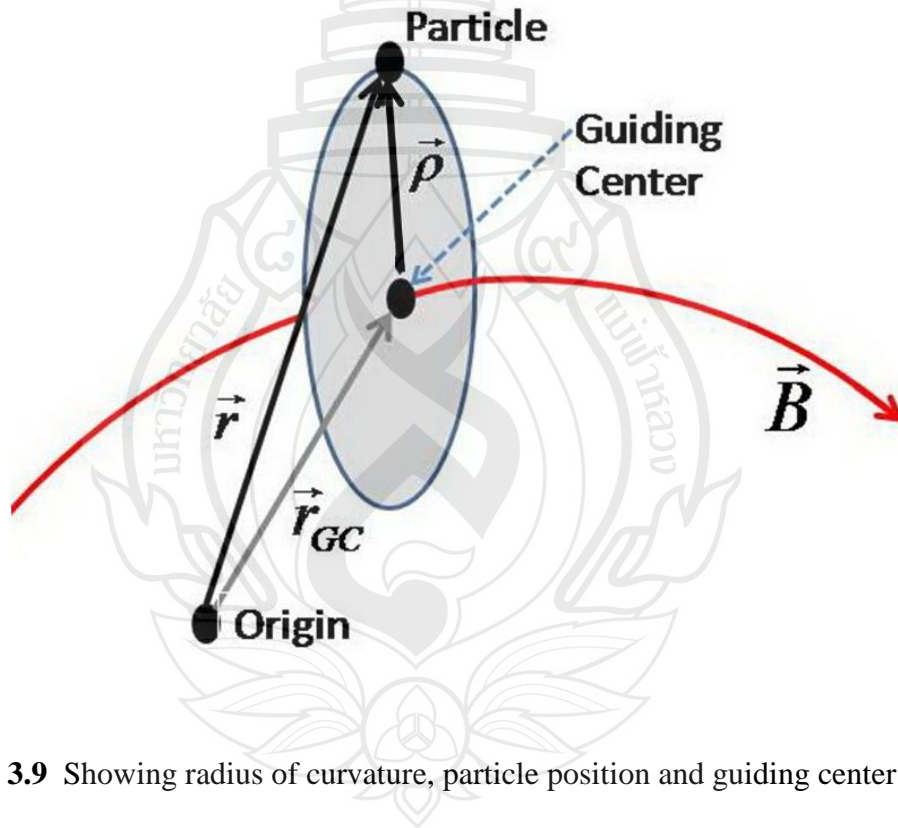


Figure 3.9 Showing radius of curvature, particle position and guiding center position.

3.6.2 In the case that the charged particles are released at all directions by using random method, so we do not know pitch angles between the charged particles and magnetic field lines. Thus we will find pitch angle (θ) before to analyze data by using equation (2.32) it can written as

$$\theta = \cos^{-1} \left[\frac{\vec{v} \cdot \vec{B}}{|\vec{v}| |\vec{B}|} \right]. \quad (3.25)$$

3.6.3 We bring the initial guiding center of each charged particle to be the initial position of magnetic field line. We find solution of magnetic field line by solving magnetic field line equation. The output will be the position x_{FL} , y_{FL} and z_{FL} of the field line trajectories that correspond to the initial guiding center of particles.

3.6.4 We analyze position of magnetic field lines and guiding centers of charged particles by finding the separation of magnetic field lines and guiding centers of charged particles at anytime for various cases of the pitch angles.

3.7 Data analysis

3.7.1 From data the pitch angle will divided into several cases before calculate separation of guiding centers and magnetic field lines such as

1. The cases that we set pitch angles range as 0-30 degree, 30-60 degree and 60-90 degree in simple 2D field+slab turbulence and 2D+slab turbulence.
2. The cases that we fix initial pitch angles as 0, 30, 60 and 90 degrees in simple 2D field+slab turbulence and 2D+slab turbulence.
3. The cases that we set pitch angle range as 0-90 degree in simple (2D+Slab) turbulence.

3.7.2 From the positions of magnetic field lines, which come from initial of the guiding centers of each charged particle, we can plot the samples of the picture between trajectories of magnetic field lines and guiding centers of charged particles similar as in the diagram. We show in Figure 3.10 from the output of simulations.

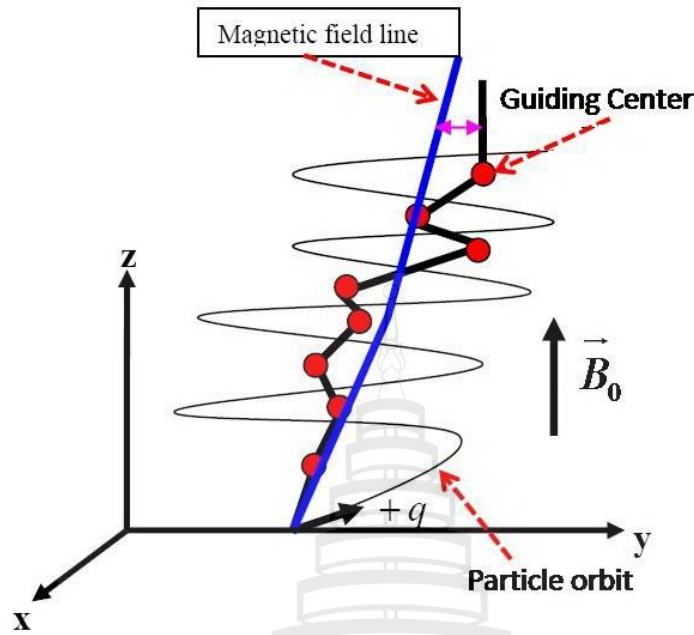


Figure 3.10 The diagram of separation between the guiding center and magnetic field line.

3.7.3 We calculate the mean squared displacement perpendicular to the mean field between guiding centers of charged particles (x_{GC}) and their corresponding magnetic field lines (x_{FL}) at anytime (Chuychai et al., 2011).

$$\langle (x_{GC}(t) - x_{FL}[z(t)])^2 \rangle, \quad (3.26)$$

where $z(t)$ is the z -coordinate of the particle guiding center at time t .

3.7.4 We find the theories or principles that can explain the results about the effects of pitch angles on the separation between charged particles and magnetic field lines.

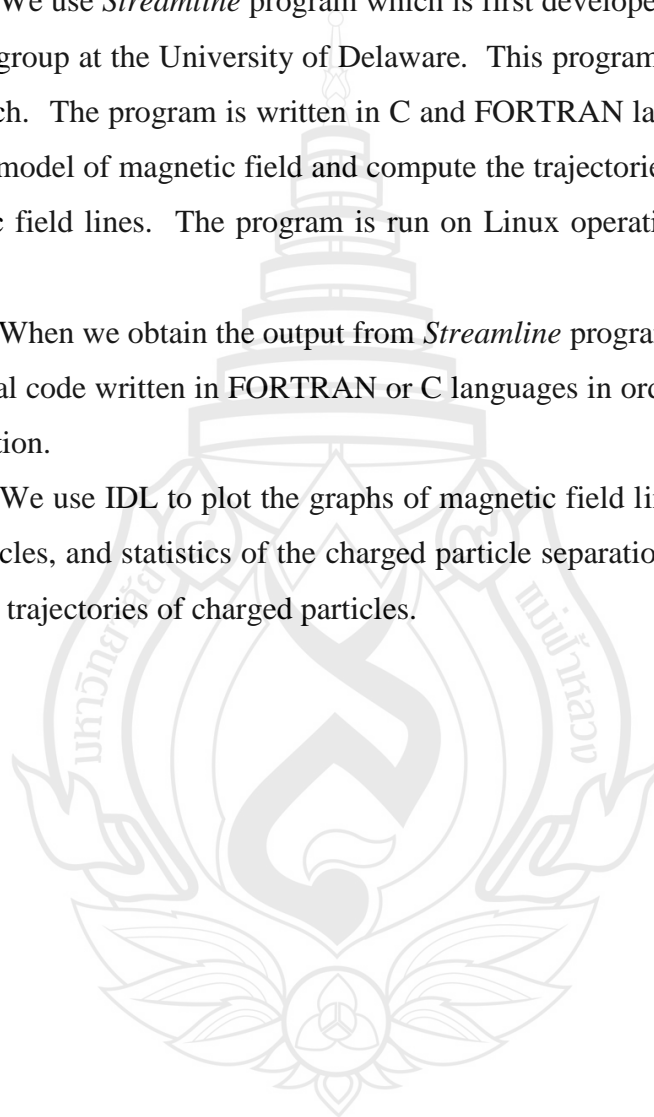
3.8 Research tools

3.8.1 The high performance of computer processing (parallel connected) has been used in this work, because it computes quickly and has high efficiency.

3.8.2 We use *Streamline* program which is first developed by Prof. William H. Matthaeus's group at the University of Delaware. This program is modified and used in our research. The program is written in C and FORTRAN languages. It is used to simulate the model of magnetic field and compute the trajectories of charged particles and magnetic field lines. The program is run on Linux operating system (Dalena et al., 2012).

3.8.3 When we obtain the output from *Streamline* program the data is analyzed by using serial code written in FORTRAN or C languages in order to see the statistics of the separation.

3.8.4 We use IDL to plot the graphs of magnetic field lines and trajectories of charged particles, and statistics of the charged particle separation from their magnetic field line and trajectories of charged particles.



CHAPTER 4

RESULTS FOR THE CHARGED PARTICLES IN SIMPLE 2D FIELD+SLAB TURBULENCE

In this chapter, we present the results of the effect of initial released radii and initial pitch angles to the separation when the particles are in Gaussian 2D field plus slab turbulence.

4.1 The effect of initial released position to the separation

The 1000 charged particles are released at random initial pitch angles from 0 to 180 degrees by using the method in section 3.2 and on various distances from the center of the 2D Gaussian island (r_0) as 0.1λ , 0.3λ , 0.5λ , 0.7λ and 0.9λ . For Gaussian function of potential function, we give the width of the Gaussian σ as 0.5λ . We define $b_{2D}^{\max} / B_0 = 1.0$ and $(b_{2D}^{\max} / \delta b_{slab})^2 = 20$ that means the 2D flux tube is very strong compared with slab turbulence. The test particles are designed to represent protons that have energy 100 MeV. In our simulations, all units of lengths are scaled with λ and the unit of the time is scaled by λ/c .

Results & discussion

The Figure 4.1 shows the example of the trajectory of the test charged particle and magnetic field line. In our work, the simulation results for 1,000 particles show that the separation behaviors between the charged particles and the corresponding field lines can be divided into several regimes as we can see in Figure 4.2. We can explain the mechanism of separation in each regime by relating to the structure of the 2D Gaussian and slab turbulent magnetic field.

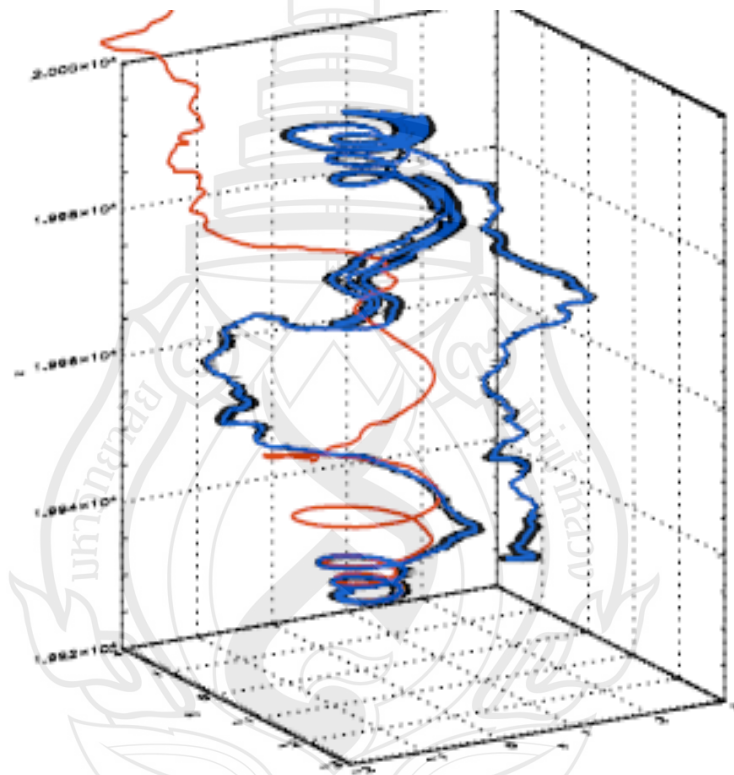


Figure 4.1 Example of the trajectory of a charged particle in our model; red line demonstrates trajectory of magnetic field line, black line and blue line demonstrate trajectories of charged particle and its guiding centers, respectively.

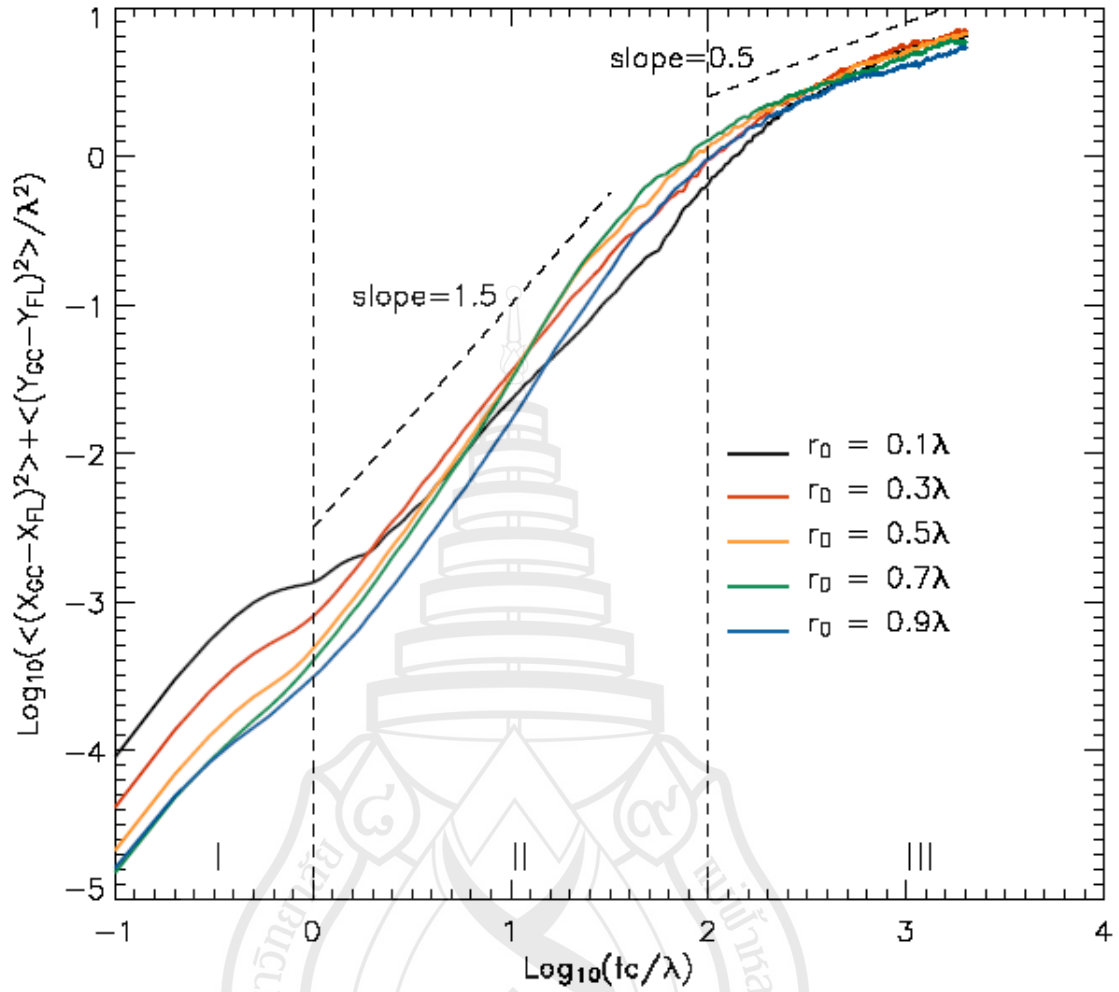


Figure 4.2 The results of the separation of charged particles and their corresponding field lines in the log-log scale.

I. At the initial times (when $tc/\lambda < 1$)

We found that the separation of the charged particles in initial time which are started at the radius of 0.1λ is highest one following by the ones started at 0.3λ and 0.5λ , respectively. For the particles started at 0.7λ and 0.9λ , the separations are very close to each other and lower than the particles started $r_0=0.5\lambda$. It seems that the separation of charged particles during this time depend on the structure of 2D field which has radius of curvature of the magnetic field and the gradient of magnetic field. The positions of 0.1λ from center of Gaussian function have the lower radius of

curvature of the magnetic field lines than the radii as 0.3λ , 0.5λ , 0.7λ and 0.9λ . The curvature is larger when the distance is far from the center. For the gradient of magnetic field, we can see from the profile of the intensity of 2D Gaussian flux can be seen in Figure 4.3. The gradient depends on the radius from the center of Gaussian 2D field. The maximum of 2D magnetic field is at the width of Gaussian function (σ) and the decrease when the radius towards to the center as well as when they go outside. Next, we compute the effect of curvature and gradient drifts due to 2D Gaussian field in order to explain the results during the beginning time. From equation (2.42) and (2.47), we plugin the Gaussian 2D magnetic field and compute the drift velocity. Then we can find that the magnitude of drift velocity of the guiding center due to the gradient and the curvature drift of the magnetic field are

$$\|\langle \vec{v}_G \rangle\| = \frac{\gamma m v^2}{3q\sigma^2 R_c} \frac{b^{2D}}{B^2} |\sigma^2 - R_c^2| \text{ and} \quad (4.1)$$

$$\|\langle \vec{v}_C \rangle\| = \frac{\gamma m v^2}{3qR_c B}. \quad (4.2)$$

Then when we consider both effects, the equation for these is

$$\|\langle \vec{v}_G \rangle + \langle \vec{v}_C \rangle\| = \frac{\gamma m v^2}{3qBR_c} \left[\left(\frac{b^{2D}(R_c)}{B\sigma^2} \right) (\sigma^2 - R_c^2) + 1 \right]. \quad (4.3)$$

After that, we insert all magnetic field parameters in our simulation into equations (4.1), (4.2), and (4.3) and make a map to see the effect of the drift for each radius from the center of Gaussian. We found that they give the shapes of drift speed like Figure 4.4. From the drift speed profile, we can see that the curvature drift has more effect than the gradient drift and it is dominated at the small radius from the center of the Gaussian function. When we combine these two effects as in equation (4.3), the particles started near the center of the Gaussian have more drift speed due to 2D field. That is why we can see the charged particles have high separation of the charged particles when they are released at the small radius as shown in Figure 4.2. Moreover, from the profile in Figure 4.4, the effect of the drift for the particles started at 0.7λ and 0.9λ is slightly different which we can also see this effect in Figure 4.2.

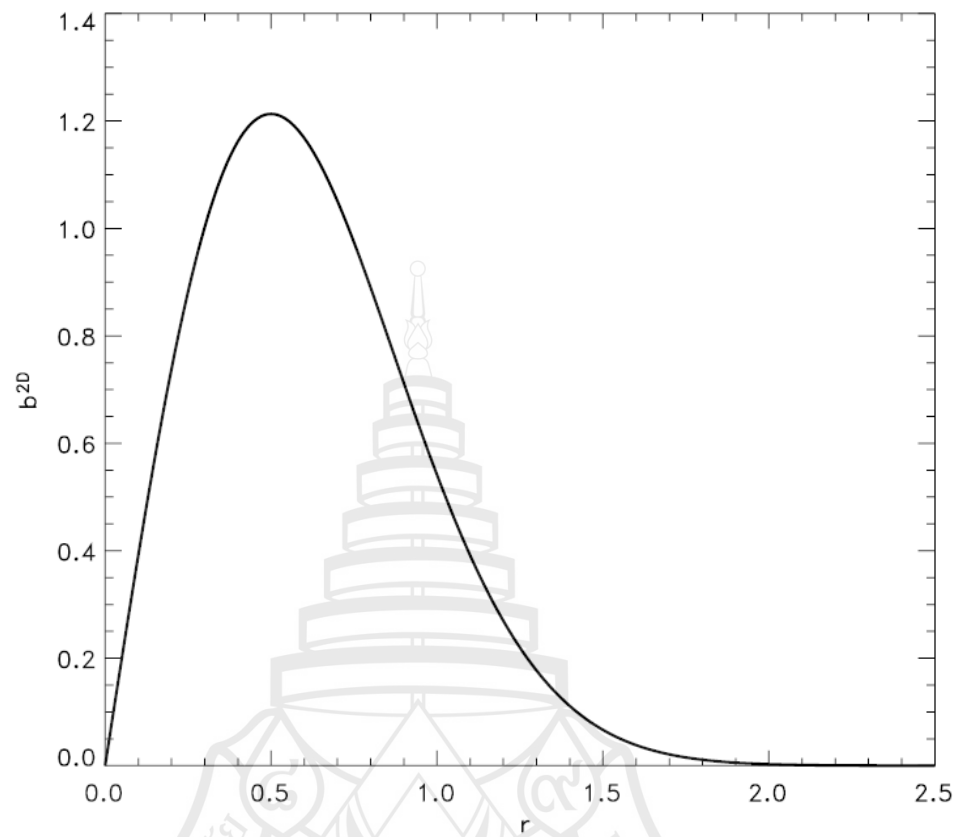


Figure 4.3 The profile of the 2D Gaussian magnetic field along the distance from the center of the flux tube.

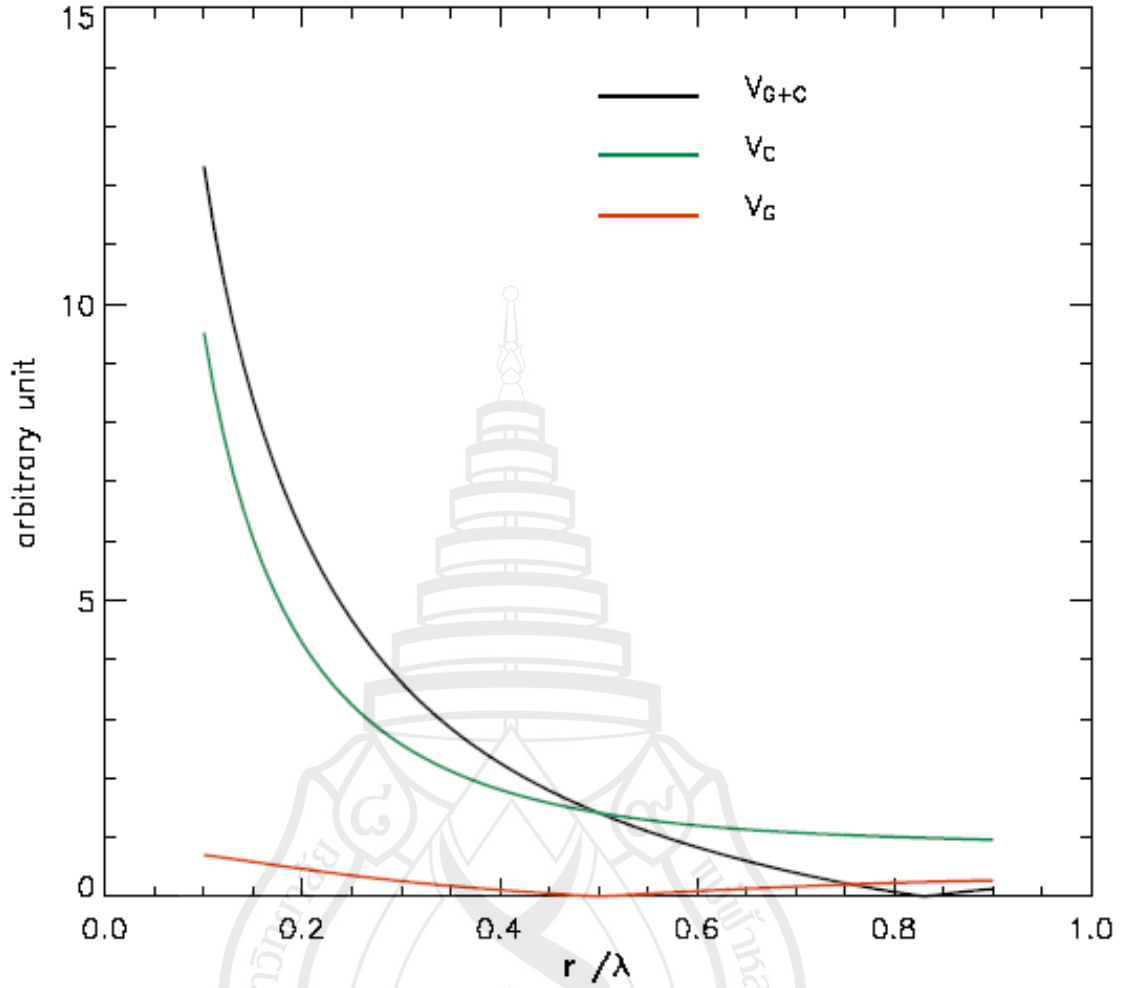


Figure 4.4 Showing shape of drift speed of guiding center due to the gradient of the magnetic field, radius of curvature of the magnetic field line and the summation of the gradient drift and curvature drift in arbitrary units.

II. At intermediate time (when $1 \leq tc/\lambda \leq 100$)

In this regime, the charged particles follow their corresponding field lines for a while and start to escape from the influence of the 2D flux tube. There are interesting features in this regime. The particles started deeper inside the 2D island have lower separation during this time and the particles started outside 2D island have almost the same slope of the separation. The particles start at $r_0 = 0.1\lambda$ and 0.3λ , at inside 2D islands, have lower separation rate than the others as shown in Figure 4.5a). Here, we can recognize the separation rate by the slope of the graph. The particles started deep

inside the 2D island slowly drift out from the field lines because both field lines and the charged particles are trapped inside 2D island. For the behaviors of the particles released outside the 2D island such as at $r_0 = 0.5\lambda$, 0.7λ and 0.9λ , they have almost the same separation rate and there is more the separation rate than the particles started at inside 2D island as shown in Figure 4.5b). That is because these particles quickly move outside and are not trapped due to the strong 2D field. This corresponds with the suppression of field line and particle diffusion when there is a strong 2D magnetic field as found in previous work (Chuychai et al., 2005, 2007; Tooprakai et al., 2007).

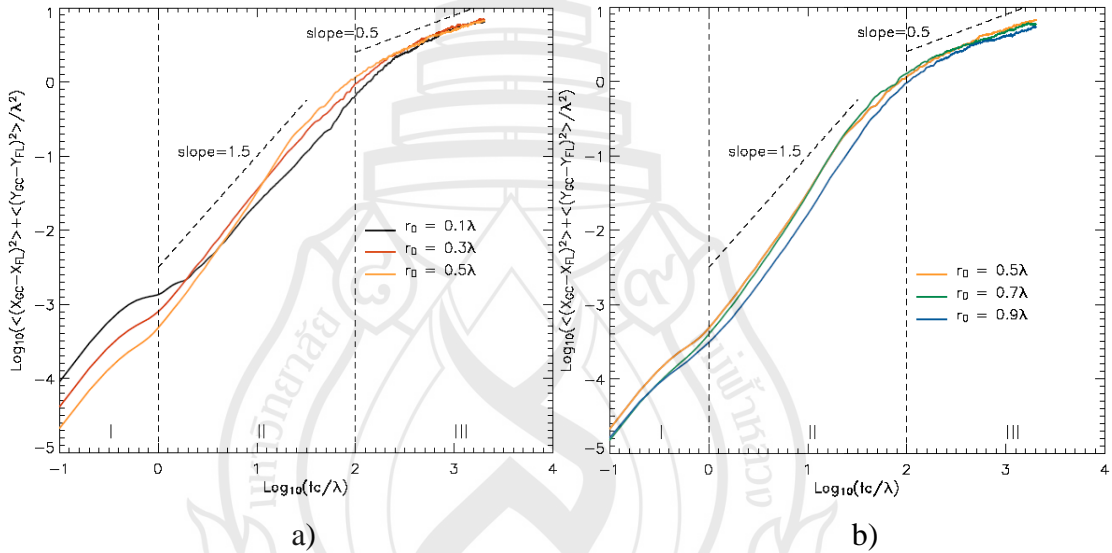


Figure 4.5 Showing the separation of the charged particles at a) inside the 2D island and b) outside the 2D island.

III. At final time (when $tc/\lambda \gg 100$)

From the final range in Figure 4.6, we can see that the charged particles released at radius as 0.1λ , 0.3λ and 0.5λ separate faster than the other radii. It seems the separation is related to the radius of releasing the charged particles. If the charged particles are released inside the center of Gaussian function, they separate from their initial field lines more than the other positions. In this range, the transition of the charged particles and their corresponding magnetic field lines are uncorrelated. Note

that the corresponding length scale of the uncorrelation between particles and field lines is in the order of coherence length scale (λ) which, within this length scale, the slab field are still correlated. The charged particles are mainly influenced by slab turbulence and undergo subdiffusive as we can see from the slope = 0.5 in Figure 4.2. We normally find subdiffusive process when charged particles transport in pure slab magnetic field (Tooprakai et al., 2007).

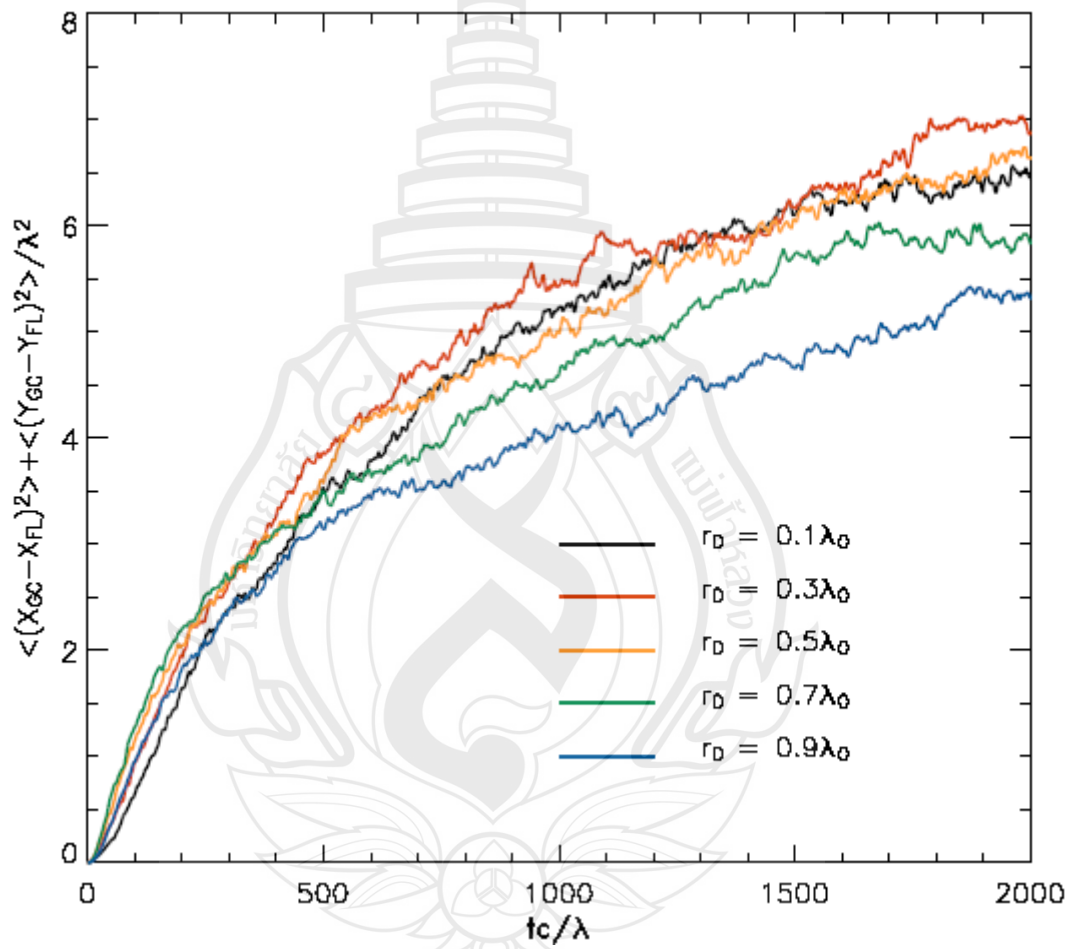


Figure 4.6 The mean squared perpendicular displacement and time in the final range.

Conclusion

From the results, the separation of the charged particles are related with the distance from the center of the Gaussian flux tube (r_0) and where they experience the different structure of the magnetic field. When the charged particles are released at low curvature of the magnetic field line, the separation is more than the others at the initial times. In our results, we show that the separation at the beginning depend on the gradient and curvature drift due to the 2D field. Then, in intermediate time, they slowly drift to outside the 2D flux tube. The sharp gradient of 2D field can be distinct behavior of the particles inside and outside the island in this regime. It corresponds with the suppressed diffusive regime in the previous work (Chuychai et al., 2007; Tooprakai et al., 2007). In addition, for final time the separation of the charged particles is uncorrected with the starting point to release the charged particles. The separation of the charged particles depends on distance from the center of the Gaussian function and becomes subdiffusive, the charged particles are released at outside of 2D Gaussian field ($r_0 = 0.7$ and 0.9λ), the separation is lower than the others radius. Finally, this work can help us to understand more about the relation of the separation between guiding centers of charged particles and magnetic field lines. In the next section, we will study more about theory and simulations in order to describe the mechanism or characteristic of the separation including the effect of pitch angle between charged particles and magnetic field lines.

4.2 The effect of fixed initial pitch angles to the separation

Here, instead of randomly generating the initial pitch angle over 0 to 180 degrees which consists of many value of pitch angles, we release the pitch angle at fixed value by using the method we show in the section 3.4, the 1000 charged particles are fixed initial pitch angles as 0, 30, 60 and 90 degrees, and released in every radius by using random positions. Moreover, we use the same condition of magnetic field and particle energy as in section 4.1 for studying the effect of initial pitch angle to the separation of charged particles.

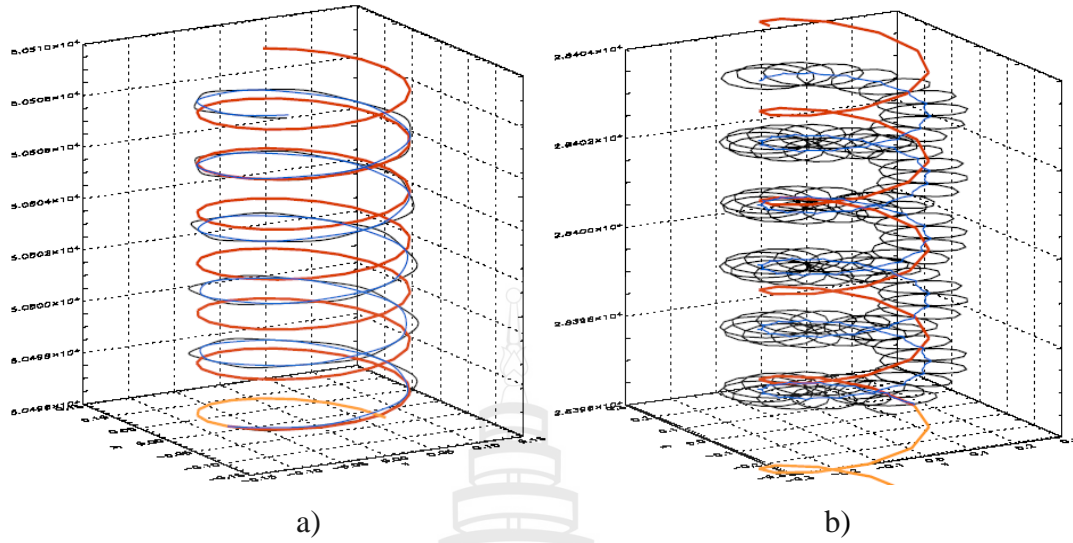


Figure 4.7 Example of the trajectories of a charged particles are released at radius as 0.1λ when the initial pitch angle as a) 0 degree and b) 90 degrees; the red line demonstrates trajectory of magnetic field line, the black line and the blue line demonstrate trajectories of charged particle and its guiding centers, respectively.

Results & discussion

In this section, we increase the condition to the experiment by using method which can specify the value of the initial pitch angle for the charged particles. This method gives us more understand about the effect of initial pitch angles to the separation. Figure 4.7 shows the examples of trajectories of magnetic field lines and particles with the guiding center when they are released at different of the pitch angles in the pure 2D Gaussian field. Here we can see the particle started at 0 degree drift faster than the one started at 90 degrees. When we have the simple 2D field + slab field and release the particles with various pitch angles, we found that the separation of the charged particles are released at every radius is highest when initial pitch angle as 0 degree [see also Figure 4.8a) to 4.8e)]. For the charged particles have the least separation when the initial pitch angle as 90 degrees.

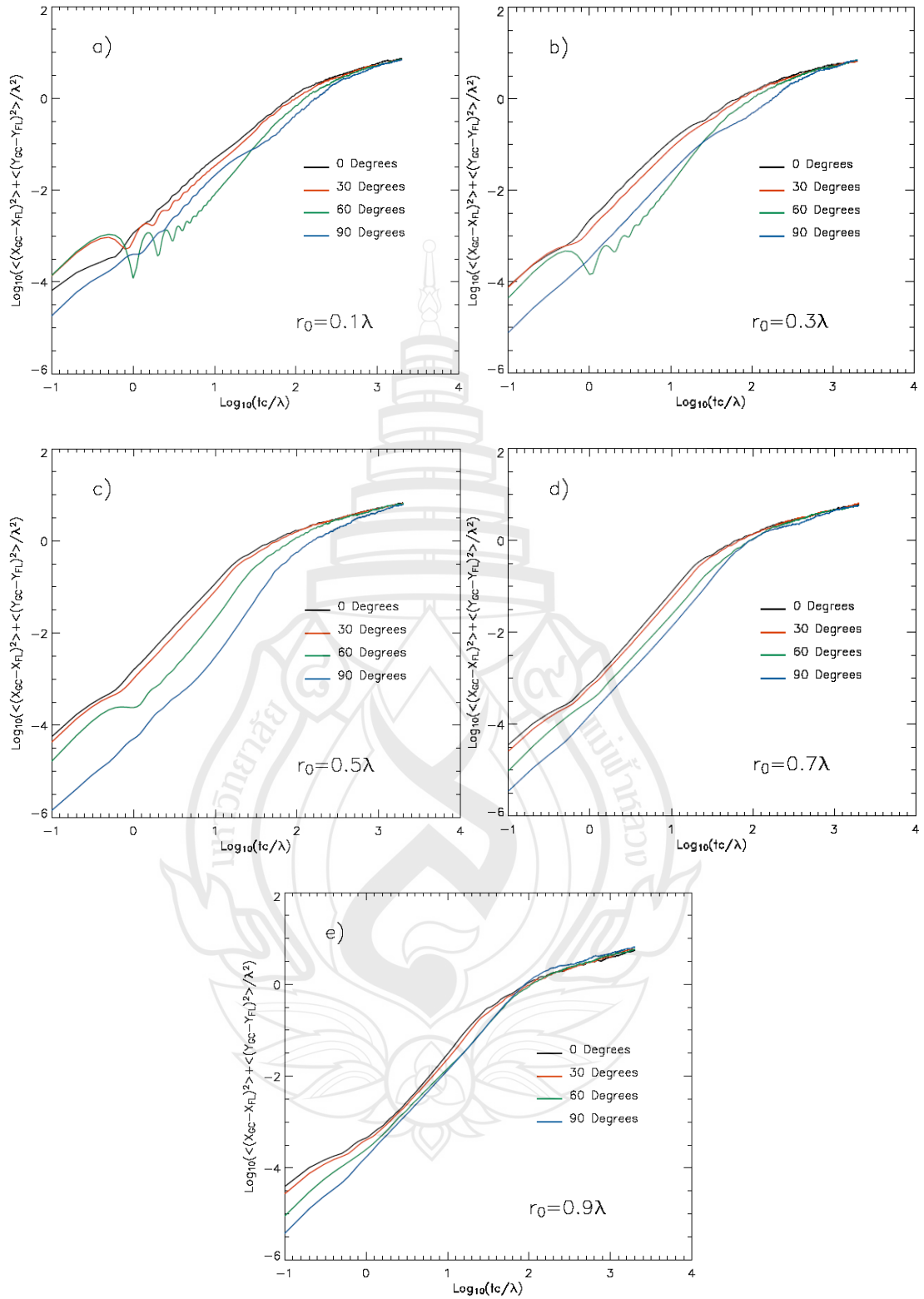


Figure 4.8 Showing the separation of the charged particles at the radii as $0.1, 0.3, 0.5, 0.7, 0.9\lambda$ in the figure 4.8a)-e) respectively.

Moreover, for better understand about the separation of charged particle we eject one particle in the simple pure 2D field at initial pitch angles as 0 and 90 degrees and vary radii as 0.1, 0.5 and 0.9λ , we found that the radius of curvature of the magnetic field line has affect to the separation of the charged particle. From Figure 4.9a) and b), the charged particle is released at radius as 0.1λ has least separation because here it has a little the radius of curvature of the magnetic field line. The particle is confined and drift along z direction with the flux tube at its radius (see also in Figure 4.7). The charged particle released at radius as 0.9λ has highest separation because maximum the radius of curvature of the magnetic field line. In addition, the charged particle is released at deep inside the island, it is trapped by the effect of 2D flux tube, has a smaller period than other radii (see in Figure 4.9a) which is because of the size of the 2D flux tube.

Next, let's compare of pitch angle to the separation at the beginning. From the drift velocity in equation (2.42) and (2.47), we can see that the gradient drift depends on the velocity in perpendicular component and the curvature drift depends on velocity in parallel component. That means the curvature drift plays most important role for the particles with the pitch angle near 0 degree and has less effect to the ones with the pitch angle near 90 degrees while the gradient drift has more effect to the pitch angle near 90 degrees but not for 0 degree. As we discuss in Section 4.1, the curvature drift is dominated more than the gradient, so we can see the separation in for 0 degree pitch angle higher than the pitch angle at 90 degrees (see also in Figure 4.10). Also from Figure 4.8a) to 4.8e), the charged particles are released at initial pitch angle as 0 degree have more separation than initial pitch angles as 30, 60 and 90 degrees in every radii.

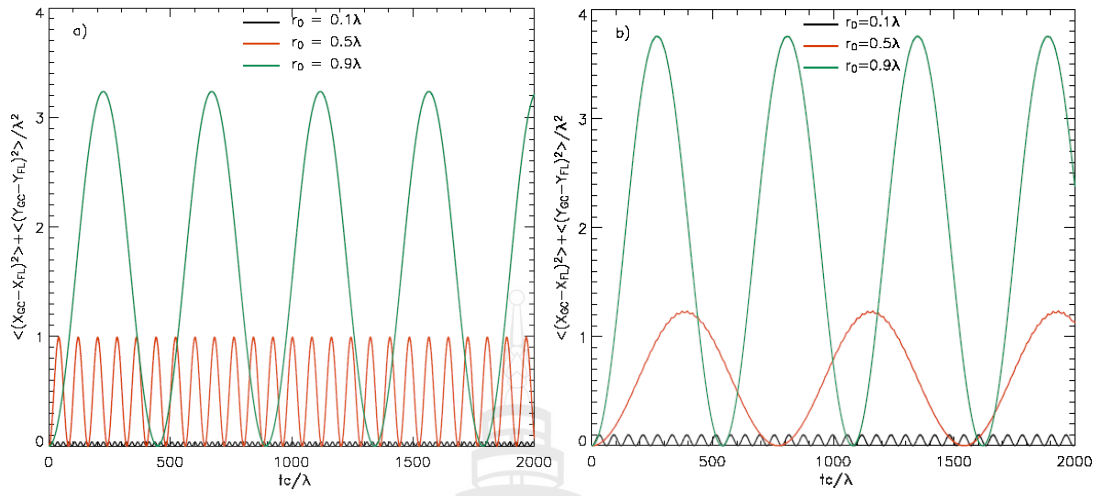


Figure 4.9 Showing the separation of the charged particles at the radius as 0.1λ , 0.3λ and 0.9λ by using fix initial pitch angles as a) 0 degree and b) 90 degrees in the simple pure 2D field.

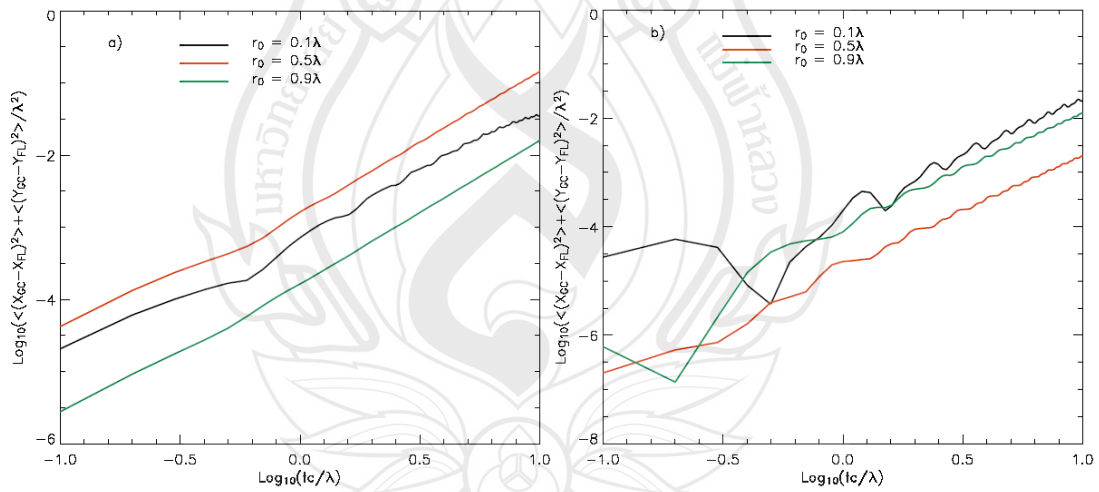
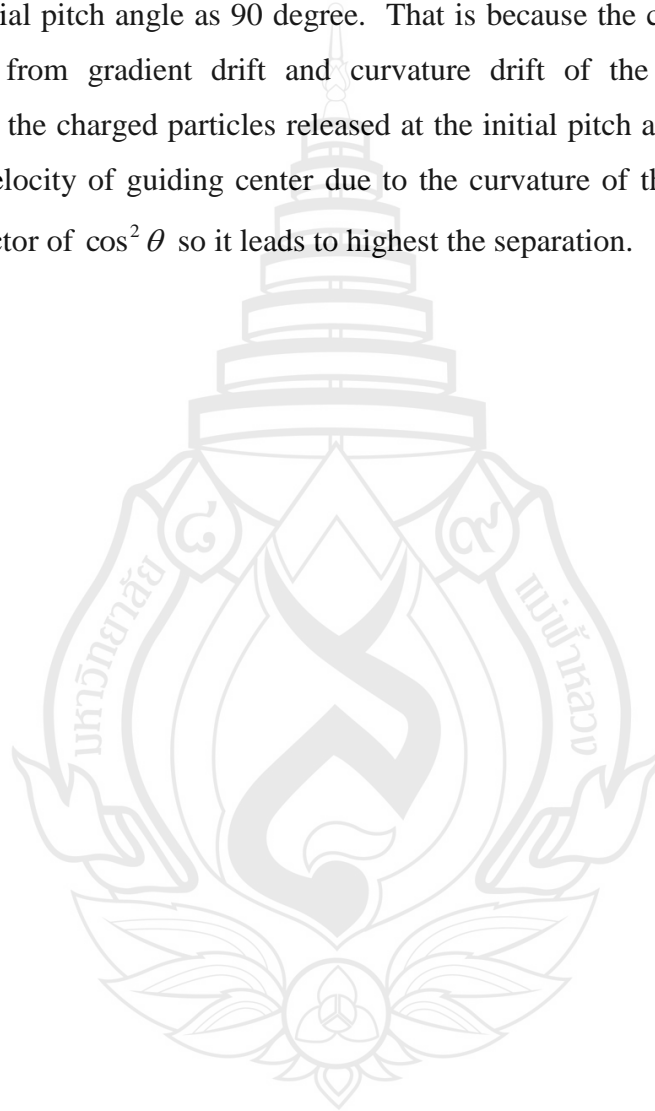


Figure 4.10 Showing the separation of the charged particles in log-log scale at the radius as 0.1λ , 0.3λ and 0.9λ by using fix initial pitch angles as a) 0 degree and b) 90 degrees in simple pure 2D field.

Conclusions

When the results are plotted graph in the same scale, the charged particles have the least separation when initial pitch angle as 90 degree in every radius, no matter that the magnetic field is strong or not. The separations of the charged particles are highest when they are released at initial pitch angle as 0 degree and lowest at initial pitch angle as 90 degree. That is because the charged particles have more effect from gradient drift and curvature drift of the magnetic field line. Furthermore, the charged particles released at the initial pitch angle as 0 degree have more drift velocity of guiding center due to the curvature of the magnetic field line due to the factor of $\cos^2 \theta$ so it leads to highest the separation.



CHAPTER 5

RESULTS FOR THE CHARGED PARTICLES IN 2D+SLAB TURBULENCE

This chapter presents the results for the effect of the pitch angles to the separation when the charged particles are in 2D+slab turbulent magnetic field. We perform 2 cases here. The first case is that the particles are released at various pitch angle ranges. For the second one, the particles are released at specific initial pitch angles.

5.1 The effect of various initial pitch angle ranges on the separation

We generate magnetic field which is static and homogeneous by using 2D+slab model of magnetic field turbulence. The magnetic field is generated in simulation box, the ratio of 2D and slab magnetic energy $E^{2D} : E^{slab} = 80 : 20$. In this numerical experiment, 1,000 100-MeV charged particles are released at various pitch angle ranges from 0-30, 30-60, 60-90 degrees in simulation box that we model with random positions (see section 3.4).

Results & discussion

For better understand about the motion of charged particles in turbulent magnetic field, we release a sample of charged particles at initial pitch angles near 0 and near 90 degrees to observe trajectories of charged particles and to see the difference between guiding center of them with magnetic field lines that are traced

from initial guiding centers of charged particles. We found the trend that the charged particle released at pitch angle near 0 degree has more separation better than the one near 90 degrees in the initial time. For nearly 90 degrees, the particle stays around the released position at the beginning time before it leaves the field line while, the particle quickly travel along the field line for the one released nearly 0 degree (see Figure 5.1). However, this is just only a few examples of particle trajectories in turbulent field which the particle trajectories are very sensitive with the turbulent magnetic field at each location. Therefore, we need to explore the statistics of the separation of 1000 charged particles and their corresponding magnetic field lines.

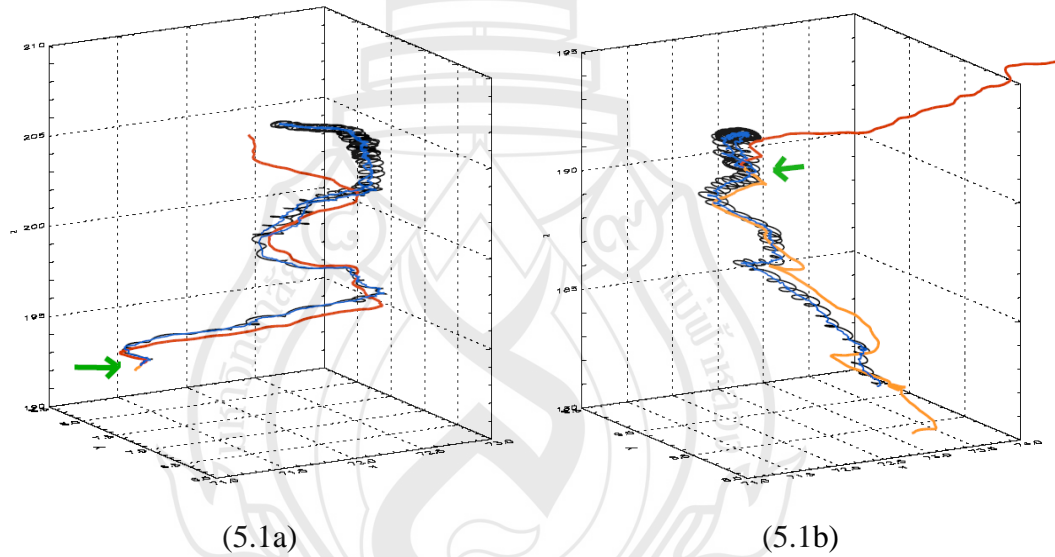


Figure 5.1 Illustration of the examples of charged particles and their corresponding magnetic field line trajectories. a) The charged particle is released at initial pitch angle near 0 degree. b) The charged particle is released at initial pitch angle near 90 degrees. They are released at the same position where the green arrow indicates. The red line shows trajectory of magnetic field line, the blue line shows trajectory of guiding center, and dark line show trajectory of charged particle.

In the simulations, we choose bins for initial pitch angles as 0-30, 30-60, and 60-90 degrees and release 1000 charged particles for each bin. Then we compute the mean squared displacement as in equation (10). The results from the experiment at the initial time are shown in Figure 5.2. For the charged particles released at the pitch angle as 0-30 degrees, the separation is larger than at the pitch angle as 30-60, and 60-90 degrees (Wikey, Chuychai, Ruffolo & Matthaeus, 2012). If the pitch angles are 60-90 degrees, the charged particles have a little separation at the beginning time. In initial range, the different of separation of charged particles due to the effect of initial pitch angle is clearly seen.

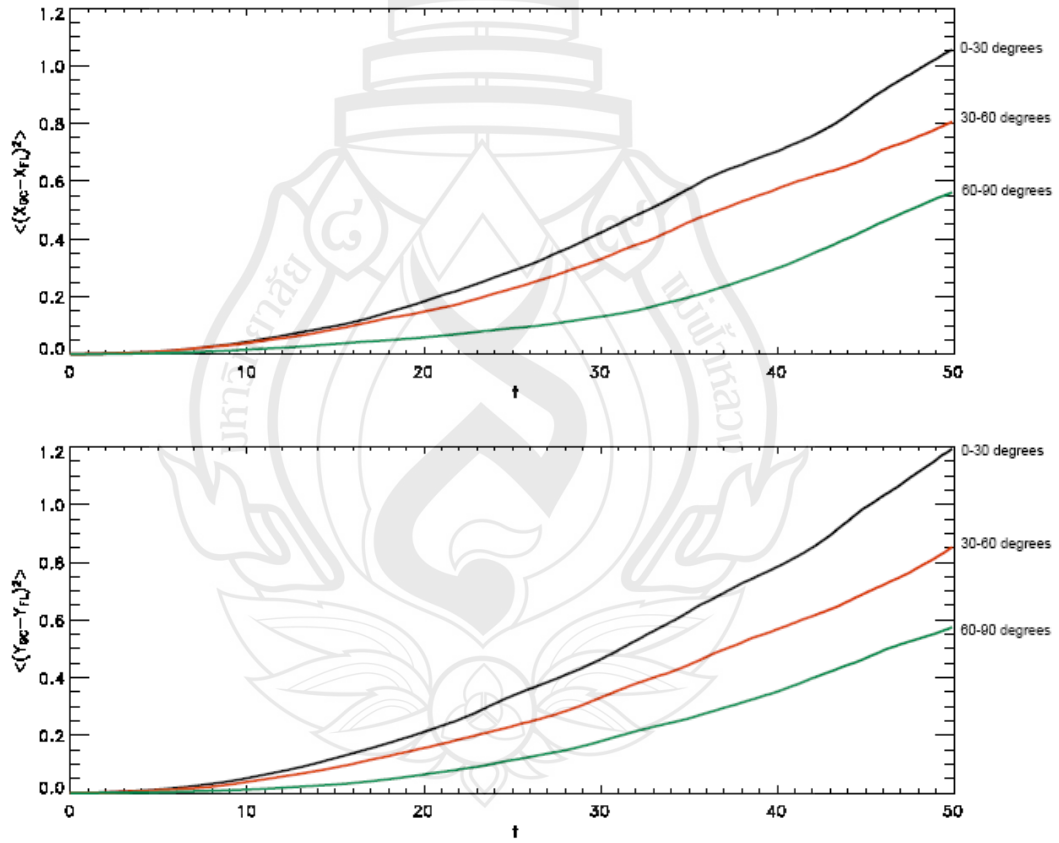


Figure 5.2 Displacement mean squared perpendicular to the mean field between guiding centers of charged particles (x_{GC}, y_{GC}) and their corresponding magnetic field lines (x_{FL}, y_{FL}) at initial in linear-linear scale.

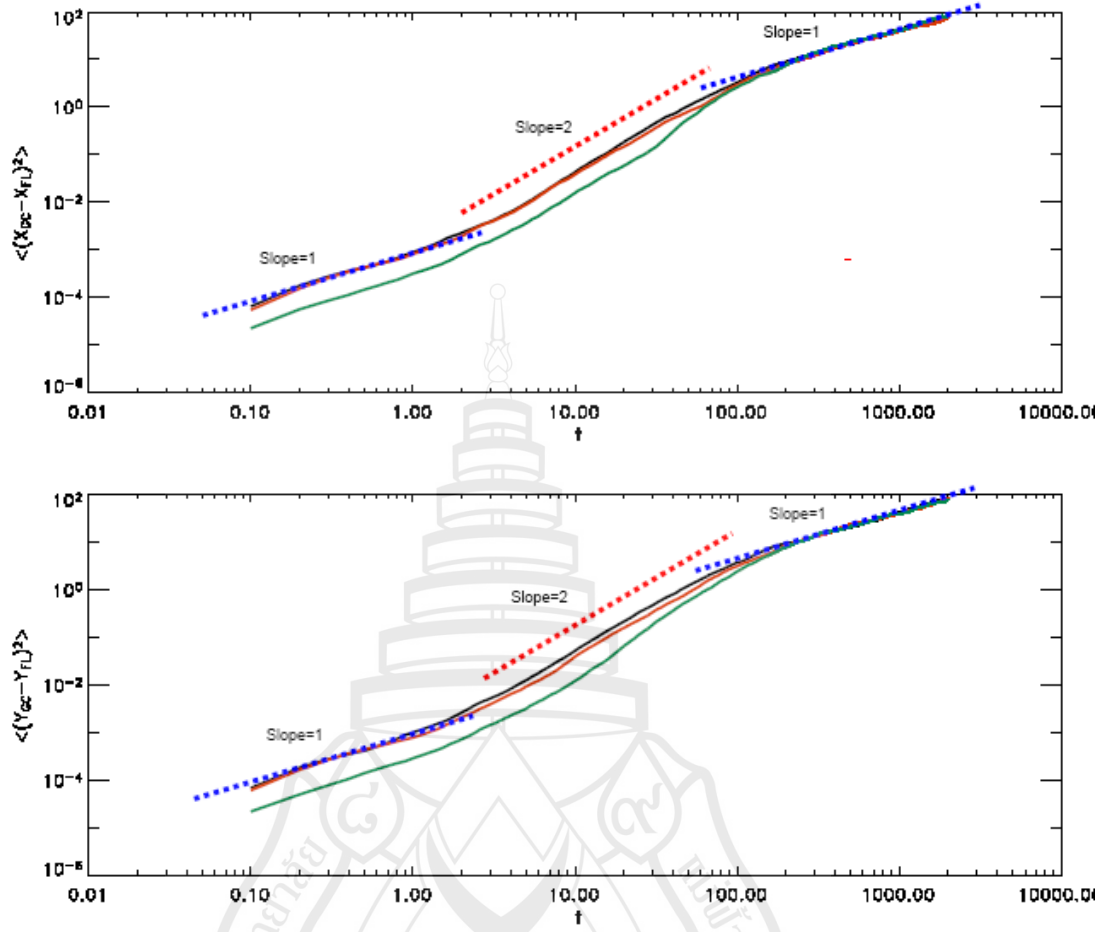


Figure 5.3 Showing relation between mean squared displacement perpendicular to the mean field between guiding centers of charged particles (x_{GC}, y_{GC}) and their corresponding magnetic field lines (x_{FL}, y_{FL}) and time in log-log scale.

After that we plot the data in the log-log scale to see the separation process at each range as presented in Figure 5.3. We found that trajectory of the charged particles can be divided into two characteristics. At the very short time and long time limit, the slope is 1 that means in this regime the separations are diffusive and for long time limit the field line random walk is dominated by 2D-dimensional component of turbulence (Ruffolo et al., 2004). For the intermediate regime the separation grows as free streaming process. It seems that the particles still depend on the initial field lines

in intermediate range before they undergo diffusive and are uncorrelated with their initial field lines. Note that we also did the initial pitch angle between 90-180 degrees. The results are similar to 0-90 degrees. The initial pitch angles near 180 degrees have the separation more than the one nearby 90 degrees.

Conclusions

We have found that there is the effect of the initial pitch angles of charged particles to the separation on the turbulent magnetic field lines. If the initial pitch angle is close to 0 degree, the separation is more than the one that is close to 90 degrees at the initial time before the separation are diffusive and the trajectories of the particles are uncorrelated with their initial magnetic field lines. Finally, this study helps us to know the effect of the initial pitch angles on the separation between guiding center of charged particles and magnetic field line. In the next section, we released the initial pitch angles at specific values in order to study in more detail for better understanding about the mechanism of separation between charged particles and magnetic field.

5.2 The effect of fixed initial pitch angles on the separation

The 1000 charged particles are released at random position in (2D+slab) turbulence magnetic field by using fixed initial pitch angles as 0, 30, 60, 90 degrees (see section 3.4 for procedure to fixed initial pitch angle). We generate magnetic field which is static and homogeneous by using 2D+slab model of magnetic field turbulence. The magnetic field is generated in simulation box, the ratio of 2D and slab magnetic energy $E^{2D} : E^{slab} = 80 : 20$, in this numerical experiment, 1,000 100-MeV.

When we plot the graph of the results of the separation of the charged particles between guiding centers of charged particles (x_{GC}, y_{GC}) and their corresponding magnetic field lines (x_{FL}, y_{FL}) at any each time on linear-linear scale, we found that the separation of them is not clear, we cannot describe that which the initial pitch

angle has the effect to the separation of the charged particles or has more separation than other initial pitch angles [see Figure 5.4a]. Thus we instead plot the graph, on log-log scale for the separation and linear scale for times as shown in Figure 5.4b). We found that the initial pitch angle as 90 degrees has effect to the separation of charged particles in time as $tc/\lambda \sim 0.1$ to 900 because the charged particles have least separation when the initial pitch angles of them are 90 degrees. However, it is only initial time to the separation of the charged particles are dominated, when long distance the charged particles and their corresponding magnetic field lines are uncorrelated, so their initial pitch angles do not effect to the separation.

Results & discussion

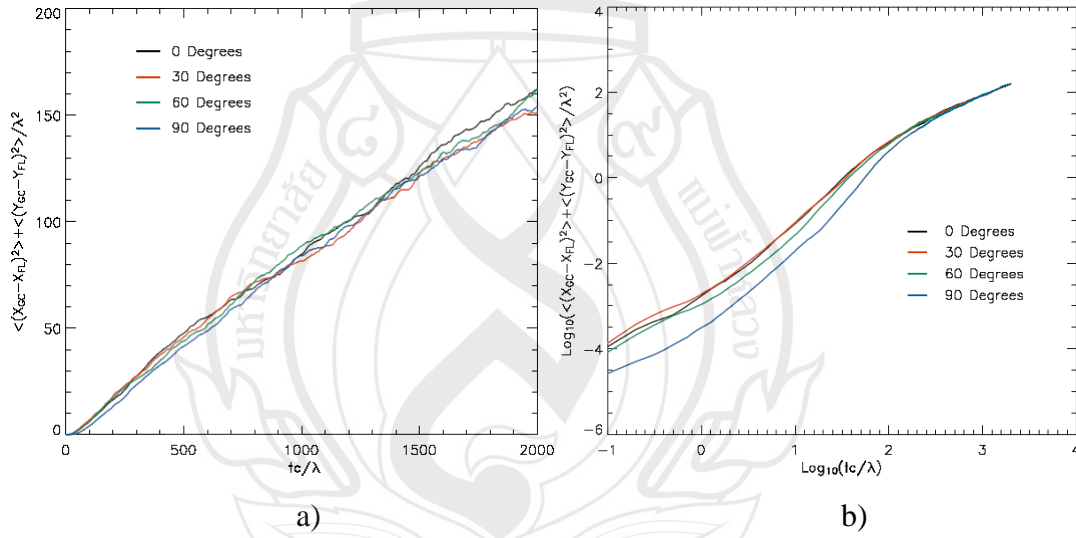


Figure 5.4 Showing the separation of the charged particles between guiding centers of charged particles (x_{GC}, y_{GC}) and their corresponding magnetic field lines (x_{FL}, y_{FL}) at any each time in a) linear-linear scale and b) log-log scale(5.4b).

1. At the initial range, when $tc / \lambda < 1$

When we take log-log scale to the results, we can describe behavior of the charged particles in various ranges. We found that the separation of the charged particles in initial time at every initial pitch angles has slope = 1.0. In this range, the particles have begun influence from 2D+slab turbulence magnetic field and also start separation. Moreover, we note that the charged particles are released at initial pitch angle as 30 degree has more separation than the other initial pitch angles, the charged particles are released at initial pitch angle as 90 degrees has least separation. If we estimate gyrofrequency of the charged particles in this range, we found that their transition have almost a 1 period, so the charged particles are released at initial pitch angle as 90 degree has less distance in z direction than 0, 30 and 60 degrees, but the charged particles are released at initial pitch angle as 0, 30 degrees have long distance until they move complete 1 period. Thus, the charged particles are released in parallel direction to their corresponding magnetic field lines such as at initial pitch angle as 0 and 30 degrees, they have separation more than other initial pitch angles.

2. At intermediate range, when $1 \leq tc / \lambda \leq 100$

From the Figure 5.5, we found that the slope has highest gradient, which is 2.0 here. The particles orbit around the field lines which are mainly affected by the 2D turbulence magnetic field and the effects of the slab turbulence on these trajectories are small at this range (Tooprakai et al., 2007). The guiding center charged particles in this range are quickly diffusive from their corresponding magnetic field lines.

For this range the charged particles pass through the different intensity magnetic field. If they are in the stronger magnetic field, the radius of particle's trajectory is small while the weaker field gives the larger radius. Because the change of magnetic field intensity, the guiding centers of the charged particles drift from their initial magnetic field lines and perpendicular to \vec{B} and to the magnetic field gradient (∇B) follow Figure 2.13, we call this effect as "gradient drift". Moreover, the magnetic field line also has curvature. Due to the curvature of magnetic field, the moving charged particle has acceleration relate to the field line curvature follow equation (2.46) and their directions follow Figure 2.14. Because the magnetic field lines have both gradient and curvature, this range the charged particles have different

separation suddenly, and have slope as 2.0. In the other view, for slope = 2.0, it tells us that the particles behave as free-streaming which means they are not diffusive or follow the field lines but they are freely moving from their initial field lines.

3. At final time, when $tc / \lambda \gg 100$

For long time limit, the displacement between the guiding centers of the charged particles and their corresponding magnetic field lines are very large and transition of the charged particles are increasingly not related to their corresponding magnetic field lines. Moreover, the charged particles are diffusive due to 2D+Slab turbulence and they are uncorrelated with their initial field lines that why we obtained the slope from this range as 1.0. Thus, we call this range as diffusion regime (Ruffolo et al., 2008).

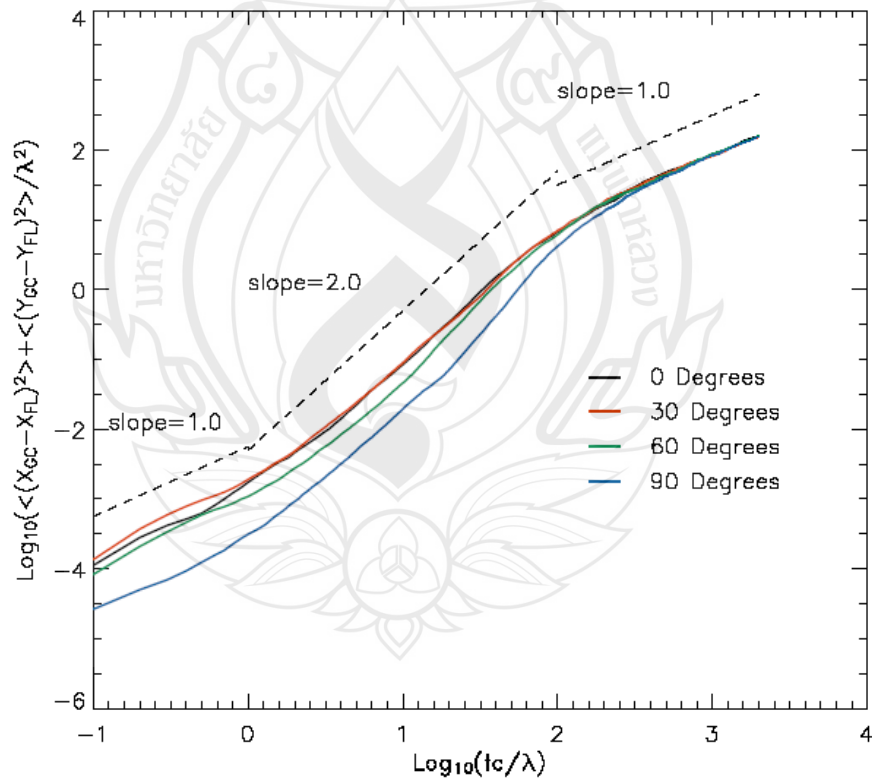


Figure 5.5 The results of the separation of charged particles and their corresponding field lines in the log-log scale.

In addition, when we plot the graph of the results between the initial pitch angles and the separation of the charged particles in log scale on the same picture, we found that at the initial pitch angles at 90 degrees has least separation at each time. For long time, the separations of the charged particles are not different as shown that the separation does not depend on the initial pitch angles (see Figures 5.6 and 5.7).

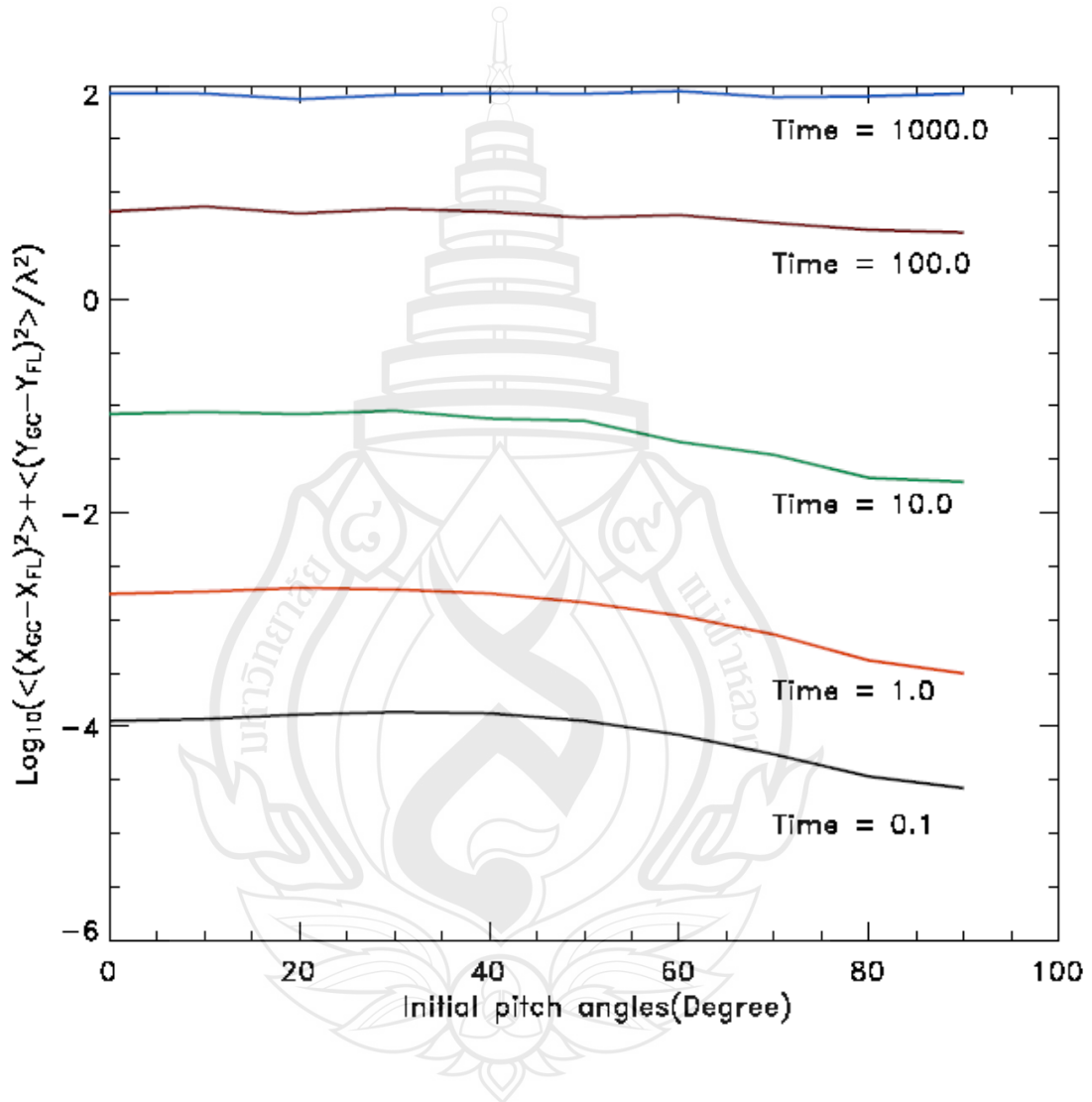


Figure 5.6 Showing the results between the initial pitch angles and the separation of the charged particles in log scale on the same picture at the time as $tc/\lambda = 0.1, 1.0, 10.0, 100.0$ and 1000.0 .

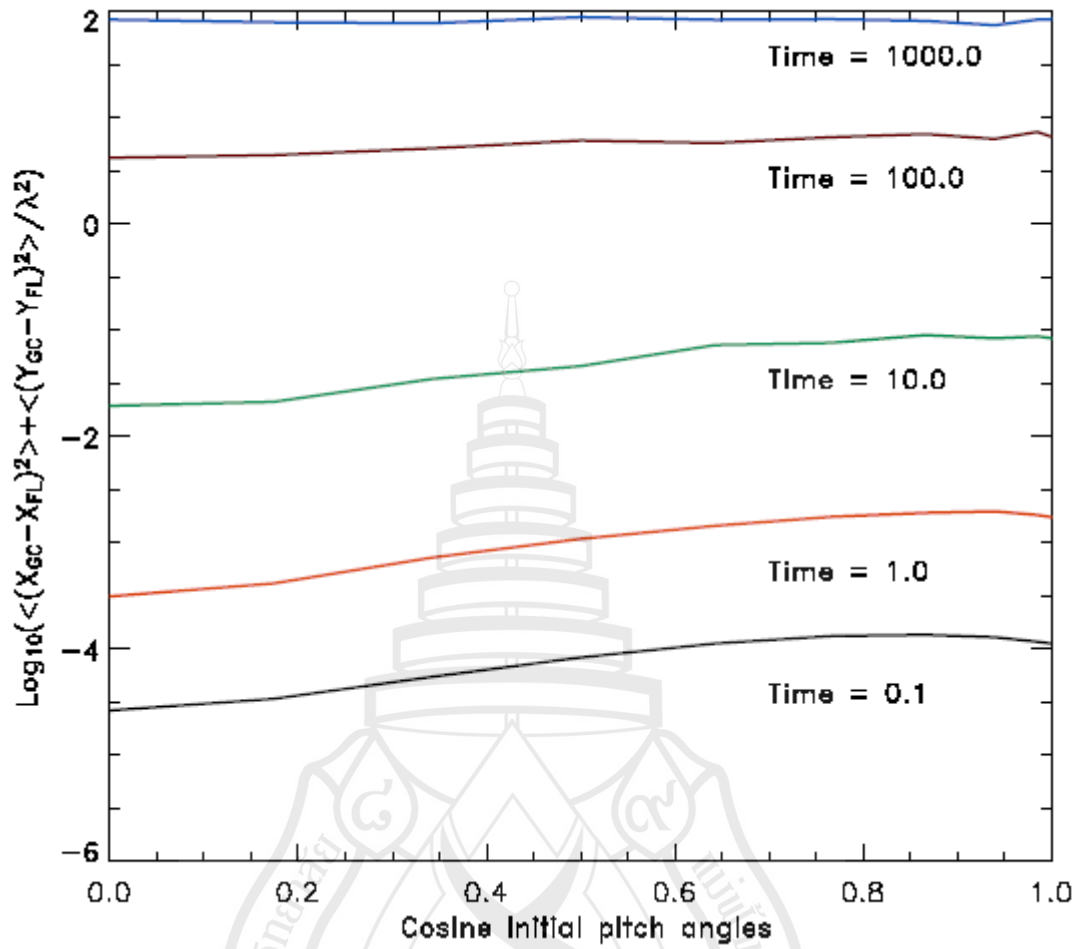
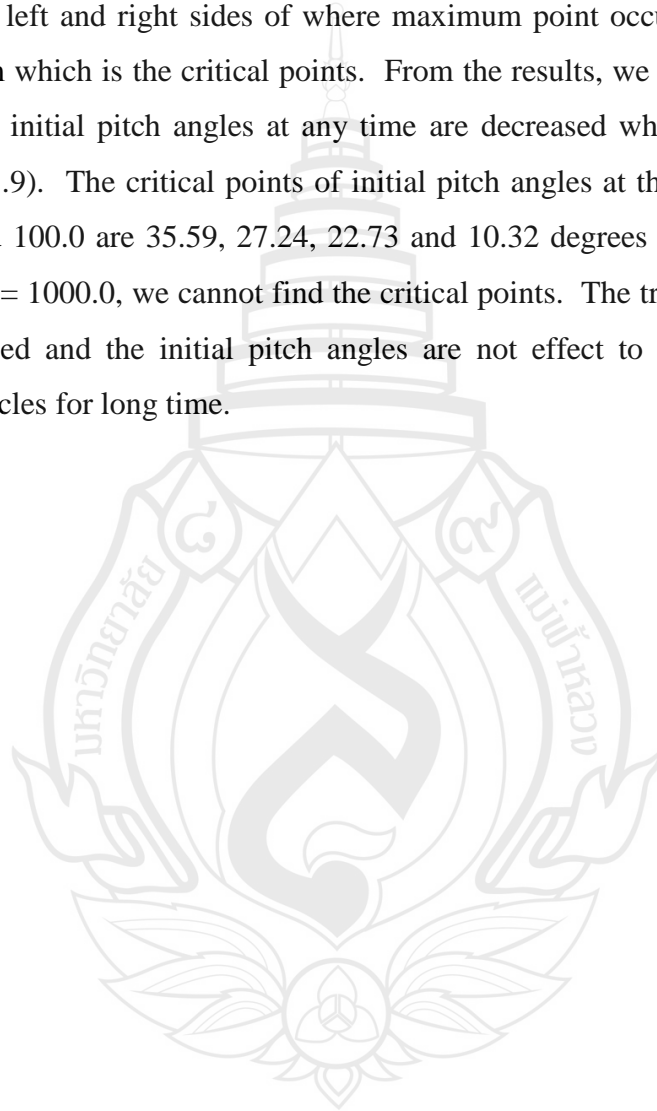


Figure 5.7 Showing the results between the cosine initial pitch angles and the separation of the charged particles in log scale on the same picture at the time as $tc/\lambda = 0.1, 1.0, 10.0, 100.0$ and 1000.0 .

Since the plots in Figures 5.6 and 5.7 have not yet provided quantitative explanation, we find the new method to explain the results here. When the results are plotted between the initial pitch angles and the separation at the time as $tc/\lambda = 0.1, 1.0, 10.0, 100.0$, and 1000.0 , we found that at the time as $tc/\lambda = 0.1, 1.0, 10.0$, and 100.0 have decrease separation of the charged particles when the initial pitch angles closely 90 degrees, but there are not much different for the separation of the charged particles at the time as $tc/\lambda = 1000.0$ in any initial pitch angles (see Figure 5.8) which shown that the initial pitch angles are not affect to the separation of the charged

particles for long time. Note that at the time as $tc/\lambda = 0.1, 1.0$ and 10.0 have high separation of the charged particles in the range of initial pitch angles as $20-40$ degrees. Then we find the critical point of initial pitch angles which is the angle that the separation of the charged particles have maximum at each time as shown in Figure 5.9. To compute the critical point of the initial pitch angles, we use linear least square fitting in the left and right sides of where maximum point occurs and find intercept point of them which is the critical points. From the results, we found that the critical points of the initial pitch angles at any time are decreased when the time increases (see Figure 5.9). The critical points of initial pitch angles at the time as $tc/\lambda = 0.1, 1.0, 10.0$ and 100.0 are $35.59, 27.24, 22.73$ and 10.32 degrees respectively. For the time as $tc/\lambda = 1000.0$, we cannot find the critical points. The trends of critical points have decreased and the initial pitch angles are not effect to the separation of the charged particles for long time.



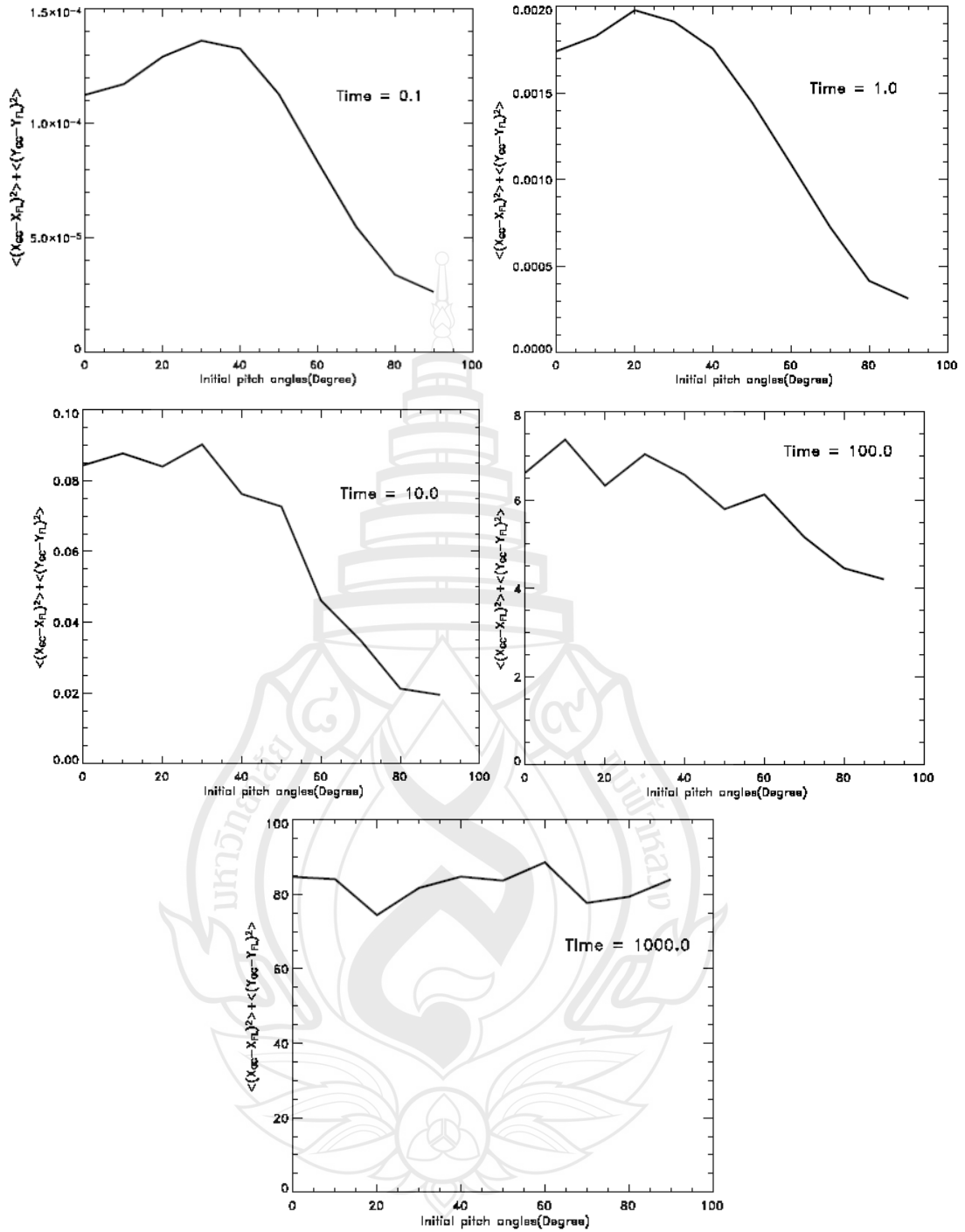


Figure 5.8 These figures show the separation of a charged particles in turbulence magnetic field model when initial pitch angle and time are different.

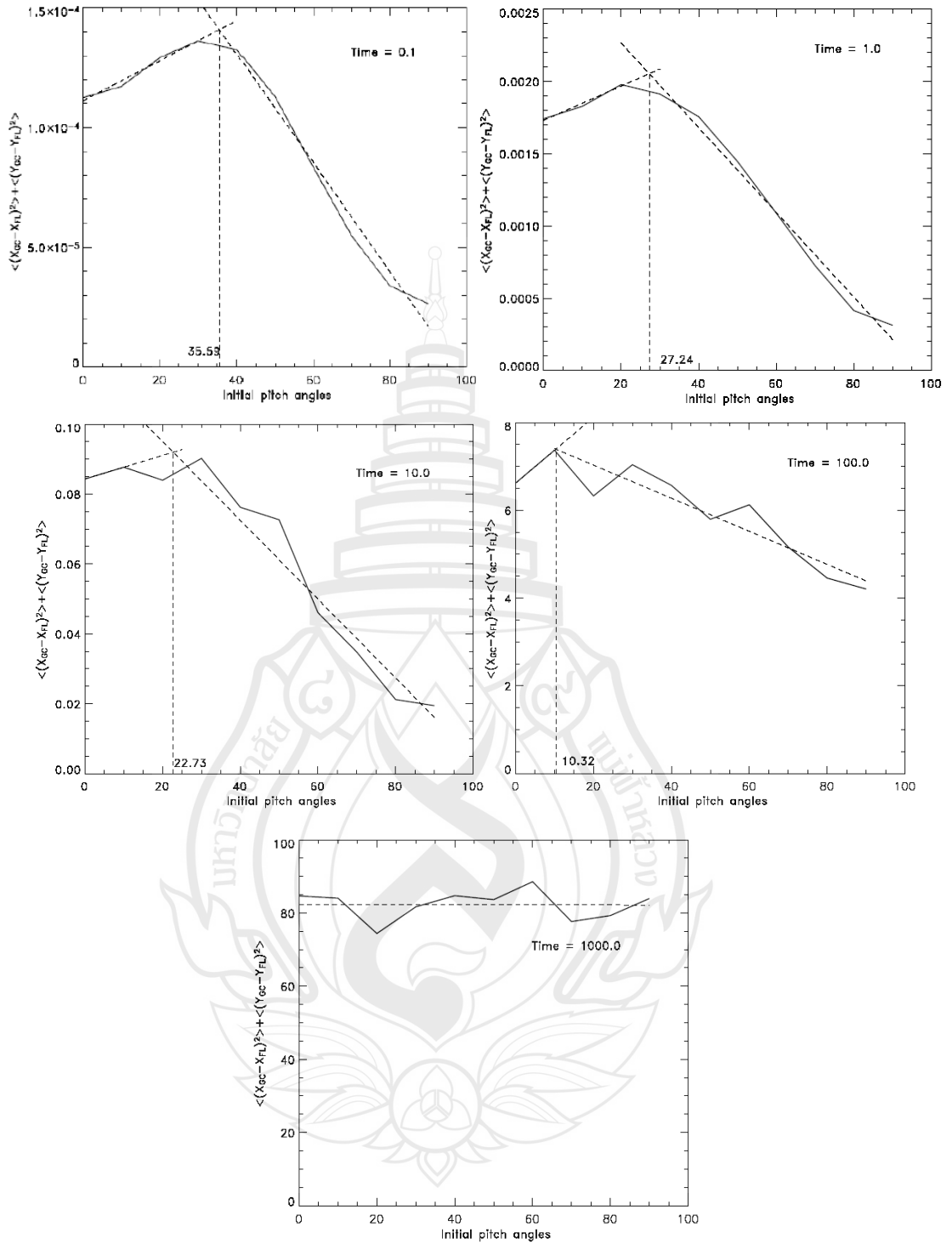


Figure 5.9 These figures show the critical points of initial pitch angles at the time as $tc/\lambda = 0.1, 1.0, 10.0, 100.0$, and 1000.0 by using linear least square fitting.

Moreover, when we plot the graph of differential pitch angle at each time for a selected particle, we found that the pitch angle of the charged particle will slowly change on decreasing or increasing in range as 0-180 degrees, as shown in Figure 5.10 a). If we plot the graph of the average pitch angle at each time of 1000 charged particles at each time as $0 \leq tc/\lambda \leq 2000$ for the initial pitch angles as 0, 30, 60 degrees, they have differential increasing of the pitch angles and later converge to 90 degrees. The charged particles that released at initial pitch angle as 90 degrees, there are a little difference of the pitch angles and nearly always 90 degrees (see Figure 5.10 b). Finally, the charged particles are released at every initial pitch angles, there are pitch angles almost 90 degrees. That is because the pitch angles of each particle are distributed over the range 0 to 180 degrees. Then the mean values of them are about 90 degrees.

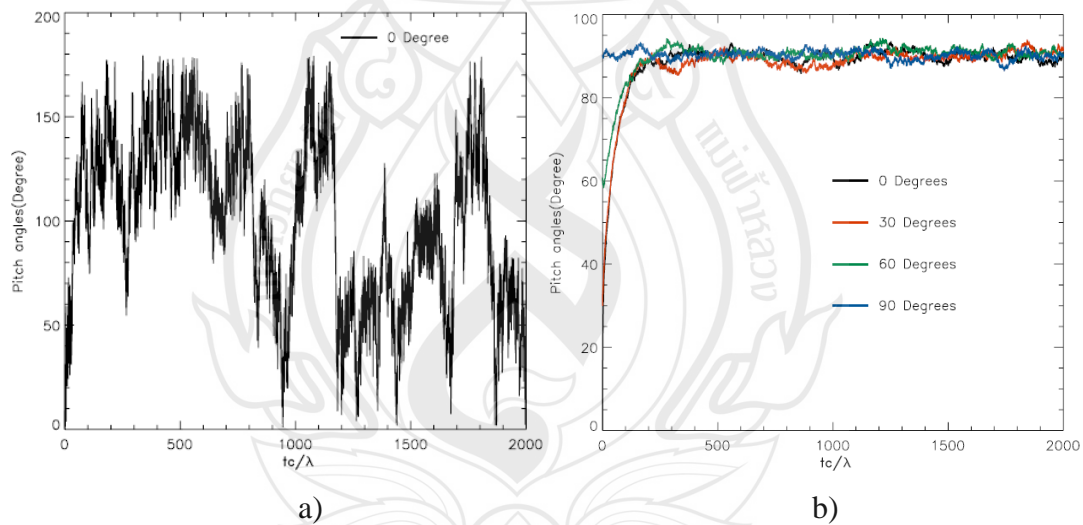


Figure 5.10 These figures show the changing of pitch angles and time in a) a selected particle at initial pitch angle as 0 degree and b) the average pitch angle of 1000 particles at initial pitch angles as 0, 30, 60 and 90 degrees.

Conclusions

When we see the results from Figure 5.4b, we know that the charged particles have least separation when the initial pitch angles of them are 90 degrees and if we find slope of graph in log-log scale at each range, we know the behavior of the charged particles and effect of the magnetic field to separation. At the initial range the charged particles have begun effect from 2D+slab turbulence magnetic field, the charged particles are released at initial pitch angle as 30 degrees has more separation than the other initial pitch angles and the charged particles are released at initial pitch angle as 90 degrees has least separation. In the intermediate range, the charged particles are quickly separated away of guiding center of them from their corresponding magnetic field lines due to the drift effect and the charged particles have diffusion due to effect of 2D+slab turbulence magnetic field at the final time. Moreover, we can find the critical point of initial pitch angles at various time, we found that the trend of the critical points of initial pitch angles have decreased and the initial pitch angles are not effect to the separation of the charged particles for long time. The averages of pitch angles at each time are also presented. The values of them approximately approach to 90 degrees at long time limit.

CHAPTER 6

CONCLUSIONS

We study the effect of initial pitch angles of the charged particles to their corresponding magnetic field lines in interplanetary space. In our research, we consider solar energetic particles (SEPs) as charged particles for case study. We assume that the charged particles orbit around their corresponding magnetic field lines. We determine the guiding centers of the charged particles for starting points of magnetic field lines when particles are released at different pitch angles and after that we will compute the separation of the guiding center of the charged particle and their corresponding magnetic field lines. We find the trajectory of the charged particles and magnetic field lines by using fourth-order Runge-Kutta method with adaptive time stepping regulated by a fifth-order error estimate step to solve Newton Lorentz force and magnetic field line equation. For the magnetic field, we use 2D+slab model. The first case is a simple case which is 2D Gaussian field + slab turbulence and another one is (2D+slab) turbulence field model we will specify the power spectrum for both 2D and slab magnetic field as Kolmogorov spectrum.

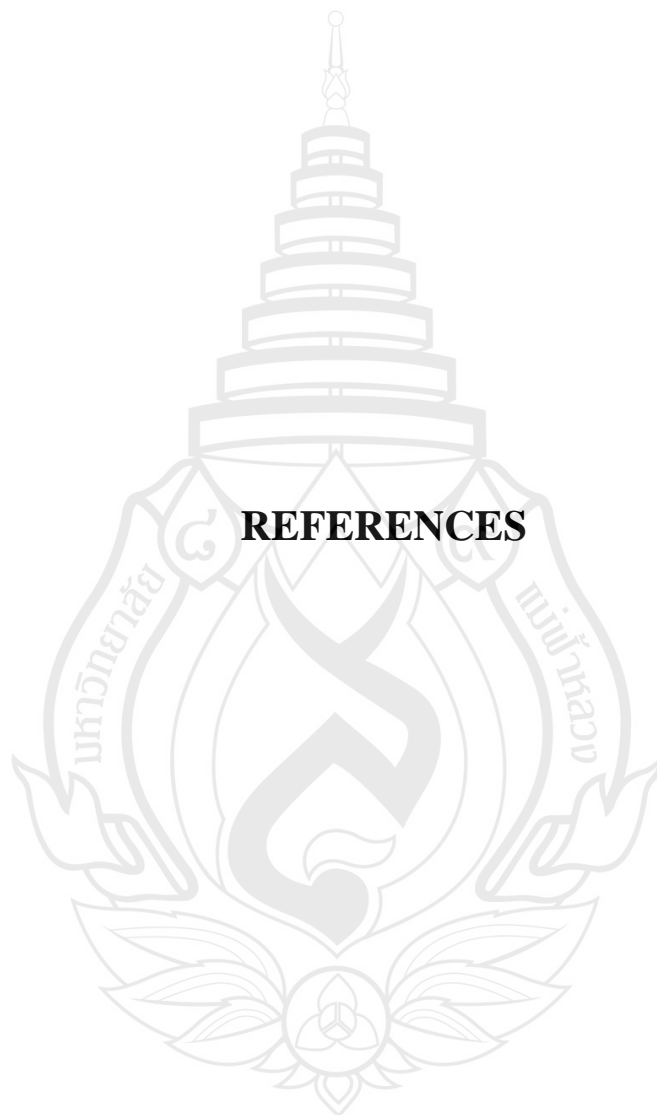
For the effect of the initial pitch angles of the charged particles and their corresponding magnetic field lines in simple case as we presented in Chapter 4, the results from this case is divided into 2 cases. For the first, the 1000 charged particles are released at random initial pitch angles from 0 to 180 degrees and on various distances from the center of the 2D Gaussian island (r_0) as 0.1λ , 0.3λ , 0.5λ , 0.7λ and 0.9λ . We found that the separation of the charged particles are related to the distance from the center of the Gaussian flux tube (r_0), where they experience the different

structure of the magnetic field. When the charged particles are released at low curvature of the magnetic field line, the separation is more than the others at the initial times. They try to follow the field line and slowly drift to outside the 2D flux tube. Figure 4.4 shows that the influence of drift velocity of guiding center due to the gradient and curvature of the magnetic field has more effect to the separation of the charged particles at the beginning. Especially, when the charged particles are released at radius as 0.1λ , the curvature drift has more effect to the separation of the charged particles than other radius. At intermediate time, the particles start at $r_0 = 0.1\lambda$ and 0.3λ , at inside 2D islands, have lower separation than the others radius. The particles slowly drift out from the field lines. There are low the separation rates here because the charged particles are trapped inside 2D island. The different behaviors of the particles are found for the particles started outside 2D islands, the particles are started at $r_0 = 0.5\lambda$, 0.7λ and 0.9λ have almost the same separation rate and there is more the separation rate than the particles start at inside 2D island. It is because the particles outside the sharp gradient are not suppressed due to strong 2D field. In addition, for the final time the separation of the charged particles is uncorrected with the starting point to release the charged particles. The separation of the charged particles depends on distance from the center of the Gaussian function and become subdiffusive, the charged particles are released at outside of 2D Gaussian field ($r_0 = 0.7$ and 0.9λ), the separation is lower than the others radius. For the second case, the 1000 charged particles are fixed initial pitch angles as 0, 30, 60 and 90 degrees and released in various radii (r_0). The charged particles have least separation when initial pitch angle as 90 degrees in every radius and initial pitch angle as 0 degree has highest separation. From the result, we found that the drift velocity of guiding center has more influence to the separation of the charged particle due to the curvature of the magnetic field line, that depends on $\cos^2 \theta$. So the initial pitch angle as 0 degree gives the highest drift velocity of guiding center, we can see from Figure 4.4 and that confirm our results in section 4.2.

The results for 2D+slab turbulence are presented in Chapter 5. Two cases are performed here. First, 1,000 charged particles are released at various pitch angles range from 0-30, 30-60, 60-90 degrees in simulation box that we model with random

positions. We found the trend of the charged particle released at initial pitch angle near 0 degree have more separation better than the one near 90 degrees in the initial time. In the second case, 1000 charged particles are released at random position in (2D+slab) turbulence magnetic field by fixing initial pitch angles as 0, 30, 60, 90 degrees. The initial pitch angle as 90 degree has less separation than the other angles. We know the behavior of the charged particles and effect of the magnetic field to separation of the charged particles at any time. In addition, we can find the critical point of initial pitch angles at any time.

From all results, we know that the magnetic field has effect to the separation of the charged particles supported by using simple case (2D Gaussian field + slab turbulence) and they give us a new idea about initial pitch angle to make least separation from (2D+slab) turbulence, that is 90 degree which is shown that if the charged particles are released perpendicular to their magnetic field lines, they have a little drift from effect of magnetic field but if they are released along their magnetic field lines they have a lot of drift. We can also conclude about the influence of drift motion of the charged particles. The curvature drift is dominated and has affect to the separation of the charged particle (see Figure 4.4) at the initial time. The separation of the charged particle is mostly depended on radius of curvature of the magnetic field line. The second is the gradient drift, it has a little effect to the separation of the charged particle and it is dominate when the charged particles are released at initial pitch angle as 90 degree (see from Figure 4.4). Moreover, for pure simple 2D field case, when the charged particles are released inside Gaussian island, they are confined within along 2D flux tube that they are started. So the period of the separation has smaller than outside one [see from Figures 4.9a) and 4.9b)]. This research is very useful to help us understanding about mechanisms of the transport of the solar energetic particles in heliosphere and developing the theory of diffusion of charged particles in turbulent magnetic field.



REFERENCES

REFERENCES

- Achara Seripienlert. (2006). *Tracing charged particle motion in a turbulent magnetic field*. Master's Thesis. Mahidol University, Bangkok.
- Bieber, J. W., Wanner, W. & Matthaeus, W. H. (1996). Dominant two-dimensional solar wind turbulence with implications for cosmic ray transport. *Journal of Geophysical Research*, 101(A2), 2511-2522.
- Bittencourt, J. A. (2004). *Fundamentals of plasma physics: Uniform magnetostatic field* (3rd ed.). New York: Springer-Verlag.
- Chuychai, P., Ruffolo, D., Matthaeus, W. H. & Meechai, J. (2007). Trapping and diffusive escape of field lines in two-component magnetic turbulence. *The Astrophysical Journal*, 659, 1761-1776.
- Chuychai, P., Ruffolo, D., Matthaeus, W. H. & Rowlands, G. (2005). Suppressed diffusive escape of topologically trapped magnetic field lines. *The Astrophysical Journal*, 633, L49-L52.
- Chuychai, P., Ruffolo, D., Wikee, C. & Matthaeus, W. H. (2011). Effect of reduced dimensionality of the magnetic field fluctuations on the cross-field motion of charged particles. *The 6th Annual Conference of the Thai Physics Society (SPC2011)*. Pattaya, Thailand: Thai physics society & Department of Physics, King Mongkut's University of Technology Thonburi.

- Dalena, S., Chuychai, P., Mace, R. L., Greco, A., Qin, G. & Matthaeus, W. H. (2012). Streamline generation code for particle dynamics description in numerical models of turbulence. *Computer Physics Communications*, 183, 1974-1985.
- Giacalone, J. & Jokipii, J. R. (1994). Charged-particle motion in multidimensional magnetic-field turbulence. *The Astrophysical Journal*, 430, L137-L140.
- Goldstein, M. L., Roberts, D. A. & Matthaeus, W. H. (1995). Magnetohydrodynamic turbulence in the solar wind. *The Astrophysical Journal*, 33, 283-325.
- Grant, H. L., Stewart, R. W. & Moilliet, A., (1962). Turbulence spectra from a tidal channel. *Journal of Fluid Mechanics*, 12, 241-263.
- Jokipii, J. R. (1966). Cosmic-ray propagation. I. Charged particles in a random magnetic field. *The Astrophysical Journal*, 146(2), 480-487.
- Jokipii, J. R. (1973). The rate of separation of magnetic lines of force in a random magnetic field. *The Astrophysical Journal*, 183(3), 1029-1036.
- Jokipii, J. R. & Parker, E. N. (1968). Random walk of magnetic lines of force in astrophysics. *Physical Review Letters*, 21(4), 44-47.
- Jokipii, J. R., Kota, J. & Giacalone. (1993). Perpendicular transport in 1- and 2-dimensional shock simulation. *Geophysical Research Letters*, 20(17), 1759-1761.
- Jones, F. C., Jokipii, J. R. & Matthaeus, W. H. (1998). Charged-particle motion in electromagnetic fields having at least one ignorable spatial coordinate. *The Astrophysical Journal*, 509, 238-243.
- Kolmogorov, A. N. (1941). Dissipation of energy in the locally isotropic turbulence. *Mathematical and Physical Science*, 434(1890), 15-17.

- Matthaeus, W. H., Goldstein, M. L. & Robert, D. A. (1990). Evidence for the presence of Quasi-two-dimensional nearly incompressible fluctuations in the solar wind. *Journal of Geophysical Research*, 95(A12), 20,673-20,683.
- Matthaeus, W. H., Gray, P. C., Pontius, D. H., Jr. & Bieber, J. W. (1995). Spatial structure and field-line diffusion in transverse magnetic turbulence. *Physical Review Letters*, 75, 2136-2139.
- Matthaeus, W.H., Qin, G., Bieber, J. W. & Zank, G. P. (2003). Nonlinear collisionless perpendicular diffusion of charged particles. *The Astrophysical Journal*, 590, L53-L56.
- Piyanate Chuychai. (2004). *Models of random magnetic fields and some implications for turbulence structure and particle transport in the heliosphere*. Doctoral Dissertation. Chulalongkorn University, Bangkok.
- Press, W. H., Teukolsky, S. A., Vetterling, W. T. & Flannery, B. P. (1992). *Numerical recipes in FORTRAN: The art of scientific computing*. Cambridge: Cambridge University Press.
- Qin, G., Matthaeus, W. H. & Bieber, J. W. (2002). Subdiffusive transport of charged particles perpendicular to the large scale magnetic field. *Geophysical Research Letters*, 29(4), 1048.
- Qin, G., Matthaeus, W. H. & Bieber, J. W. (2002). Perpendicular transport of charged particles in composite model turbulence: Recovery of diffusion. *The Astrophysical Journal*, 578, L117-L120.
- Richardson, L. F. (1922). *Weather prediction by numerical process*. Cambridge: Cambridge University Press.

- Ruffolo, D., Matthaeus, W. H. & Chuychai, P. (2003). Trapping of solar energetic particles by the small-scale topology of solar wind turbulence. *The Astrophysical Journal*, 597, L169-L172.
- Ruffolo, D., Matthaeus, W. H. & Chuychai, P. (2004). Separation of magnetic field lines in two-component turbulence. *The Astrophysical Journal*, 614, 420-434.
- Ruffolo, D., Chuychai, P., Wongpan, P., Minnie, J., Bieber, J. W. & Matthaeus, W. H. (2008). Perpendicular transport of energetic charged particles in nonaxisymmetric two-component magnetic turbulence. *The Astrophysical Journal*, 686, 1231-1244.
- Schindler, K. (2007). *Physics of space plasma activity*. New York: Cambridge University Press.
- Shalchi, A. (2010). Random walk of magnetic field lines in dynamical turbulence: A field line tracing method. I. Slab turbulence. *Physics of Plasmas*, 17.
- Tooprakai, P., Chuychai, P., Minnie, J., Ruffolo, D., Bieber, J.W. & Matthaeus, W.H. (2007). Temporary topological trapping and escape of charged particles in a flux tube as a cause of delay in time asymptotic transport. *Geophysical Research Letters*, 34, L17015.
- Tu, C.-Y. & Marsch, E. (1995). MHD Structures. Waves and Turbulence in the Solar Wind. *Space Science Review*, 73, 1-210.
- Watcharawuth Krittinatham. (2010). *Drift motions of energetic particles in an interplanetary magnetic cloud*. Doctoral Dissertation. Mahidol University, Bangkok.

Wikee, C., Chuychai, P., Ruffolo, D. & Matthaeus, W. H. (2012). The effect of the initial pitch angles of charged particles to the separation on the turbulent magnetic field lines. *Proceedings of the 16th international annual symposium on computational science and engineering (ANSCSE 16)* (pp. 175-180). Chiang Mai: Chiang Mai University.





APPENDICES

APPENDIX A

THE LINEAR INTERPOLATION AND BI-LINEAR INTERPOLATION FOR 2D+SLAB TURBULENT FIELD

From the section 3.2, we have the 2D and slab magnetic fields only on each grid point in the simulation box. From Figure A.1, we want the magnetic field at red point, we can compute the magnetic field by using linear interpolation from nearest known grid points for slab turbulence or z direction and bi-linear interpolation for 2D field, it shown in Figure A.2a) and A.2b) respectively.

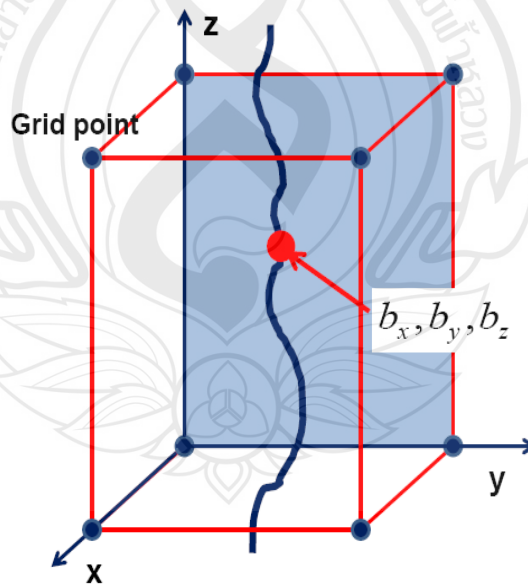


Figure A1 shows a position between grid points for finding magnetic field by using interpolation method.

For slab turbulence, if we want to find the magnetic field at any point in z direction, we can find the magnetic field by using linear interpolation. Here the magnetic field is not different on the same plane in z direction but in the different plane the magnetic field is not the same.

From the Figure A.2a), we know the magnetic field on grid points at (x_1, y_1, z_2) and (x_1, y_1, z_1) which correspond to the magnetic field values of b_2 and b_1 respectively. Suppose we want to find the magnetic field b at (x_1, y_1, z) . The linear interpolation method is applied to find magnetic field. Then we obtained the linear equation as

$$b = \left(\frac{b_2 - b_1}{z_2 - z_1} \right) z. \quad (\text{A.1})$$

Finally, we can find the magnetic field at (x_1, y_1, z) . as b .

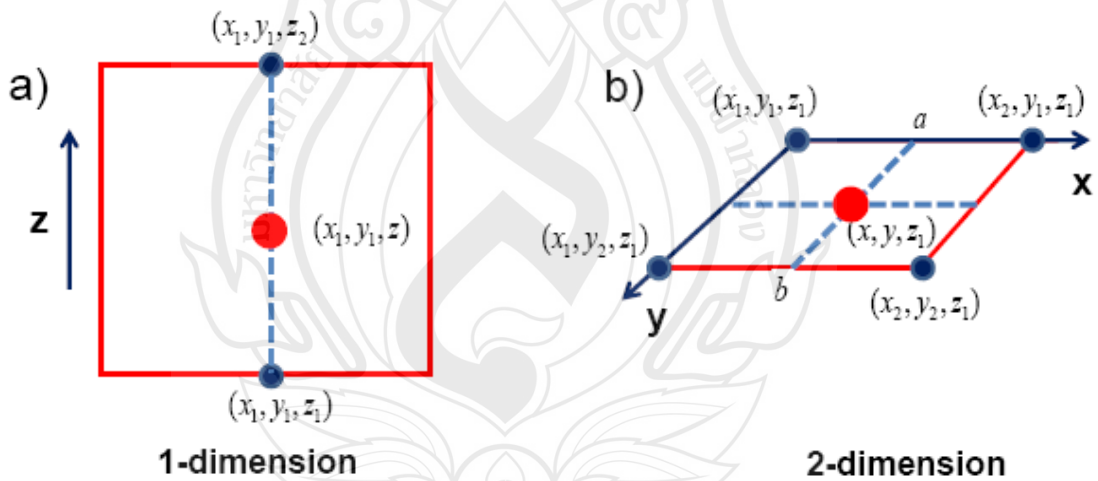


Figure A2 Illustrates the magnetic field at any position between grid points by using a) linear interpolation in z direction and b) bi-linear interpolation in x, y direction.

For 2D field, when we use simple model for 2D field, we can directly find the magnetic field on the same x, y plane by using Gaussian function. For 2D turbulence,

we compute the magnetic field by using bi-linear interpolation, it shown that in Figure A.2b). We can find the magnetic field at (x, y, z_1) if we known the magnetic field on grid points at $(x_1, y_1, z_1), (x_2, y_1, z_1), (x_1, y_2, z_1)$ and (x_2, y_2, z_1) which are corresponds to magnetic field value of b_3, b_4, b_5 and b_6 , respectively. From equation A.1, we obtained the magnetic field at a and b points as

$$b_a = \left(\frac{b_4 - b_3}{x_2 - x_1} \right) x \text{ and} \quad (\text{A.2})$$

$$b_b = \left(\frac{b_6 - b_5}{x_2 - x_1} \right) x. \quad (\text{A.3})$$

After that we use linear interpolation at (x, y, z_1) again, finally we obtain the equation as

$$b_{x,y,z_1} = \left(\frac{b_b - b_a}{y_2 - y_1} \right) y. \quad (\text{A.4})$$

APPENDIX B

THE CORRECTION OF UNIT VECTOR OF CROSS PRODUCT BETWEEN VELOCITY AND UNIT VECTOR FOR GENERATING A NEW VELOCITY VECTOR

The equation (3.22) is corrected if $|\vec{v} \times \hat{n}| = |\overline{\text{NP}}|$, when $|\vec{v} \times \hat{n}| = |\vec{v}||\hat{n}|\sin\theta$, $|\hat{n}| = 1$.

So the magnitude of vector $\overline{\text{NP}}$ as

$$|\overline{\text{NP}}| = \left| \vec{v} - \frac{\vec{B}}{|\vec{B}|} |\vec{v}| \cos\theta \right| \quad (\text{B.1})$$

$$\left(|\overline{\text{NP}}| \right)^2 = \left(\vec{v} - \frac{\vec{B}}{|\vec{B}|} |\vec{v}| \cos\theta \right)^2$$

$$\left(|\overline{\text{NP}}| \right)^2 = (|\vec{v}|)^2 + \left(\left| \frac{\vec{B}}{|\vec{B}|} |\vec{v}| \cos\theta \right| \right)^2 - 2 \left| \vec{v} \right| \left| \frac{\vec{B}}{|\vec{B}|} |\vec{v}| \cos\theta \right| \cos\theta.$$

Since $\left| \frac{\vec{B}}{|\vec{B}|} \right| = 1$, it is written as

$$\left(|\overline{\text{NP}}| \right)^2 = (|\vec{v}|)^2 + (|\vec{v}|^2 \cos^2\theta) - 2(|\vec{v}|^2 \cos^2\theta)$$

$$\left(|\overline{\text{NP}}| \right)^2 = (|\vec{v}|)^2 - (|\vec{v}|^2 \cos^2\theta)$$

$$\left(|\overline{\text{NP}}| \right)^2 = (|\vec{v}|)^2 (1 - \cos^2\theta).$$

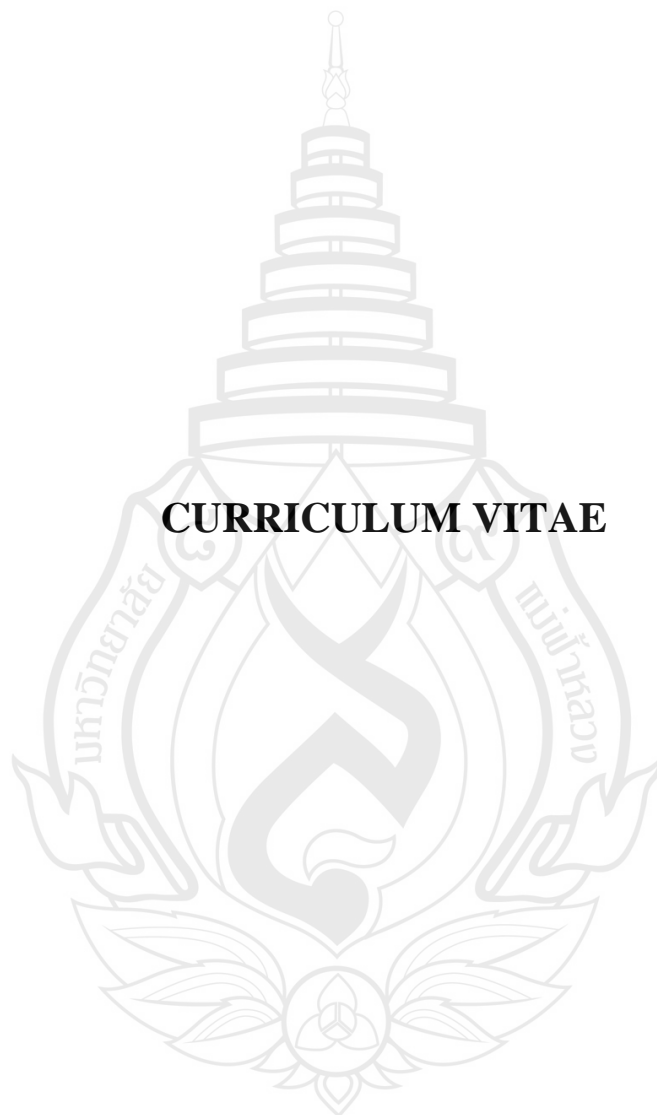
Since $\sin^2\theta = (1 - \cos^2\theta)$, then

$$\left(\overrightarrow{NP}\right)^2 = \left(\vec{v}\right)^2 \sin^2 \theta ,$$

$$\left|\overrightarrow{NP}\right| = \left|\vec{v}\right| \sin \theta .$$

Therefore, $\left|\vec{v} \times \hat{n}\right| = \left|\overrightarrow{NP}\right|$.





CURRICULUM VITAE

CURRICULUM VITAE

NAME

Mr. Chart Wikee

DATE OF BIRTH

23 December 1978

ADDRESS

House No.2, Village No.7,
Pasang sub-district
Maechan district, Chiang Rai province,
Thailand
57110

E-mail: chartwikee_2010@hotmail.com

EDUCATIONAL BACKGROUND

1999-2001

Bachelor of Science
Physics
Ramkhamhaeng University

WORK EXPERIENCE

2007-Present

Scientist
Scientific and Technological Instrument Center
Mae Fah Luang University